Deep Neural Network acoustic models for ASR

by

Abdel-rahman Mohamed

A thesis submitted in conformity with the requirements
for the degree of Doctor of Philosophy
Graduate Department of Computer Science
University of Toronto

Abstract

Deep Neural Network acoustic models for ASR

Abdel-rahman Mohamed

Doctor of Philosophy

Graduate Department of Computer Science

University of Toronto

2014

Automatic speech recognition (ASR) is a key core technology for the information age. ASR systems have evolved from discriminating among isolated digits to recognizing telephone-quality, spontaneous speech, allowing for a growing number of practical applications in various sectors. Nevertheless, there are still serious challenges facing ASR which require major improvement in almost every stage of the speech recognition process. Until very recently, the standard approach to ASR had remained largely unchanged for many years. It used Hidden Markov Models (HMMs) to model the sequential structure of speech signals, with each HMM state using a mixture of diagonal covariance Gaussians (GMM) to model a spectral representation of the sound wave.

This thesis describes new acoustic models based on Deep Neural Networks (DNN) that have begun to replace GMMs. For ASR, the deep structure of a DNN as well as its distributed representations allow for better generalization of learned features to new situations, even when only small amounts of training data are available. In addition, DNN acoustic models scale well to large vocabulary tasks significantly improving upon the best previous systems.

Different input feature representations are analyzed to determine which one is more suitable for DNN acoustic models. Mel-frequency cepstral coefficients (MFCC) are inferior to log Mel-frequency spectral coefficients (MFSC) which help DNN models marginalize out speaker-specific information while focusing on discriminant phonetic features.

Various speaker adaptation techniques are also introduced to further improve DNN performance.

Another deep acoustic model based on Convolutional Neural Networks (CNN) is also proposed. Rather than using fully connected hidden layers as in a DNN, a CNN uses a pair of convolutional and pooling layers as building blocks. The convolution operation scans the frequency axis using a learned local spectro-temporal filter while in the pooling layer a maximum operation is applied to the learned features utilizing the smoothness of the input MFSC features to eliminate speaker variations expressed as shifts along the frequency axis in a way similar to vocal tract length normalization (VTLN) techniques.

We show that the proposed DNN and CNN acoustic models achieve significant improvements over GMMs on various small and large vocabulary tasks.

Acknowledgements

First, I would like to thank my supervisors, Gerald Penn and Geoff Hinton, for being great teachers and providing guidance for me over the past few years, and for their great support and encouragement to pursue my own ideas. I am really grateful to have been their student. I would like to thank my committee members Brendan Frey, Ruslan Salakhutdinov, and Graeme Hirst for all their help and insights throughout my PhD. I am grateful for Jim Glass for his help and valuable comments and discussions.

I am fortunate to be part of two amazing research groups: the computational linguistics group and the machine learning group. I want to thank all the current and past ML and CL professors, students and post-docs for the great and fruitful environment they created: Aditya Bhargava, Afsaneh Fazly, Aida Nematzadeh, Alex Graves, Alex Krizhevsky, Andriy Mnih, Anthony McCallum, Charlie Tang, Chris Maddison, Chris Parisien, Cosmin Munteanu, Craig Boutilier, Danny Tarlow, Eric Corlett, Frank Rudzicz, George Dahl, Graham Taylor, Hugo Larochelle, Iain Murray, Ilya Sutskever, Jackie Cheung, Jake Snell, James Martens, Jasper Snoek, Josh Susskind, Julian Brooke, Katie Fraser, Kevin Swersky, Kinfe Tadesse, Laurent Charlin, Libby Barak, Maksims Volkovs, Marc'Aurelio Ranzato, Michael Reimer, Navdeep Jaitly, Nikola Karamanov, Nitish Srivastava, Nona Naderi, Patricia Araujo Thaine, Paul Cook, Radford Neal, Richard Zemel, Rouzbeh Farahmand, Ryan Adams, Ryan Kiros, Sean Robertson, Shunan Zhao, Siavash Kazemian, Suzanne Stevenson, Tijmen Tieleman, Timothy Fowler, Tong Wang, Tyler Lu, Ulrich Germann, Vanessa Wei Feng, Varada Kolhatkar, Vinod Nair, Volodymyr Mnih, Wesley May, Xiaodan Zhu, and Yujia Li. I owe special thanks to Julian Brooke and Katie Fraser for proof reading my thesis. I would like to thank Relu Patrascu, Luna Keshwah, Marina Haloulos, and Lisa DeCaro for their great support.

I am indebted to the speech research group at Microsoft for their support for my work in its earliest stage. Special thanks to Li Deng, Dong Yu, Geoff Zweig, Dan Povey, Patrick Nguyen, Mike Seltzer, Jasha Droppo, Asela Gunawardana, and Ivan Tashev for

making my internship at MSR a great pleasure.

Over the past three years, I had the great opportunity of collaborating with the speech research group at IBM. I owe many thanks to Tara Sainath, Bhuvana Ramabhadran, Brian Kingsbury, George Saon, Hagen Soltau, Peder Olsen, Mohamed Omar, Steven Rennie, David Nahamoo, Michael Picheny, Lidia Mangu, Abhinav Sethy, Ebru Arisoy, and Vaibhava Goel.

But most of all, I want to express my deepest gratitude to my family who supported me in every possible way. Especially, I want to thank my wife Maryam for her support and motivation all the time.

Contents

Chapter 1

Introduction

Traditional ASR systems use Hidden Markov Models (HMM) to model acoustic sequences, with each HMM state modeling a frame (typically 10 msec) of a spectral representation of the sound wave, using a mixture of diagonal covariance Gaussians (GMM). Due to the quasi-random nature of the speech production process, similar spoken sounds exhibit a wide range of spectral realizations. Major causes of variation include: the influence of neighboring phones (i.e. coarticulation), prosody, the vocal characteristics of individual speakers, and background noise. Given all the different sources of variation that affect speech spectral structure, it is not at all clear that models which learn rigid templates of acoustic inputs, e.g. Gaussian Mixture Models (GMM), represent the best approach to ASR acoustic modeling.

This dissertation proposes alternative acoustic models based on Deep Neural Networks (DNN) which use input speech segments as long as the average phone (about 150 msec), and utilize the time-varying spectro-temporal structure of speech data to recognize the many different forms of a spoken phone. Deep Neural Networks (DNN) model the conditional probability distribution of the correct phone label given the observed speech segment.

The central claim of the dissertation is that the variable nature of speech data is

better captured with deep neural network (DNN) acoustic models than with Gaussian Mixture Models (GMM). The proposed DNN acoustic models have the flexibility necessary to assimilate different spectro-temporal realizations of the same phone under various conditions using higher level representations that marginalize out undesirable information. Each layer of the DNN learns distributed representations of features presented at the layer below where multiple experts (i.e. hidden units) collaborate together to explain various hidden causes of input data. Such a representation allows the model to focus more and more on aspects that are important for accurate ASR at deeper layers. Also, the distributed nature of the model's representation helps generalize better to unseen situations (e.g. different speakers, noise sources, and languages), even with limited amounts of training data. By contrast, each expert (i.e. Gaussian) in a GMM models the whole input feature vector which makes GMMs inefficient when there are multiple simultaneous hidden causes, because a GMM requires a large number of Gaussian components to deal with the cross-product of all the causes.

We, however, found that DNN acoustic models prefer features that smoothly change both in time and frequency, like the log mel-frequency spectral coefficients (MFSC), to the **decorrelated** mel-frequency cepstral coefficients (MFCC). MFSC features make it easier for DNNs to discover linear relations as well as higher order causes of the input data, leading to a better overall system performance.

Such slowly changing features along the frequency axis makes it possible to deal explicitly with speaker variations in a manner similar to vocal tract length normalization (VTLN) techniques using Convolutional Neural Networks (CNN). The convolution and pooling operations of a CNN are performed along the frequency axis to spot local spectro-temporal structures with tolerance for the small translations caused by the different vocal tract lengths of different speakers.

1.1 Thesis structure

This thesis is organized as follows:

- Chapter 2 discusses previous ASR acoustic modeling efforts. The state-of-the-art HMM/GMM system is presented as well as various enhancements related to speaker and environment adaptation, covariance modeling, and the objective functions to be optimized. The database used in this dissertation and the experimental setup are also covered in this chapter.

- Chapter 3 presents layer-wise unsupervised feature learning for spoken data using a stack of Restricted Boltzmann Machines (RBM) that are used to initialize a Deep Neural Network (DNN). Each RBM learns a distributed representation of the input from the layer below using an approximate maximum likelihood training algorithm called Contrastive Divergence (CD). The resulting network is used as an initial state for the fine tuning phase, which uses the backpropagation algorithm.

- Chapter 4 investigates the appropriate input feature representation for DNN acoustic models. The typical feature representation choice for diagonal covariance GMM acoustic models, MFCCs, co-evolved with that model and therefore is not necessarily the best choice for the very different DNN acoustic model.

- Chapter 5 investigates various ways of performing speaker adaptation, required for higher ASR accuracy, in the context of DNN acoustic models. Speaker-adapted input features are used and two new speaker adaptation techniques are presented which have the flavor of eigenvoice speaker adaptation methods and do not require extra speaker label information.

- Chapter 6 introduces a new acoustic model based on Convolutional Neural Networks (CNN) which performs speaker normalization by convolving and pooling learned filters along the frequency axis. It is motivated by the wide range of vocal tract

lengths across speakers. Deep CNN acoustic models achieved the best published results over many small and large vocabulary tasks.

- Chapter 7 provides a brief summary of contributions made in the thesis and discusses future research directions.

1.2 Thesis contributions

This thesis introduces Deep Neural Networks (DNN) acoustic models for ASR. DNN acoustic models outperform other previously proposed methods on various standard benchmarks. It demonstrates the drawbacks of using Mel Frequency Cepstral Coefficients (MFCCs) rather than Mel Frequency spectral Coefficients (MFSCs) as the input features for DNN acoustic models. Also, it presents a variety of speaker adaptation techniques for DNN acoustic models. A new Convolutional Neural Networks (CNN) acoustic model is introduce which performs speaker normalization by acting along the frequency axis achieving the best published results to date on various large vocabulary tasks.

Chapter 2

Background and experimental setup

2.1 Past and current research trends in acoustic modeling

2.1.1 A basic HMM/GMM system for ASR

A typical ASR system represents the speech signal with Mel Frequency Cepstral Coefficients (MFCC) which are computed every 10 ms using an overlapping analysis window of around 25 ms. MFCCs are generated by applying a discrete cosine transformation (DCT) to a log spectral estimate computed by smoothing an FFT with around 20 frequency bins distributed non-linearly (on a mel scale) across the speech spectrum to approximate the frequency response of the human ear.

Hidden Markov Models (HMMs) are used to model the MFCC observation sequence. The HMM, which is a special case of the regular Markov model, has a sequence of state transitions that are not directly visible. However, the HMM output observations are visible and are used to infer the hidden state sequence. Each HMM state is modeled by a Gaussian mixture model (GMM) with many diagonal covariance Gaussians which are cheaper to train compared to full covariance Gaussians of the same size. MFCCs are a

good fit to this framework because they have been already decorrelated by the DCT.

Phones are used as the atomic speech unit to be modeled by HMMs. A phone can be defined as a speech segment that possesses distinct physical or perceptual properties. Each phone is modeled by a three-state HMM plus start and end dummy nodes. Figure 2.1 shows an HMM representation of a phone.

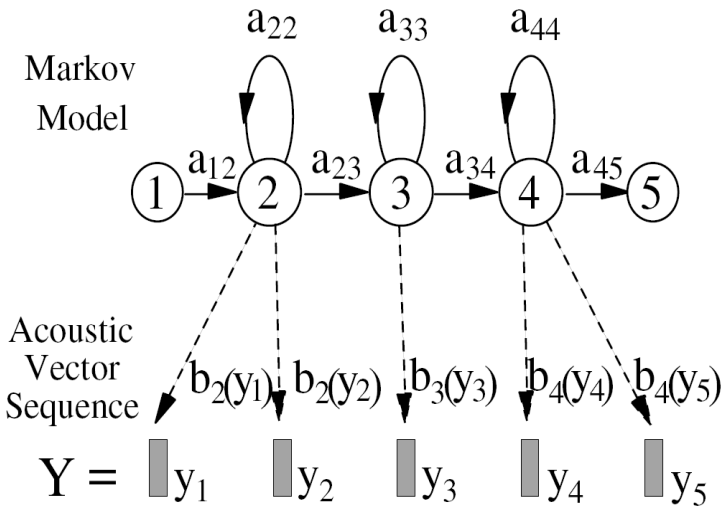

Figure 2.1: HMM-based phone model (from [23])

HMM parameters (the transition matrices and the GMMs) are trained by maximizing the training data likelihood:

$$\mathcal{F}_L = \sum_{n=1}^{N} \log(p(O^n_{1:T_n}|L^n_{1:m_n})). \tag{2.1}$$

During decoding all label sequences are searched to find L^* that maximizes the posterior probability $p(L|O)$ using the Viterbi algorithm such that:

$$L^* = \arg\max_i p(L_i|O) = \arg\max_i p(O|L_i)p(L_i) \tag{2.2}$$

where the term $p(L_i)$ represents the language model which is normally trained separately on a huge amount of text. Many proposals have been made to fine-tune the generatively trained acoustic model using another discriminative objective function which maximizes

the posterior probability $p(L|O)$ directly (i.e. using the language model probabilities $p(L)$ while training the acoustic model) which will be discussed in section 2.1.3.

There are many simplistic assumptions that are made in this basic model. HMMs have two unrealistic conditional independence assumptions: First, the current observation frame o_t, which is about 25ms long, is conditionally independent from all other frames in the utterance given the current state s_t. The second is that the current state at time s_t is conditionally independent from all other states given the previous state s_{t-1}. GMMs are easily trained using the EM algorithm, especially when they have diagonal covariance matrices but they are statistically inefficient at modeling high dimensional data that has any kind of componential structure (e.g. the speech spectrum), because in GMMs the whole data vector must be generated by a single Gaussian component. In the signal representation phase, MFCCs throw away a lot of the information in the sound wave using a fixed filter bank, i.e., with a fixed center and cut-off frequencies, for all speakers. This misses some discriminative spectral information.

Although these assumptions make inference and learning easy, they cause this basic system to lose lots of interesting structure inherent to the speech spectrum, which is crucial in discriminating among different acoustic units.

These limitations in the basic HMM/GMM system have triggered many proposals for modifications to it.

2.1.2 Improvements over the basic HMM/GMM model

In a heuristic attempt to compensate for the conditional independence assumption made by the HMM, first order (delta) and second-order (delta-delta) regression coefficients are often appended to the MFCC features [20]:

$$\Delta o_t = \frac{\sum_{i=1}^{n} w_i * (o_{t+i} - o_{t-i})}{2 \sum_{i=1}^{n} w_i^2} \tag{2.3}$$

where n is the regression window width and w_i are the regression coefficients. Delta-delta parameters ($\Delta^2 o_t$) are derived in the same way starting from the delta features. So the new feature vector is:

$$o_t^{new} = [o_t^T \ \Delta o_t^T \ \Delta^2 o_t^T]^T. \tag{2.4}$$

The temporal differences also assist diagonal covariance Gaussians in modelling the strong temporal covariances in the signal by reducing these particular pairwise covariances to individual coefficients. By variance normalization of input features, these differences got exaggerated which help improve recognition performance. On the other hand, it models only short term dependencies without explicit modeling of longer term trajectories [15].

As mentioned in section 2.1.1, HMM-based recognizers do not usually include any explicit modeling of correlations between different dimensions in the feature vector, i.e., conditioned on the hidden states, acoustic features are modeled by Gaussian distributions with diagonal covariance matrices. This is because it is cheaper both in running time and in the amount of data required (for each Gaussian) than reliably estimating the full covariance matrices.

Factor analysis has been proposed to model the correlations between acoustic features [87]. The idea behind factor analysis is to map systematic variations of the data into a lower dimensional subspace. This enables one to approximate, in a very compact way, the full covariance matrices for high dimensional data. These matrices are expressed in terms of a small number of parameters that model the most significant correlations.

Let $x \in \mathcal{R}^D$ be a feature whose covariance we want to model, and which is normally distributed with mean μ, and let $z \in R^f$ be a Gaussian latent factor that generates x, where $f \ll D$. So the probability density of $p(x|z)$ is also Gaussian with mean $\mu + \Lambda z$ and diagonal covariance ψ where Λ is the factor loading matrix that relates the hidden factor z to the observations x. Marginalizing out z, the probability density of x under the factor analysis model is Gaussian with mean μ and covariance $\psi + \Lambda\Lambda^T$. This model allows for

modeling the important correlations between features using only $D + Df$ variables per Gaussian component rather than D^2 variables.

It follows that when the diagonal elements of ψ are small, most of the variation in x occurs in the subspace $S(\Lambda)$ spanned by the columns of Λ. The variances ψ_{ii} measure the typical size of component-wise fluctuations outside this subspace.

[87], used filter bank outputs as input features for x, which are strongly correlated, while [80] used MFCCs as features which, although they are decorrelated by the DCT, have non-zero off-diagonal elements in their covariance matrices. Improvements were introduced by sharing covariances between Gaussian components and using a GMM to model the latent variable z [80]. Further improvements were achieved by modeling the precision matrix [91] rather than the covariance matrix so that no inversion was needed during decoding.

The precision matrix can be approximated as, [24, 91]:

$$\Sigma_m^{-1} = \sum_{i=1}^{B} \nu_{mi} S_i \tag{2.5}$$

where ν_m is a Gaussian-component-specific weight vector that specifies the contribution from each of the B global positive semi-definite matrices. Further refinement takes B to be the number of dimensions with symmetric basis matrices that have rank 1 so that $S_i = a_i^T a_i$ where a_i is the i^{th} row of the matrix A:

$$\Sigma_m^{-1} = \sum_{i=1}^{d} \nu_{mi} a_i^T a_i = A \Sigma_{diag}^{(m)-1} A^T. \tag{2.6}$$

$\Sigma_{diag}^{(m)}$ is specific to each component whereas the A matrices are shared between many components.

As discussed earlier, HMMs use a single-state variable to encode all state information (typically, just the identity of the current phonetic unit) while Dynamic Bayesian Networks (referred to here as "DyBNs"), a generalization of HMMs, provide a convenient method for defining acoustic models that maintains an explicit representation of

the speech articulators (e.g. lips, tongue, jaw, etc...) as they change over time. They can therefore naturally handle coarticulation effects [99]. In addition, dependencies between multiple acoustic features could be modeled to relax the strong independence assumption of HMMs, which makes DyBNs more accurate models for speech recognition and generation [9]. As the DyBN becomes more powerful, by introducing connections between its hidden states to encode dependencies, learning becomes harder as the exact inference of the hidden variables becomes intractable, so variational and approximate inference models are used in such complex models [27].

2.1.3 Discriminative objective functions for training GMMs

Many proposals have been made to fine-tune generatively trained acoustic models using another discriminative objective function that maximizes the posterior probability $p(L|O)$ directly and is directly related to the performance metric, e.g., word error rates (WER).

Using Bayes' rule, the posterior probability of the correct label sequence L_c is

$$p(L_c|O) = \frac{p(O|L_c)p(L_c)}{\sum_l p(O|l)p(l)} \tag{2.7}$$

where the summation in the denominator is over all possible label sequences. In practice this summation is performed over only strong competing sequences (they are represented either in a lattice or an N-best list). The language model probabilities $p(l)$ are normally fixed while optimizing the acoustic model parameters. This family of training methods is harder to optimize than ML because they include all other competing models, i.e., it is a joint optimization of many models that constrain each other. Discriminative objectives are prone to overfitting unless coupled with another generative objective as a regularizer [70].

Maximum Mutual Information (MMI) training [6, 75] tries to maximize the mutual information between the training data and the correct label sequence:

$$
\begin{aligned}
I(L,O) &= H(L) - H(L|O) \\
&= \sum_{l}\sum_{o} p(l,o)\log(\frac{p(l,o)}{p(l)p(o)}) \\
&\approx \frac{1}{N}\sum_{n=1}^{N}\log(p(L|O)) \\
\mathcal{F}_{MMI} &= \sum_{n=1}^{N}\log(\frac{p(O_n|L_n)^{\kappa}p(L_n)}{\sum_l p(O_n|l)^{\kappa}p(l)})
\end{aligned}
\tag{2.8}
$$

where κ is a smoothing factor ($\kappa < 1.0$) to make less likely sequences contribute to the objective function, make the objective more smoothly differentiable, and improve model generalization. The expectation in the second equation was approximated by averaging over all the training data samples N and dropping the label entropy term. MMI training, while being well-motivated from an information-theoretic prospective, does not relate directly to the required performance metric, e.g., word error rates (WER).

The Minimum phone error training (MPE) objective function directly optimizes weighted phone transcription accuracy [78]:

$$
\begin{aligned}
\mathcal{F}_{MPE} &= \sum_{n=1}^{N}\sum_{u} p(u|O_n)A(u,u_n) \\
&= \sum_{n=1}^{N}\frac{\sum_u p(O_n|u)^{\kappa}p(u)A(u,u_n)}{\sum_l p(O_n|l)^{\kappa}p(l)}
\end{aligned}
\tag{2.9}
$$

where $A(u,u_n)$ is the raw phone transcription accuracy of the sequence u given the reference sequence u_n (which equals the number of reference phones minus the number of errors).

Even when overall system performance is measured by Word Error Rate (WER), maximizing the phone transcription accuracy (the edit distance on the phone level) has been found to be more helpful than directly maximizing word transcription accuracy (the edit distance on the word level) [78].

Another proposal is Large Margin training (LM). The main idea here is to maximize the classification margin [48, 90], i.e., to separate the correct versus incorrect label sequences by margins proportional to the number of mislabeled units like phones or words, while using a convex objective function to avoid local minima.

We define $D(O, L)$ as:

$$D(O, L) = \sum_t (\lambda(l_{t-1}, l_t) + \rho(o_t, l_t)) \tag{2.10}$$

where λ and ρ are state transition and state output score functions respectively.

The set of constraints that the model should satisfy are:

$$\begin{aligned} D(O_n, L_n) - D(O_n, U) \geq H(L_n, U), \forall U \neq L_n \\ -D(O_n, L_n) + log \sum_{U \neq L_n} exp(D(O_n, U) + H(L_n, U)) \leq 0 \end{aligned} \tag{2.11}$$

where $H()$ is the hamming distance between two sequences. The objective function becomes:

$$\begin{aligned} \mathcal{F}_{LM} = \gamma \sum_{c,m} trace(\phi_{cm}) + \sum_{n=1}^{N} [-D(O_n, L_n) + log \sum_{U \neq L_n} exp(D(O_n, U) + H(L_n, U))]_+, \\ \text{subject to the positive semidefinite constraints } \phi_{jm} > 0 \end{aligned} \tag{2.12}$$

where ϕ_{cm} is a matrix containing the parameters of the Gaussian mixture m for state c. $[a]_+$ is a hinge function which equals zero unless $a > 0$, in which case it equals a.

Affected by the success of the large margin training of HMMs, The MMI objective was changed to have a large margin flavour in Boosted maximum mutual information training (BMMI) [76]:

$$\mathcal{F}_{BMMI} = \sum_{n=1}^{N} log \frac{p(O_n|L_n)^\kappa p(L_n)}{\sum_l p(O_n|l)^\kappa p(l) exp(-bA(l, L_n))} \tag{2.13}$$

where $A()$ is the raw phone transcription accuracy. In this objective function, the likelihood of the sentences that have more errors is emphasized to enforce a soft margin that is

proportional to the number of errors in a hypothesized sentence. The objective is related to the MPE objective with no consistent superiority in performance [76].

Following the success of using the MPE and BMMI objective functions for training HMMs, the same objectives have been proposed for training acoustic features [76, 77] so that they are more discriminative. The first stage is to project the low (e.g. 39) dimensional features into high (e.g. 100,000) dimensional ones. A set of Gaussians is created by likelihood-based clustering in the acoustic space, each frame being represented by its sparse Gaussian responsibility vector. Then a contextual window (e.g. 7 frames of context) of these high-dimensional vectors is formed into the vector h_t. The new features y_t are:

$$y_t = x_t + Mh_t \tag{2.14}$$

where the matrix M projects back the high-dimensional vector h_t into the original feature space. The main work is in training the matrix M using an MPE or BMMI objective function.

2.1.4 Speaker adaptation

There are a few terms related to adapting acoustic models that need clarification. A speaker-independent (SI) model is one created using utterances from many speakers which contain both intraspeaker (within the same speaker) and interspeaker (between different speakers) variabilities. A speaker-dependent (SD) model is one created using utterances recorded from one speaker only which, when practical, contains intraspeaker variations only. For applications in which there will be only one speaker interacting with the ASR system, e.g., a dictation system, ideas have been proposed to adapt an existing SI model to one test speaker, e.g., the one who will be using the dictation system, during an enrollment session to ensure the best performance for this speaker. After collecting speaker data, a speaker transformation is created, called speaker profile, which shifts the SI model closer to this speaker's point in the acoustic space [96].

Building on that idea, pre-existing transforms are built *a priori* using data clustered based on speaker similarity so that, during decoding, every utterance is mapped to the closest cluster. The cluster's transform is then used for very fast adaptation.

The idea of speaker adaptation has also been used during training where, as opposed to SI models, every utterance in the training data is normalized (moved from its speaker point in the acoustic space to a certain canonical speaker point) before building the acoustic model so that the resulting training data, while keeping the intraspeaker variations, will not contain interspeaker differences. This is called speaker-adaptive training (SAT) [4] which offers a more practical alternative to SD models which are then adapted during test time to match test speakers. One major drawback of the proposed adaptation techniques is that they are performed separately from GMM training, which sometimes cause a degradation of performance. A better method would train the GMM and speaker transforms jointly to reduce WER.

One major source of interspeaker variability is the variation of vocal-tract shape among speakers. The spectral formant peaks are related to the length of the vocal tract and the formant center frequencies can vary by as much as 25% between speakers. Systems that use MFCCs as their features will not be able to recover the missing data from mislocated filter banks. One basic solution to this problem is to warp the spectrum so that we have normalized features with speaker-specific vocal-tract length information removed [5, 17, 61]. For training, given a set of HMM models λ, a grid search is done to choose the optimal linear warping frequency factor α_i^* for each speaker i which maximizes the data likelihood:

$$\alpha_i^* = \arg\max_{\alpha} p(O_i^{\alpha}|\lambda, L_i) \tag{2.15}$$

where O_i^{α} are the warped features using the factor α. A new HMM model is created using the new warped features and then the whole process is repeated until the warping factor stabilizes. For testing, a first-pass decoding finds approximate labels then, α is

selected to warp the input features for this utterance before the final decoding. An improved version uses a piece-wise linear function [32] for warping the spectrum.

Maximum likelihood linear regression (MLLR) adaptation applies a linear transformation to the learned model parameters to improve system performance for a certain test speaker s by transforming the model means and covariances to maximize the likelihood of the test data under the new model [21,62]. If μ^m and Σ^m are the mean and covariance of the Gaussian m, then:

$$\begin{aligned} \mu^{sm} &= A^s \mu^m + b^s \\ \Sigma^{sm} &= H^s \Sigma^m H^{sT} \end{aligned} \tag{2.16}$$

where μ^{sm} and Σ^{sm} are the mean and covariance of the Gaussian m adapted to speaker s. To perform adaptation with as little data as possible, all Gaussians in the system are pooled together in a tree so that Gaussians that are closer in the acoustic space will share the same linear transforms. As the amount of data available for speaker s increases, we descend deeper into the tree to have more specific transformations of the Gaussians. If we constrain the mean and covariance transforms to be the same:

$$\begin{aligned} \mu^{sm} &= A_c^s \mu^m + b_c^s \\ \Sigma^{sm} &= A_c^s \Sigma^m A_c^{sT} \end{aligned} \tag{2.17}$$

it can be shown also that:

$$O^s = A^s O + b^s \tag{2.18}$$

where:

$$\begin{aligned} A^s &= inv(A_c^s) \\ b^s &= -inv(A_c^s) b_c^s. \end{aligned} \tag{2.19}$$

This is called Constrained MLLR (CMLLR) or Feature-space MLLR (fMLLR) [21] where the learned transformation could be applied directly in the feature space.

During the estimation of both MLLR and CMLLR, an adaptation-data transcript is needed. Thus we may distinguish between a supervised adaptation mode where the transcript is known *a priori* (e.g. user enrollment in voice enabled software) and an unsupervised adaptation mode where the adaptation-data transcript should be provided with one pass of the recognizer using an existing acoustic model before the transform is estimated (this process is repeated until convergence) [95].

As mentioned in section 2.1.1, the failure of GMMs to model componential structure in the data requires MLLR to have many transforms (which requires a lot of more adaptation data) to model the huge number of Gaussians used in such systems.

For Speaker-independent (SI) systems, acoustic model parameters are estimated using a large number of speakers, which is less accurate than Speaker-dependent (SD) acoustic models where the training data is collected from only one speaker. Spectral variations in SI models are caused by interspeaker variability, e.g., the anatomy of the vocal tract and the vocal cords, by regional dialects and by speaking style, in addition to phonetically relevant sources of variation. As a result, the SI spectral distributions often have higher variance than the corresponding SD distributions and hence higher overlap among different speech units. In Speaker Adaptive Training (SAT) [4], these two sources of variation are separated by explicit MLLR transformations modeled jointly with the GMM density estimation so that one focuses on speaker variations and the other on phonetically relevant variations of the speech signal.

Another formulation of SAT can be reached by using the CMLLR idea where speaker adaptation take place in the feature domain rather than in the model domain. In [21], training data from different speakers are transformed to a canonical speaker feature space where interspeaker variability is removed and then a new HMM/GMM model is estimated in this space, which focuses on the intraspeaker variability only.

The speaker-adaptation process when applied in the test phase is a compromise between the correctness of the estimated adapted model (Which benefits from more data) and how fast the enrollment/adaptation phase is. Some speaker adaptation techniques arrange training speakers in a tree based on their gender and speaker rate with a separate HMM/GMM model built for each leaf node in the tree. So during the test phase, a new test speaker is quickly assigned to one leaf cluster and its model is used [36].

Furthermore, every test speaker can be represented as a weighted sum of previously trained speaker cluster HMM/GMMs [25, 36]. So the mean of certain Gaussians for speaker s is:

$$\mu^s = \sum_{c=1}^{C} \lambda_{cs} \mu_c \tag{2.20}$$

where μ_c is a Gaussian in the GMM of cluster c, C is the total number of clusters, and the λ vector contains the speaker specific mixing proportions. The λ parameters are trained using ML.

2.1.5 Neural networks for ASR

Feedforward neural networks NN have been used in many ASR systems [8,10,73] because they offer several potential advantages over GMMs:

- Their estimation of the posterior probabilities of HMM states does not require detailed assumptions about the data distribution.
- They allow an easy way of combining diverse features, including both discrete and continuous features.
- They use far more of the data to constrain each parameter because the output on each training case is sensitive to a large fraction of the weights.

It is harder to train a neural network model using gradient descent on mini-batches than it is to fit a GMM using EM, and there are usually more decisions to be made about meta-parameters such as learning rates and regularization terms. The use of special-purpose

hardware with multiple DSP chips by [72] led to a large reduction in the training time needed for neural nets and helped make neural networks competitive with GMMs for speech recognition.

Conditioned on an acoustic feature vector, NNs provide the posterior probability distribution over the class labels. In a hybrid HMM-NN model [10], the posterior probabilities are fed to a Viterbi decoder to produce word sequences (i.e. the NN replaces the GMM component). In the Tandem model [37], the decorrelated log posterior probabilities (sometimes augmented with MFCC features) are fed as feature vectors to a basic HMM/GMM system so that it compromises between the high modeling power of NNs and all of the algorithms and tools developed for GMMs.

Recurrent neural networks (RNNs) have been also applied to ASR in the same way that the hybrid system works [79]. The advantage of the RNN is that the previous hidden state vectors of the network are used along with the current input features to determine the current hidden state vector which makes RNNs a very powerful model for time sequences. RNNs are harder to train than feed forward NNs with only a few hidden layers because, as when they are unfolded in time, they correspond to a deep network with T layers, where T is the sequence length.

In the previously mentioned NN systems, the input acoustic feature vector is a context window of n MFCC frames (with 10 ms frame shift) which covers $10 * n$ ms of the input speech (i.e. features are $10 * n$ ms thick vertical slices from the MFCC spectrogram that covers all the frequency bands). In the TRAPS architecture [40], features are horizontal slices such that each one focuses on one frequency band (could be more than one band) for about $1sec$. A *band filter* is a NN that keeps focusing on one horizontal slice over time to produce a posterior probability distribution over class labels. Many band filters, e.g., 15, are then combined using the output NN to produce the final posterior probability distribution for each frame which could be used in hybrid or tandem systems. The TRAPS architecture provides robust frame accuracies in noisy conditions because decisions are

made reliably by some band filters even if others are corrupted by band-limited noise. This architecture is inspired by human speech recognition findings, as shown in the next section.

2.1.6 Human speech recognition

Thinking of biological systems as the ultimate information processors, many studies have been performed to understand how humans perceive, process and recognize speech [3, 19, 31]. Human speech recognition (HSR) is believed to be largely bottom-up, where speech is recognized based on a hierarchy of feature layers that use progressively longer contexts. Feature extractors and event detectors start from the filters in the cochlea. As we go higher in the hierarchy, more context is integrated, leading to a decrease in entropy and the appearance of more abstract representations (e.g. phones, syllables, words,etc ...) [3].

Existing automated speech recognition systems do not work the way humans work. This is because automatic speech recognition (ASR) uses spectral templates, while humans work with partial (i.e. local) recognition information across frequencies (e.g., formants). It has been shown in humans, for example, that forcing partial recognition errors in one frequency region does not affect partial recognition at other frequencies, i.e., the partial recognition errors across frequency are independent [3]. It seems to be this local feature-processing, uncoupled across frequency, that makes human speech recognition (HSR) robust to noise and reverberation. These extracted features are then integrated into basic sound units (phones), and the phones are then grouped into syllables, then words, and so forth [3].

HSR studies show that current ASR systems, while good for some tasks, are too shallow and model human processing of speech poorly. The work in [64] compares the performance of humans and speech recognizers using six modern speech corpora with vocabularies ranging from 10 to 65,000 words. Error rates of machines are often more

than an order of magnitude greater than those of humans for quiet, clearly spoken speech. Machine performance degrades by a larger margin below that of humans in noisy conditions. Human performance remains high with natural variability caused by new speakers, spontaneous speaking styles, noise, and reverberation. Human performance also remains high with unnatural degradation caused by waveform clipping, band-reject filtering, and analog waveform scrambling.

2.1.7 Segmental and landmark based methods

Many speech scientists believe that the acoustic cues important for phonetic contrasts are best characterized in relation to specific temporal landmarks in the speech signal, such as points of oral closure or release, or other points of maximal constriction or opening in the vocal tract which are produced during speech production [29]. Many of these locations correspond to phonetic boundaries, leading some speech researchers to consider segment- and landmark-based approaches for ASR. Work in [35] recognizes different streams of phonological features (e.g. voice, manner, and place of articulation) and uses these temporal landmarks to synchronize between them.

The work in [47] proposes a hierarchical framework where each layer is designed to capture a set of distinctive feature landmarks. For each feature, a specialized acoustic representation is constructed in which that feature is easy to detect.

The "SUMMIT" speech recognizer [98] used a segment-based framework for its acoustic-phonetic representation of the speech signal. The observation space takes the form of a graph where different paths through the graph are associated with different sets of feature vectors. During decoding, proper normalization of likelihoods is needed as different paths through the graph compute likelihoods on different observation spaces.

2.2 Experimental Setup

In this section the database and the experimental setup used in the reminder of the thesis are described.

2.2.1 TIMIT corpus

Phone recognition experiments were performed on the TIMIT corpus.[1] We used the 462 speaker training set and removed all SA records (i.e., identical sentences for all speakers in the database) since they could bias the results. **A separate validation set of 50 speakers, as defined in [34], was used for testing all of the meta-parameters. Results are then reported using the 24-speaker core test set, which is different from the validation set. Running Multiple rounds of cross-validation was not necessary given that the validation set is not part of the training data, and the training data size is sufficiently large.**

The speech was analyzed using a 25-ms Hamming window with a 10-ms fixed frame rate. In most of the experiments, we represented the speech using 12th-order Mel frequency cepstral coefficients (MFCCs) and energy, along with their first and second temporal derivatives. For other experiments, we used a Fourier-transform-based filter-bank with 40 coefficients distributed on a mel-scale (and energy) together with their first and second temporal derivatives (MFSC).

The data were normalized so that, averaged over the training cases, each coefficient, first derivative, and second derivative had zero mean and unit variance. We used 183 target class labels, i.e., 3 states for each one of the 61 phones. After decoding, the 61 phone classes were mapped to a set of 39 classes as in [60] for scoring. All of our experiments used a bigram language model over phones, estimated from the training set.

[1] http://www.ldc.upenn.edu/Catalog/CatalogEntry.jsp?catalogId=LDC93S1.

2.2.2 Computational setup

The acoustic models proposed in this thesis are quite computationally expensive. Training was accelerated by exploiting graphics processors, in particular GPUs in an NVIDIA Tesla S1070 system, using the CUDAMAT library [69].

Chapter 3

Generatively trained DNN for acoustic modeling

The state-of-the-art Automatic Speech Recognition (ASR) system, for many decades, has used Hidden Markov Models (HMMs) to model the sequential structure of speech signals, with local spectral variability modeled using mixtures of Gaussian densities. Until recently, Feedforward neural networks have been also used in many ASR systems [8, 10, 73] but with limited success compared to GMMs. In this chapter we propose revisiting neural networks with two important modifications. First, the network weights are generatively pretrained to maximize the data likelihood before applying the backpropagation algorithm in a fine tuning phase. This way, the training process of neural networks is closer to how GMMs are normally trained in ASR systems where they are trained first to maximize the data likelihood then a discriminative training objective is used to improve GMM recognition performance. Second, the network structure is extended to have many hidden layers with each hidden layer containing many more hidden units than the usual neural networks that have been applied to acoustic modeling in the past. This *deep* neural network acoustic model is the current state-of-the-art for ASR. This chapter is divided into two sections that align with these two directions for acoustic modeling: generative

training of neural networks and building deep networks. For each section, the main idea is first motivated and presented, then evaluated on the TIMIT phone recognition task [1].

3.1 Generative training of one-hidden-layer neural network acoustic models

3.1.1 Motivation

Previous applications of the neural network (NN) approach for acoustic modeling have used the backpropagation algorithm to train the neural networks discriminatively. These approaches coincide nicely with a trend initiated by [11] in which generative modeling is replaced by discriminative training.

Discriminative models have one major disadvantage, that is, the amount of constraint each data point imposes on the parameters of the model equals the number of bits required to specify the correct label for the data point. For generative models, the amount of constraint equals the number of bits required to describe the observed data point itself. So when the input data vectors contain much more structure than the labels, a generative model can learn many more parameters before it overfits. The benefit of learning a generative model is greatly magnified when there is a large supply of unlabeled speech in addition to the training data that have been labeled.

Generative pretraining of NNs is achieved using Restricted Boltzmann Machines (RBMs) [44]. An RBM is a bipartite graph in which visible units that represent observations are connected to hidden units using undirected weighted connections. The hidden units learn non-linear features that allow the RBM to model the statistical structure in the vectors of visible states.

[1] The TIMIT dataset turned out to be quite a good predictor of LVCSR performance.

3.1.2 Restricted Boltzmann Machines (RBMs)

An RBM is a particular type of Markov Random Field (MRF) that has one layer of stochastic visible units and one layer of stochastic hidden units. An RBM is restricted in the sense that there are no visible-visible or hidden-hidden connections. In the simplest type of RBM, the binary RBM, both the hidden and visible units are binary and stochastic. To deal with real-valued input data, we use a Gaussian-Bernoulli RBM in which the hidden units are binary but the input units are linear with Gaussian noise. We will explain the Gaussian-Bernoulli RBM later after first explaining the simpler binary RBM.

In a binary RBM, the weights on the connections and the biases of the individual units define a probability distribution over the joint states of the visible and hidden units using an energy function. The energy of a joint configuration is:

$$E(\mathbf{v}, \mathbf{h}|\theta) = -\sum_{i=1}^{\mathcal{V}}\sum_{j=1}^{\mathcal{H}} w_{ij} v_i h_j - \sum_{i=1}^{\mathcal{V}} b_i v_i - \sum_{j=1}^{\mathcal{H}} a_j h_j \tag{3.1}$$

where $\theta = (\mathbf{w}, \mathbf{b}, \mathbf{a})$, w_{ij} represents the symmetric interaction term between visible unit i and hidden unit j, and b_i and a_j are their bias terms. $\mathcal{V}$ and $\mathcal{H}$ are the numbers of visible and hidden units.

The probability that an RBM assigns to a visible vector $\mathbf{v}$ is:

$$p(\mathbf{v}|\theta) = \frac{\sum_{\mathbf{h}} e^{-E(\mathbf{v},\mathbf{h})}}{\sum_{\mathbf{u}}\sum_{\mathbf{h}} e^{-E(\mathbf{u},\mathbf{h})}}. \tag{3.2}$$

Since there are no hidden-hidden connections, the conditional distribution $p(\mathbf{h}|\mathbf{v}, \theta)$ is factorial and is given by:

$$p(h_j = 1|\mathbf{v}, \theta) = \sigma(a_j + \sum_{i=1}^{\mathcal{V}} w_{ij} v_i) \tag{3.3}$$

where $\sigma(x) = (1 + e^{-x})^{-1}$. Similarly, since there are no visible-visible connections, the conditional distribution $p(\mathbf{v}|\mathbf{h}, \theta)$ is factorial and is given by:

$$p(v_i = 1|\mathbf{h}, \theta) = \sigma(b_i + \sum_{j=1}^{\mathcal{H}} w_{ij} h_j). \tag{3.4}$$

Exact maximum likelihood learning is infeasible in a large RBM because it is exponentially expensive to compute the derivative of the log probability of the training data. Nevertheless, RBMs have an efficient *approximate* training procedure called "contrastive divergence" [42] which makes them suitable as building blocks for learning DNNs. We repeatedly update each weight, w_{ij}, using the difference between two measured, pairwise correlations:

$$\Delta w_{ij} \propto \langle v_i h_j \rangle_{\text{data}} - \langle v_i h_j \rangle_{\text{recon.}}. \tag{3.5}$$

The first term on the right hand side of Eq. 3.5 is the measured frequency with which visible unit i and hidden unit j are on together when the visible vectors are samples from the training set and the states of the hidden units are determined by Eq. 3.3. The second term is the measured frequency with which i and j are both on when the visible vectors are "reconstructions" of the data vectors and the states of the hidden units are determined by applying Eq. 3.3 to the reconstructions. Reconstructions are produced by applying Eq. 3.4 to the hidden states that were computed from the data when computing the first term on the right hand side of Eq. 3.5.

For Gaussian-Bernoulli RBMs the energy of a joint configuration is:

$$E(\mathbf{v}, \mathbf{h}|\theta) = \sum_{i=1}^{\mathcal{V}} \frac{(v_i - b_i)^2}{2} - \sum_{i=1}^{\mathcal{V}} \sum_{j=1}^{\mathcal{H}} w_{ij} v_i h_j - \sum_{j=1}^{\mathcal{H}} a_j h_j. \tag{3.6}$$

To keep the equation simple, we assume that the Gaussian noise level of all the visible units is fixed at 1. We also normalize the input data to have a fixed variance of 1 for each component over the whole training set.

Since there are no visible-visible connections, the conditional distribution $p(\mathbf{v}|\mathbf{h}, \theta)$ is factorial and is given by:

$$p(v_i|\mathbf{h}, \theta) = \mathcal{N}\left(b_i + \sum_{j=1}^{\mathcal{H}} w_{ij} h_j, 1\right) \tag{3.7}$$

where $\mathcal{N}(\mu, V)$ is a Gaussian with mean μ and variance V. Apart from these differences, the inference and learning rules for a Gaussian-Bernoulli RBM are the same as for a binary RBM, though, in practice, the learning rate needs to be smaller.

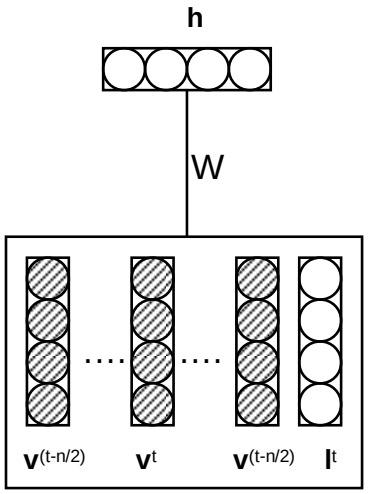

(a) RBM

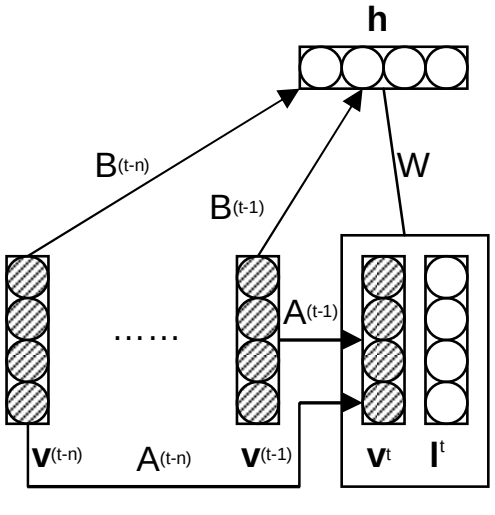

(b) CRBM

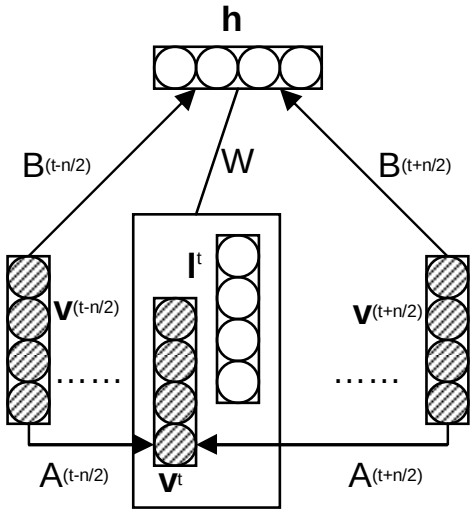

(c) ICRBM

Figure 3.1: Different RBM architectures. (a) shows an RBM that models the joint density of the label and all the frames in the window. (b) and (c) show two types of conditional RBM that model the joint density of the label and a single frame conditional on the other frames in the window.

3.1.3 The conditional RBM

The Conditional RBM (CRBM) [93] is a variant of the standard RBM that models vectors of sequential data by considering the visible variables in previous time steps as additional, conditioning inputs. Two types of directed connections are added; autoregressive connections from the past n frames of the visible vector to the current visible vector, and connections from the past n frames of the visible vector to the hidden units as in figure (3.1-b). Given the data vectors at times $t, t-1, ..., t-n$ the hidden units at time t are conditionally independent. One drawback of the CRBM is that it ignores future frames when inferring the hidden states, so it does not do backward smoothing. Performing backward smoothing correctly in a CRBM would be intractable because, unlike an HMM, there are exponentially many possible hidden state vectors, so it is not possible to work with the full distribution over hidden vectors when the hidden units are not independent.

If we are willing to give up on the ability to generate data sequentially from the model, the CRBM can be modified to have both autoregressive and visible-hidden connections from a limited set of future frames as well as from a limited past. So we get the interpolating CRBM (ICRBM) [figure (3.1-c)]. The directed, autoregressive connections from temporally adjacent frames ensure that the ICRBM does not waste the representational capacity of the non-linear hidden units by modeling aspects of the central frame that can be predicted linearly from the adjacent frames.

3.1.4 Application to phone recognition

A context window of successive frames of feature vectors is used to set the states of the visible units of the RBM. To train the RBM to model the joint distribution of a set of frames and the $\mathcal{L}$ possible phone labels of the last or central frame, we add an extra "softmax" visible unit that has $\mathcal{L}$ states, one of which has value 1. The energy function

becomes:

$$E(\mathbf{v},\mathbf{l},\mathbf{h};\theta) = -\sum_{i=1}^{\mathcal{V}}\sum_{j=1}^{\mathcal{H}} w_{ij}h_j v_i - \sum_{k=1}^{\mathcal{L}}\sum_{j=1}^{\mathcal{H}} w_{kj}h_j l_k - \sum_{j=1}^{\mathcal{H}} a_j h_j - \sum_{k=1}^{\mathcal{L}} c_k l_k + \sum_{i=1}^{\mathcal{V}} \frac{(v_i - b_i)^2}{2} \tag{3.8}$$

$$p(l_k = 1|\mathbf{h};\theta) = \text{softmax}(\sum_{j=1}^{\mathcal{H}} w_{kj}h_j + c_k). \tag{3.9}$$

And, $p(\mathbf{l}|\mathbf{v})$ can be computed exactly using:

$$p(\mathbf{l}|\mathbf{v}) = \frac{\sum_{\mathbf{h}} e^{-E(\mathbf{v},\mathbf{l},\mathbf{h})}}{\sum_{\mathbf{l}}\sum_{\mathbf{h}} e^{-E(\mathbf{v},\mathbf{l},\mathbf{h})}}. \tag{3.10}$$

The value of $p(\mathbf{l}|\mathbf{v})$ can be computed efficiently by utilizing the fact that the hidden units are conditionally independent. This allows the hidden units to be marginalized out in a time that is linear in the number of hidden units. To generate phone sequences, the values of $\log p(\mathbf{l}|\mathbf{v})$ per frame are fed to a Viterbi decoder.

Following the Contrastive Divergence (CD) approximation to the gradient of the joint likelihood function of data and labels, the update rule for the visible-hidden weights is:

$$\Delta w_{ij} = \langle v_i h_j \rangle_{data} - \langle v_i h_j \rangle_{recon.}. \tag{3.11}$$

The update rule for the autoregressive visible-visible links is:

$$\Delta A_{ij}^{(t-q)} = v_i^{(t-q)}(\langle v_j^t \rangle_{data} - \langle v_j^t \rangle_{recon.}) \tag{3.12}$$

where $A_{ij}^{(t-q)}$ is the weight from unit i at time $(t-q)$ to unit j. For the visible-hidden directed links it is:

$$\Delta B_{ij}^{(t-q)} = v_i^{(t-q)}(\langle h_j^t \rangle_{data} - \langle h_j^t \rangle_{recon.}). \tag{3.13}$$

Discriminative and hybrid training of an RBM

Since the log conditional probability, $\log p(\mathbf{l}|\mathbf{v})$, can be computed exactly, the gradient can also be computed exactly. If the correct label is m, the discriminative update rule for the visible-hidden weights is:

$$\Delta w_{ij} = v_i \sigma \left(a_j + w_{jm} + \sum_{i=1}^{\mathcal{V}} w_{ij} v_i \right) - v_i \sum_{k=1}^{\mathcal{L}} p(l_k = 1|\mathbf{v}) \sigma \left(a_j + w_{jk} + \sum_{i=1}^{\mathcal{V}} w_{ij} v_i \right). \tag{3.14}$$

To avoid model overfitting, we follow the gradient of a hybrid function $f(\mathbf{v}, \mathbf{l})$ which contains both generative and discriminative components:

$$f(\mathbf{v}, \mathbf{l}) = \alpha \log p(\mathbf{l}|\mathbf{v}) + \log p(\mathbf{v}|\mathbf{l}) \tag{3.15}$$

where $\log p(\mathbf{v}|\mathbf{l})$ works as a regularizer and is learned by using the original labels with the reconstructed data to infer the states of the hidden units at the end of the sampling step. The α parameter is used to control the emphasis given to the discriminative component in the objective function. Since the original labels are used during hidden layer reconstruction for evaluating the gradient of $\log p(\mathbf{v}|\mathbf{l})$, the label biases are updated using the gradient of $\log p(\mathbf{l}|\mathbf{v})$ only.

3.1.5 Experiments

CD training of three types of RBM

[2] The three types of RBM shown in figure (3.1-a) were trained using a window of 11 frames as the visible states. 2000 hidden units were used for all architectures.

Mini-batch gradient descent with momentum was used for pre-training and fine-tuning of all architectures. The learning rate was fixed during the pre-training phase. For the

[2]Results presented in this section on the TIMIT database are different from other ones in the rest of the dissertation because these results use an early stopping criteria that is based on the cross entropy on the development set. Also a more restrictive scoring criterion has been used where the start and end silences are not counted as correctly recognized phones.

fine-tuning phase, an early stopping criterion that is based on the cross entropy on the development set was used along with learning rate annealing. Training stops when the learning rate falls below a certain threshold.

Table 3.1 shows the phone error rate (PER) when the RBMs are trained generatively.

Table 3.1: *The PER of different RBM architectures.*

RBM	CRBM	ICRBM
36.9%	42.7%	39.3%

The ICRBM produces a lower PER than the CRBM, presumably because the near future is more relevant than the more distant past. The unconditional RBM performs the best, probably because modeling the joint density of the entire window reduces overfitting more effectively than only modeling one frame conditional on the other frames. In the conditional RBMs, the relation between frames captured by the autoregressive connections influences what the hidden units learn, but it does not directly help in decoding as $p(\mathbf{l}|\mathbf{v})$ does not depend on the autoregressive connections.

Hybrid training of the three types of RBM

Generatively trained network parameters were used to initialize hybrid training. The parameter α in equation (3.15) was tuned to minimize PER on the development set. The best RBM model achieved 27.5% PER while the best ICRBM model achieved 26.7%. The discriminative component of the hybrid gradient forces the ICRBM to extract nonlinear features from the context that are more useful for predicting the label. It has more capacity for these features than the unconditional RBM because it does not have to model the contextual frames or the linear dependencies of the modeled frame on the context.

Comparison with other models

Since a feedforward neural network is quite similar, it was compared to the ICRBM model. A feedforward neural network with 2000 hidden units and an input window of 11 frames was trained twice using backpropagation; once from random weights and once from the generatively trained weights of the unconditional RBM. Table 4.1 shows that the ICRBM outperformed both feedforward models, probably because the generative component of the hybrid training greatly reduces overfitting.

Table 3.2: *PER of the ICRBM compared to the NN model.*

NN (random weights)	NN (RBM weights)	ICRBM
28.7%	28.3%	26.7%

A two-tailed Matched Pairs Sentence-Segment Word Error (MAPSSWE) significance test [28] was conducted with the null hypothesis that there is no performance difference between the ICRBM and the feedforward neural net models using the NIST sc_stats tool. The test finds a significant difference at the level of p=0.05.

3.2 Deep Neural Networks for acoustic modeling

3.2.1 Learning a multilayer generative model

This section focuses on using deep NNs for acoustic modeling which is inspired by human speech recognition (HSR) research. In [3], HSR has been described as a hierarchical, bottom-up process with low entropy, more abstract representation, at the top. Here we reconsider the use of deep feed-forward neural networks that take a window of feature vectors as input and produce posterior probabilities of HMM states as output.

There are two views of understanding the learning of a multi-layer generative neural network model: the directed view and the undirected view. In the directed view, we

fit a multilayer generative model that has infinitely many layers of latent variables, but uses weight sharing among the higher layers to keep the number of parameters under control [71]. This chapter focuses on the undirected, "energy-based" view, which is in line with the discussion in section 3.1. In the undirected view, we fit a Restricted Boltzmann Machine (RBM) to speech data, and then we treat the activities of the latent variables as data for the next layer and fit an RBM again to these new "data". This can be repeated as many times as we like to learn as many layers of latent variables as we desire.

Naturally, many of the high-level features learned by the generative model may be irrelevant for making the required discriminations, even though they are important for explaining the input data. However, this is a price worth paying if computation is cheap and *some* of the high-level features are very good for discriminating between the classes of interest.

The main novelty of the work presented in the remaining sections has been to show that we can achieve consistently better phone recognition performance by "pre-training" a multi-layer neural network, one layer at a time, as a *generative* model of the window of speech coefficients. This pre-training makes it easier to optimize deep neural networks that have many layers of hidden units and it also allows many more parameters to be used before overfitting occurs. The generative pre-training creates many layers of feature detectors that become progressively more complex. A subsequent phase of discriminative fine-tuning, using the standard backpropagation algorithm, then adjusts the features in every layer to make them more useful for discrimination.

Our approach makes two major assumptions about the nature of the relationship between the input data, which in this case is a window of speech coefficients, and the labels, which are HMM states produced by a forced alignment using a pre-existing ASR model. First, we assume that the discrimination we want to perform is more directly related to the underlying causes of the data than to the individual elements of the data

itself. Second, we assume that a good feature-vector representation of the underlying causes can be recovered from the input data by modeling its higher-order statistical structure.

3.2.2 Using DNNs for phone recognition

As in the previous section, we use a context window of n successive frames of speech coefficients to set the states of the visible units of the lowest RBM. Once it has been pre-trained as a generative model, the resulting network is discriminatively trained to output a probability distribution over the possible labels of the central frame. To generate phone sequences, the sequence of predicted probability distributions over the possible labels for each frame is fed into a standard Viterbi decoder.

Strictly speaking, since the HMM implements a prior over states, we should divide out the prior from the posterior distribution over HMM states produced by the DNN, although for the TIMIT task it made no difference.

3.2.3 Experiments

For all experiments conducted in this thesis, we fixed the parameters for the Viterbi decoder. Specifically, we used a zero word-insertion probability and a language-model scaling factor of 1.0.

All networks were pre-trained with a fixed recipe using stochastic gradient decent with a mini-batch size of 128 training cases. For Gaussian-binary RBMs, we ran 225 epochs with a fixed learning rate of 0.002 while for binary-binary RBMs we used 75 epochs with a learning rate of 0.02. The learning rate is applied to the average gradient over each mini-batch.

The theory used to justify the pre-training algorithm assumes that when the states of the visible units are reconstructed from the inferred binary activities in the first hidden layer, they are reconstructed stochastically. To reduce noise in the learning, we actually

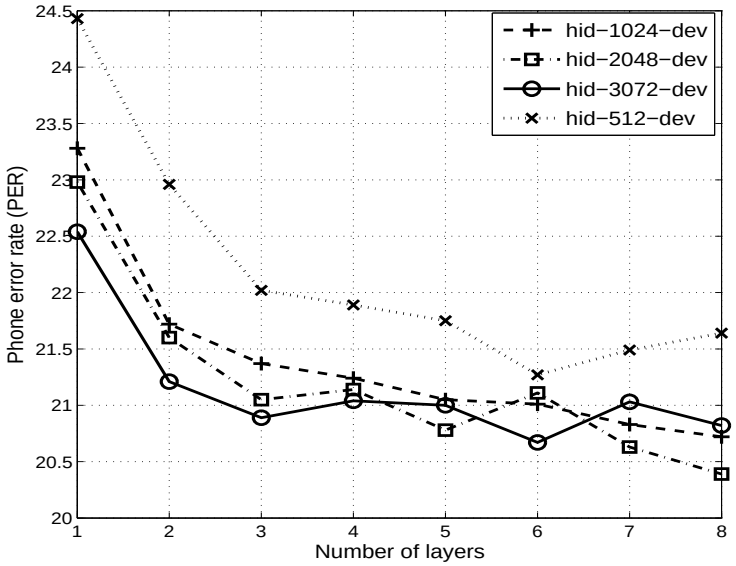

Figure 3.2: Phone error rate on the development set as a function of the number of layers and size of each layer, using 11 input frames.

reconstructed them deterministically and used the real values (see [43] for more details).

For fine-tuning, we used stochastic gradient descent with a mini-batch size 128 training cases. The learning rate started at 0.1. At the end of each epoch, if the recognition error on the development set increased, the weights were returned to their values at the beginning of the epoch and the learning rate was halved. This continued until the learning rate fell below 0.001.

During both pre-training and fine-tuning, an L2 weight penalty, half of the sum of squared weights, is used with small cost of 0.0002 and the learning was accelerated by using a momentum of 0.9 (except for the first epoch of fine-tuning which did not use momentum). [43] gives a detailed explanation of weight-cost and momentum and sensible ways to set them. This training recipe has been used in all of the experiments conducted in this thesis unless otherwise indicated.

Figure 3.2 and figure 3.3 show the effect of varying the size of each hidden layer and the number of hidden layers. For simplicity we used the same size for every hidden layer

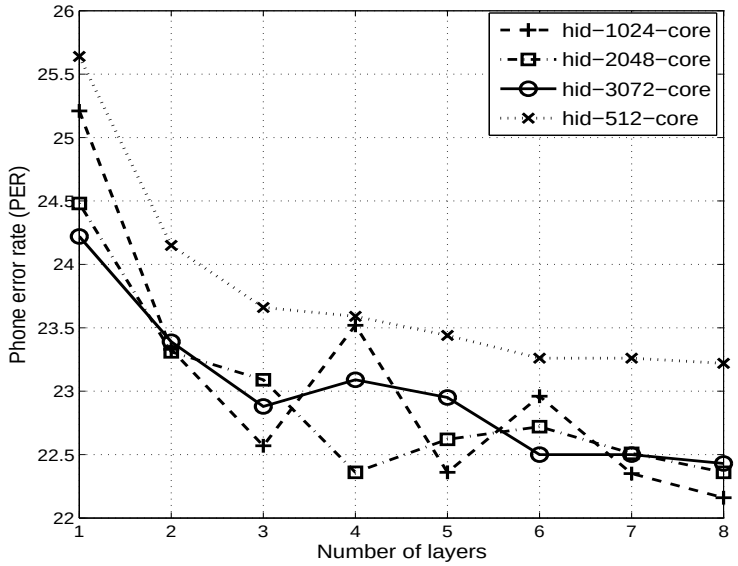

Figure 3.3: Phone error rate on the core test set as a function of the number of layers and size of each layer, using 11 input frames.

in the network. For these comparisons, the number of input frames was fixed at 11.

The main trend visible in figures 3.2, 3.3, 3.4, and 3.5 is that adding more hidden layers gives better performance, even for non pre-trained deep networks, though the gain diminishes as the number of layers increases. Using more hidden units per layer also improves performance when the number of hidden layers is less than 4, but with more hidden layers the number of units has little effect provided it is at least 1024. The advantage of using a deep architecture is clear if we consider the best way to use a total of 2048 hidden units: It is better to use two layers of 1024 or four layers of 512 than one layer of 2048.

Generative pre-training complements the performance of deep, random, networks especially for a task like TIMIT, where the number of training data points per network parameter is small. With a single hidden layer of 2048 units, generative pre-training gives a phone error rate of 24.5% and exactly the same fine-tuning algorithm started from small random weights gives 24.4%. So generative pre-training does not help. Adding a second

hidden layer causes a larger proportional increase in the number of trainable parameters than adding a third hidden layer because the input and output layers are much smaller than the hidden layers and because adjacent hidden layers are fully connected. This large increase in capacity makes the model far more flexible, but it also makes it overfit far more easily. Figure 3.4 and figure 3.5 show that for networks that are not pre-trained (but still use early stopping), these two effects apparently cancel out, whereas for pre-trained networks there is less overfitting. Although the advantage of pre-training is not as large as for some other tasks [45, 52], it still helps the network to avoid overfitting.

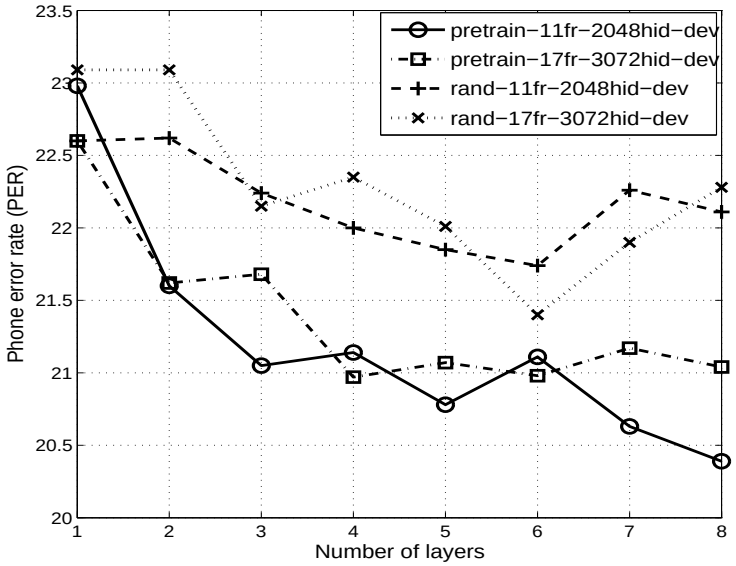

Figure 3.4: Phone error rate on the development set as a function of the number of hidden layers using randomly initialized and pretrained networks.

Fixing the number of hidden units per layer to 3072 and varying the number of frames in the input window (figures 3.6 and 3.7 and also 3.2 and 3.3) shows that the best performance on the development set is achieved using 11, 17, or 27 frames and this is true whatever the number of hidden layers. Much smaller (7 frames) and much bigger (37 frames) windows give significantly worse performance. The range from 110ms to 270ms covers the average size of phones or syllables. Smaller input windows miss

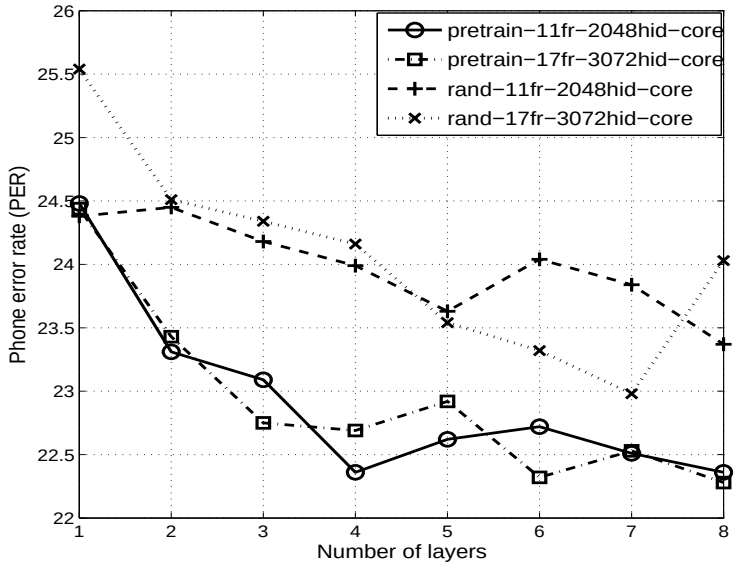

Figure 3.5: Phone error rate on the core test set as a function of the number of hidden layers using randomly initialized and pretrained networks.

important discriminative information in the context, while networks with larger windows are probably getting distracted by the almost irrelevant information far from the center of the window. The TRAP [40] architecture successfully uses 1 second long windows, but it dedicates separate networks to model different parts of the spectrum which simplifies the learning task. Larger windows would probably work better using triphone targets which provide the network with more information about the context and make the peripheral frames more relevant.

Since all but the output layer weights are pre-trained, it could be helpful to introduce a "bottleneck" at the last layer of the DNN to combat overfitting by reducing the number of weights that are not pre-trained. A bottleneck layer followed by a softmax is exactly equivalent to using a distributed output code for each class and then making the class probabilities proportional to the exponentiated squared difference between the code for a class and the activity pattern in the bottleneck layer [92]. Figure 3.8 shows that having a bottleneck layer does not actually improve PER for a typical network with 5 hidden layers

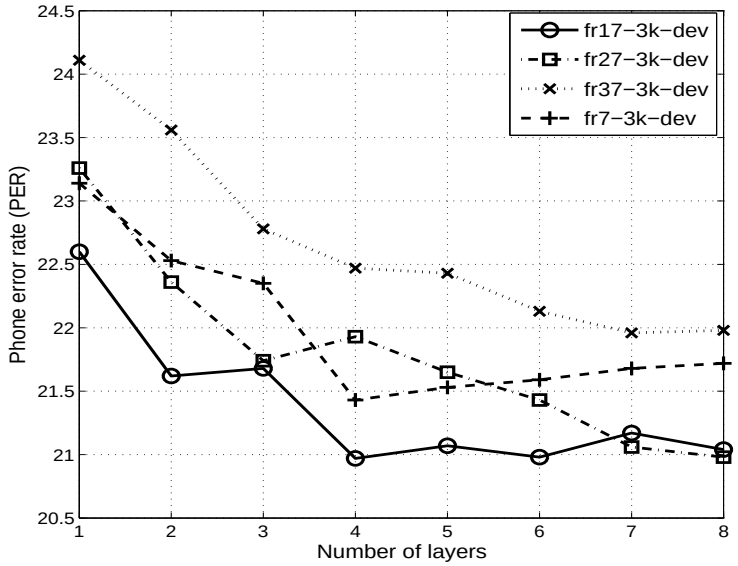

Figure 3.6: Phone error rate on the development set as a function of the number of layers, using 3072 hidden units per layer.

of 2048 units and an input window of 11 frames of MFCCs. The loss in performance from using a bottleneck layer before the soft max may be due to the low capacity of a layer of logistic units that can easily saturate. Recent results [81] show that a bottleneck works much better with linear units, i.e., matrix factorization.

Table 3.3 from [41] shows the performance of DNN systems, on various large vocabulary tasks, compared to a GMM baseline, once trained on the same amount of data and again on some cases on larger amount of data. The results found on large vocabulary tasks are in line with our findings on the TIMIT task that DNN systems outperform GMM systems. Even with way less data, DNNs are capable of providing a superior performance to GMMs.

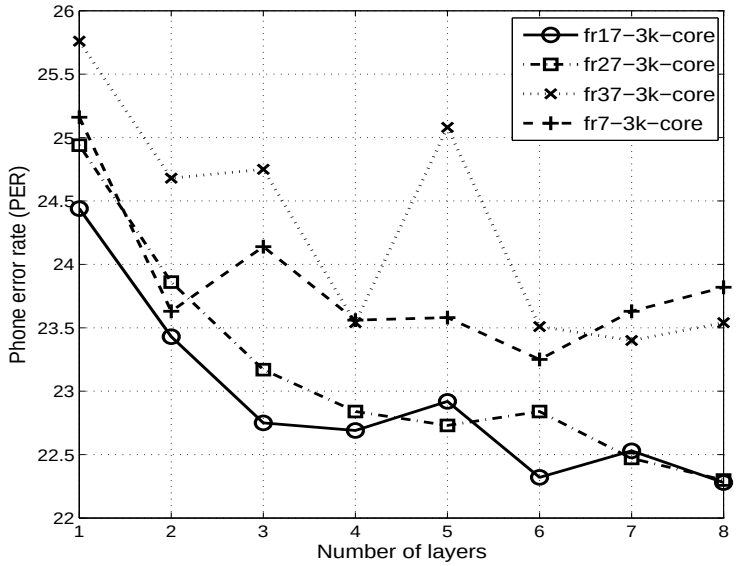

Figure 3.7: Phone error rate on the core test set as a function of the number of layers, using 3072 hidden units per layer.

3.3 Conclusion

In this chapter we introduced generatively trained deep neural networks for acoustic modeling. Experiments on phone recognition showed that generative training consistently adds to system accuracy but the major improvement came from using multiple hidden layers. In this chapter, the lowest phone recognition rates (PER), on the development set of the TIMIT benchmark, were achieved using a DNN with 8 hidden layers processing an input window of 11 MFCC frames, with each hidden layer containing 2048 hidden units. This best network achieved about 22.4% PER on the TIMIT core test set.

MFCCs were used as input features for the DNN acoustic model in all experiments presented in this chapter. However, MFCCs coevolved with a diagonal GMM acoustic model and this motivates us to reconsider MFCCs as features and search for the best features to be used with DNN acoustic models.

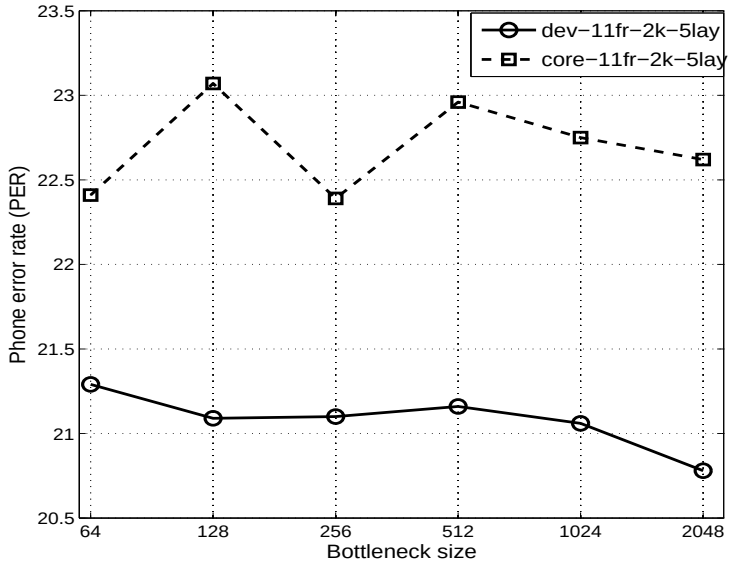

Figure 3.8: The effect of the size of the bottleneck on the phone error rate for a typical network with 11 input frames and 5 hidden layers of 2048 units per layer (except for the last hidden layer).

Table 3.3: *Comparison between DNN-HMM and GMM-HMM system on various large vocabulary tasks from [41].*

Task	Hours of training data	DNN-HMM	GMM-HMM with same data	GMM-HMM with more data
Switchboard (test set 1)	309	18.5%	27.4%	18.6% (2,000 h)
Switchboard (test set 2)	309	16.1%	23.6%	17.1% (2,000 h)
English Broadcast News	50	17.5 %	18.8%	
Bing Voice Search (Sentence error rates)	24	30.4%	36.2%	
Google Voice Input	5,870	12.3%		16.0% ($\gg$ 5,870 h)
Youtube	1,400	47.6%	52.3%	

Chapter 4

Which features to use in a DNN acoustic model

Speech data contain huge amounts of information, including aspects of the signal related to the words spoken, the speaker's emotional state, the dialect and identity of the speaker, the language used, the physical location of the speech event, and the recording channel. A key aim of the ASR feature extraction process is to ignore information in the input signal that is not relevant to the spoken content, emphasizing elements that contribute to detection of phonetic differences.

There have been various proposals for features which can represent the perceptually relevant aspects of the short-term speech spectrum, based on a variety of signal processing techniques, or based directly on the speech waveform [46]. A number of these proposals are motivated by the results of human speech recognition research [12, 38, 39]. By far, MFCCs are the most widely used input features for the state-of-the-art ASR systems.

One reason for the widespread use of MFCCs in ASR systems is that MFCCs have many characteristics that are well suited to the HMM-GMM systems (with diagonal covariance Gaussians) that have dominated the field. In this thesis, given that we are proposing DNNs as a replacement for GMMs, we also need to reconsider the choice of

MFCCs as features. MFCCs coevolved with GMMs, and there is no *a priori* reason to believe that MFCCs should be the best input representations for DNN acoustic models.

In the previous chapter, we used MFCCs as our input features to the DNN model, achieving a very competitive phone recognition performance. In this chapter, we will study the desired characteristics of input features for DNN acoustic modeling.

4.1 Mel Frequency Cepstral Coefficients (MFCCs)

Motivated by observations in human speech recognition, Mel Frequency Cepstral Coefficients (MFCCs) were developed more than three decades ago [12]. They demonstrated the best recognition accuracy relative to various other acoustic features. This is attributed to their good representation of the perceptually relevant aspects of the short-term speech spectrum. Here, we discuss briefly the main steps for producing MFCCs and the motivation behind each step.

The first step involves producing the short-term speech spectrum of an input speech window, typically between 25 to 30ms of speech. Peaks in the speech spectrum are referred to as "formants".

Human speech recognition research showed that the critical bandwidths for the human ear are non-uniformally spaced along the frequency axis. The mel scale, which is linear in low frequencies and logarithmic in high frequencies, was found to be a good candidate to represent this non-uniformity. The result is the use of more filters in low frequency regions and fewer filters in high frequency regions. The output of each filter corresponds to the total energy in frequencies that lie within the range of that filter.

Another design decision, also based on HSR research, is to take the logarithm of filter output values rather than just use the output values themselves. This is motivated by the fact that the human ear doesn't respond linearly to the amplitude of the input signal. The features derived up to this step are called "log mel-frequency spectral Coefficients"

or "MFSC".

MFSC features were found to be highly correlated, with only a few eigenvectors being sufficient to represent most of the information in the signal. This finding suggested an economical, compressed representation for the speech spectrum. The first few basis vectors of the discrete cosine transform (DCT) were found to be good, data-independent, approximations of the principal dimensions.

The resulting MFCC coefficients are therefore produced by taking the first few bases of the discrete cosine transform (DCT) of the real logarithm of the short-term energy spectrum expressed on a mel-frequency scale. So, starting from highly correlated outputs of greatly overlapping filters, the DCT concentrates energy in the first few coefficients and decorrelates them.

MFCCs possess two important characteristics that have made them an integral part of the state-of-the-art HMM-GMM systems:

- For each frame, MFCC features are decorrelated, which is preferred when diagonal covariance GMMs are used for modeling. Diagonal covariance GMMs use far fewer parameters than full covariance ones, which makes them robust for estimation as well as faster for decoding since there is no matrix inversion required to compute the Gaussian likelihoods. Diagonal covariance GMMs could be used to model correlated features, but many more Gaussian components would be needed.

- MFCC features are more compact than MFSC features because they are projections on the first few DCT basis vectors only.

As we can see, the whole process was motivated by human speech recognition findings, but then the very last step, i.e., the DCT transform, was mainly motivated by the model used, i.e., diagonal covariance GMMs, and by computational efficiency reasons. For DNN acoustic models, the covariance structure of the data is modelled implicitly, without any explicit assumptions about the data distribution, so there is no advantage in

favoring MFCCs just because they are decorrelated. Also, the computational resources available now are well beyond what was available in the past; we can easily afford higher-dimensional features, provided they offer higher recognition accuracy.

The following section takes this line of thinking further, comparing MFSC and MFCC features and the performance of DNN models using each of them.

4.2 MFCCs vs. MFSC

In this section, we want to test which feature type (MFCC or MFSC) is better suited to DNN acoustic models. Figures [4.1] and [4.2] show MFSC and MFCC features for the same utterance from the TIMIT database. It is clear that MFSC features exhibit more temporal and spectral smoothness than MFCC features. This suggests that MFSCs should be easier to model generatively than MFCCs.

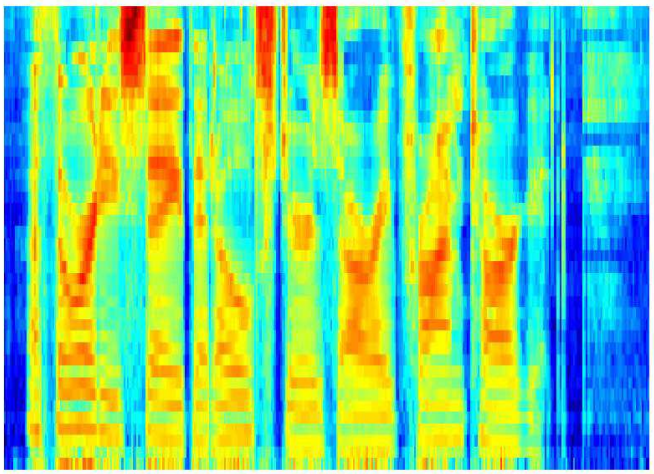

Figure 4.1: 40-dimensional MFSC features for one of the TIMIT utterances.

We compared the PER of the best performing DNNs trained with MFCCs (using 17 frames as input and 3072 hidden units per layer) and the best performing DNNs trained

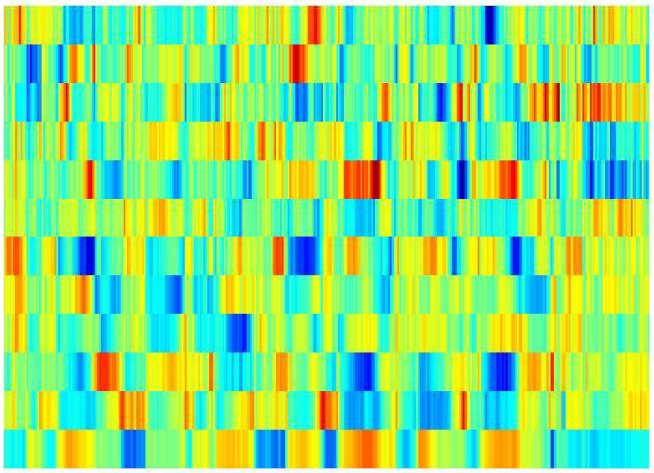

Figure 4.2: 13-dimensional MFCC features for one of the TIMIT utterances.

with MFSC features (using 15 frames as input and 2048 hidden units per layer); the result is shown in figure 4.3. All networks were first generativly pre-trained and then fine-tuned using the exact same recipe described in the previous chapter. The number of hidden units per layer and the number of input frames were tuned to achieve the best PER on the development set for each input feature type.

The performance of MFSC features is about 1.7% better than MFCCs. A two-tailed Matched Pairs Sentence-Segment Word Error (MAPSSWE) significance test [28] was conducted using the NIST sc_stats tool with the null hypothesis that there is no performance difference between the DNN models trained with MFCC features and MFSC features. The test finds a significant difference at the level of p=0.001.

One interesting observation is that DNN models trained using MFCC features and MFSC features, achieved by utilizing early stopping, were used to decode the training data. The MFCC model achieved a training PER of 5.8% while the MFSC model achieved 4.5%. There are two potential explanations for this accuracy gain: First, MFSC features

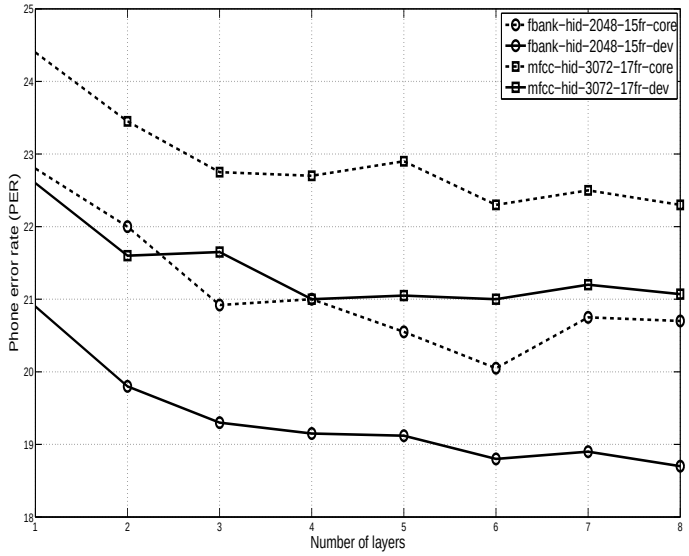

Figure 4.3: PER as a function of the number of layers.

are smoother and better correlated than MFCCs which allows DNNs to model them better which is supported by the training PER achieved by both models. The second possibility is the higher dimensionality of MFSC features compared to MFCCs. The next section will investigate these two possible explanations.

4.3 Understanding why MFSC features are better than MFCCs

4.3.1 Visualizing features using t-SNE

To understand the performance gap between MFSC features and MFCCs, it is useful to visualize the input vectors (i.e. a complete window of say n frames) as well as the learned hidden activity vectors in each layer for the two systems. DNNs with 8 hidden layers plus a softmax output layer were used for both systems).

A recently introduced visualization method called "t-SNE" [53] was used to produce

2-D embeddings of the input vectors and the hidden activity vectors. t-SNE produces 2-D embeddings in which points that are close in the high-dimensional vector space are also close in the 2-D space. It starts by converting the pairwise distances, d_{ij} in the high-dimensional space to joint probabilities $p_{ij} \propto exp(-d_{ij}^2)$. It then performs an iterative search for corresponding points in the 2-D space which give rise to a similar set of joint probabilities. To cope with the fact that there is much more volume near to a high dimensional point than a low dimensional one, t-SNE computes the joint probability in the 2-D space by using a heavy tailed probability distribution $q_{ij} \propto (1 + d_{ij}^2)^{-1}$. This leads to 2-D maps that exhibit structure at many scales [53].

For visualization only, we used SA utterances from the TIMIT core test set speakers. These utterances were not used for training or testing. These are the two utterances that were spoken by all 24 different speakers. Figures 4.4 and 4.14 show visualizations of MFSC and MFCC features for 6 speakers. Crosses are used for one utterance and circles for the other one, while different colors indicate different speakers. We removed data points from the other 18 speakers to make the map less cluttered.

Since they represent decorrelated low-dimensional feature vectors, MFCC vectors tend to be scattered across the space; by contrast, the MFSC feature vectors have stronger similarities and are often aligned across different speakers for some voiceless sounds (e.g. /s/, /sh/). This observation supports the hypothesis that MFSC features are smoother and hence easier to model generatively because the data has stronger local structure than MFCC vectors.

Figures (4.4) to (4.13) show the evolution of features from the input data to the softmax output for an 8 layer DNN using MFSC inputs. Figures (4.14) to (4.23) show the evolution for MFCC inputs for pre-trained then fine-tuned networks. For pre-trained only networks, figures (4.24) to (4.31) show their features for MFSC inputs while figures (4.32) to (4.39) show them for MFCC inputs.

In the second layer of the pretrained DNN using MFSC inputs, clusters for many

phones start to emerge like /y/,/k/,/d/,/t/,/dh/,/w/,/r/,/n/,/g/ and /oy/. Although they are not sharp, they have clearly become more speaker independent. In the higher layers of the pre-trained only DNN, observations of the formed clusters become more aligned and vowels that are closer in characteristics start to group together but with high variance. Adding frame labels and fine-tuning the DNN forces the features, as they are transformed by the network, to become more invariant to speaker differences, focusing on the content.

In the case of MFCC, the input observations are scattered, making the task of pre-training very hard. By the second layer of the pre-trained DNN, clusters for phones like /w/,/s/ and /sh/ start to appear. In the higher layers, mixed clusters for similar vowels start to form. Fine-tuning the features helps sharpen phone clusters, but they are still not as sharp and discriminating as they were for the MFSCs.

When MFSC features are used, DNNs can be thought of implicitly normalizing feature vectors across different speakers. MFSC features contain both the spoken content and the style of the utterance which allows the DNN (because of its distributed representations) to partially separate content and style aspects of the input during the pre-training phase. This makes it easier for the discriminative fine-tuning phase to enhance the propagation of content aspects to higher layers. MFCCs focus only on the smooth spectrum that is related to the spoken content while removing higher-order coefficients that contain some speaker-related information. Higher in the network, hidden activity vectors from different speakers for the same segment align for both types of feature representation, but the alignment is much clearer in the case of MFSC.

Based on our investigation of feature visualizations, it is clear that the smoothness of MFSC features and that fact that they contain both content and speaker aspects help DNNs learn better representations, boosting the overall phone accuracy.

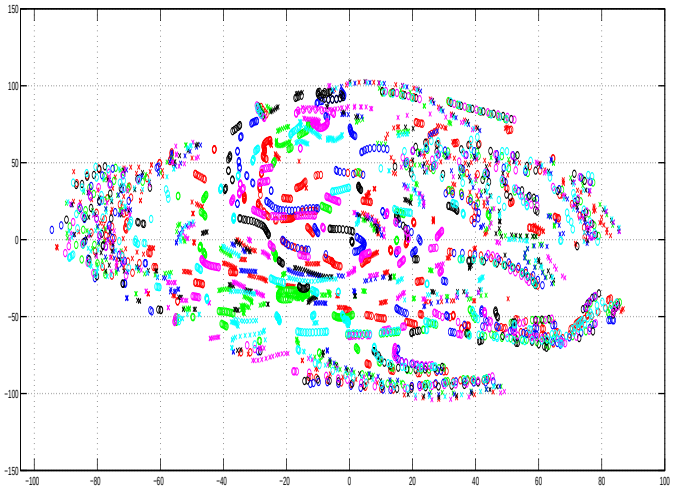

Figure 4.4: t-SNE 2-D map of MFSC inputs.

4.3.2 The effect of feature vector dimensionality

If, as we have established, MFSC feature smoothness helps with generative pre-training of DNNs as compared to MFCCs, we should remove this effect to investigate feature dimensionality only. Therefore, the following experiments perform the discriminative fine-tuning phase only using random initial network weights. To fix the number of trainable parameters, the window size for all experiments is set to 11, with hidden unit sizes of 1024 for all feature types.

All previous experiments used MFCCs with 12 coefficients and energy along with their temporal first and second derivatives while MFSC features used 40 coefficients and energy along with their temporal first and second derivatives.

To refute the hypothesis that MFSC features yield lower PER because of their higher dimensionality, we consider DCT features, which are the same as MFSC features except that they are transformed using the discrete cosine transform, which encourages decorrelated elements. The DCT features are ordered from lower-order (slow-moving) features

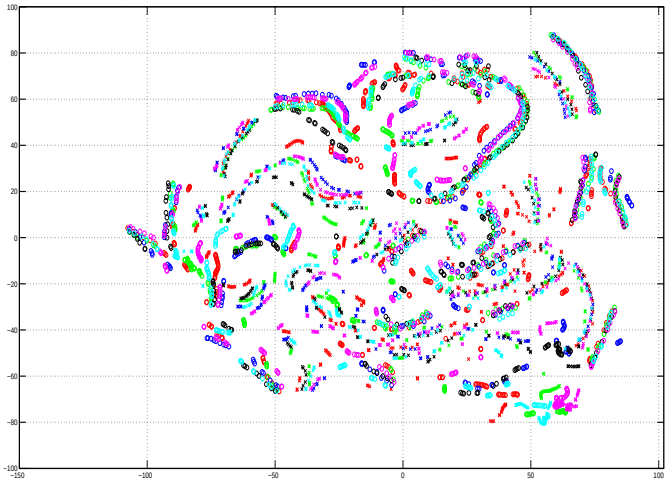

Figure 4.5: t-SNE 2-D map of the 1st layer of the fine-tuned network features using MFSC inputs.

to higher-order ones. The lower-order coefficients of the DCT features are simply the MFCC features.

Tables 4.1 and 4.2 show the PER for MFSC, DCT, and MFCC inputs for networks with different numbers of layers on the development and core test sets. Features are used twice, once with mean and variance normalization, once without.

MFSC features are clearly better than both MFCCs and DCT features, which indicates that dimensionality is not the key factor which explains the superior performance of MFSC features. The gap between MFSC features and MFCCs widens with the generative pre-training as demonstrated in the previous section. One interesting observation is that the normalized MFCCs are better than the normalized DCT features. This can be attributed to the noisy nature of the higher-order coefficients of the DCT features, which are magnified by variance normalization.

These results suggest that a linear transformation of the data space can disrupt learn-

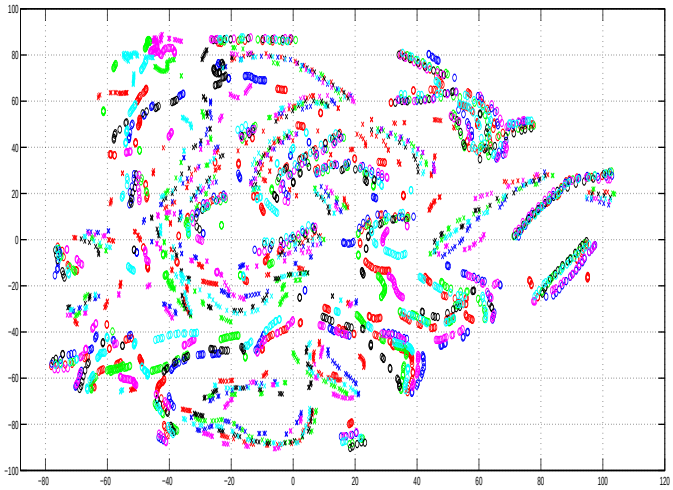

Figure 4.6: t-SNE 2-D map of the 2nd layer of the fine-tuned network features using MFSC inputs.

ing, although in theory, neural networks should recover from this transformation by undoing it. One reason this does not happen is that we have neither an oracle objective function nor a perfect optimization procedure. The following section shows another kind of linear transformation in the data space that helps improve DNN performance.

4.4 Effect of using temporal derivatives

Using first and second temporal derivatives was found to be consistently useful for GMM-based acoustic models when MFCCs are used. In this section, we examine the effect of this linear transformation on MFSC features as compared to MFCCs.

As in the last section, the following experiments perform the fine-tuning phase only on the random initial weights. The window size used for all experiments is fixed to 11, with hidden unit sizes of 1024 for all feature types. All features used are mean and variance normalized.

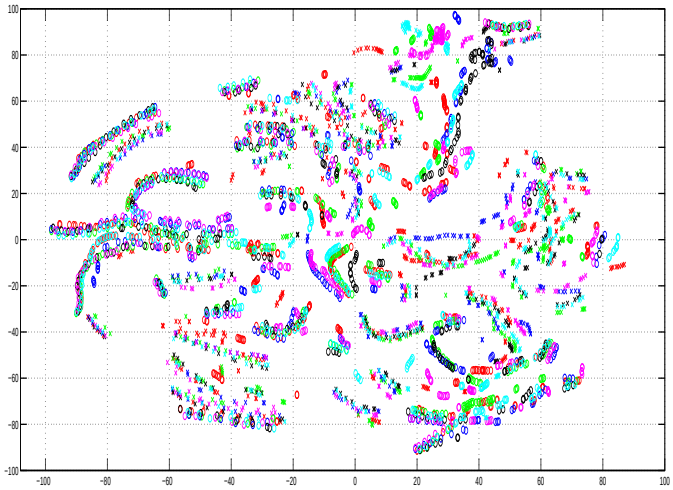

Figure 4.7: t-SNE 2-D map of the 3rd layer of the fine-tuned network features using MFSC inputs.

Tables (4.3) and (4.4) show the impact of temporal derivatives on different feature types for the development and core test sets.

It is clear that temporal derivatives are important for both MFCCs and MFSC feature types. These experiments also demonstrate that the average relative accuracy improvement for MFSC features when temporal derivatives are used is less that that of the MFCCs. This might be due to the smoothness of MFSC features; it is easier to extract linear relations between frames using MFSC features than with MFCCs, although it is still important for both.

One final thing to note is that, although the temporal derivative information is important and it can be derived linearly from the data available, DNNs were not capable of discovering it because neither the optimization procedure nor the objective function are perfect.

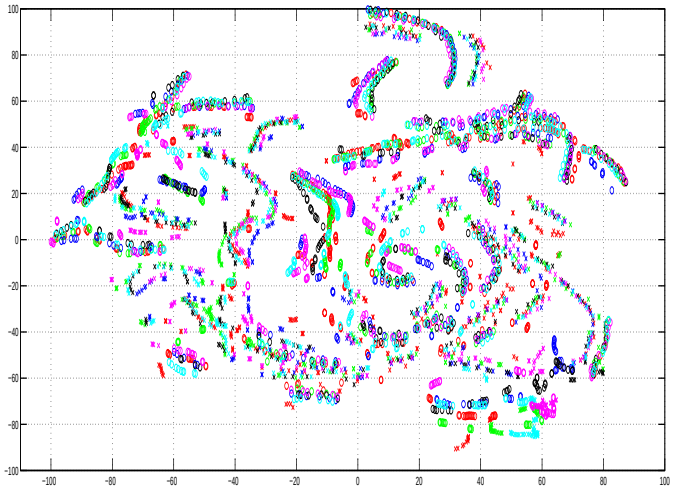

Figure 4.8: t-SNE 2-D map of the 4th layer of the fine-tuned network features using MFSC inputs.

4.5 Conclusions

In this chapter we reconsidered the selection of features for the DNN acoustic model, finding that mean-and-variance-normalized log mel-frequency spectral coefficients (MFSC features) with first and second temporal derivatives provide the best performance. The smoothness of MFSC features helps the generative pre-training procedure learn better features, widening the performance gap between MFCCs and MFSC features. In this chapter, the lowest phone recognition rates (PER), on the development set of the TIMIT benchmark, were achieved using a DNN with 8 hidden layers processing an input window of 15 MFSC frames, with each hidden layer containing 2048 hidden units. This best network achieved about 20.7% PER on the TIMIT core test set. The next chapter investigates using different types of linear transformations for the input data, with the aim of removing differences between different speakers in the training database. Channel and speaker variations are major sources of high error rates in ASR systems. Different

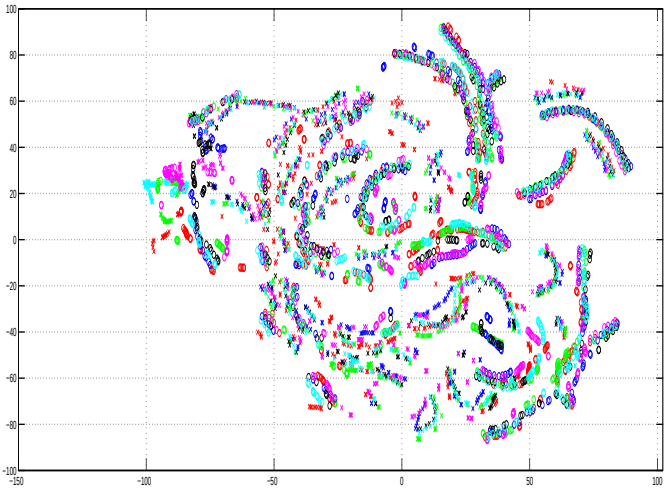

Figure 4.9: t-SNE 2-D map of the 5th layer of the fine-tuned network features using MFSC inputs.

schemes for speaker adaptation are examined; some of them were developed for GMM acoustic models while others are native to DNN acoustic models.

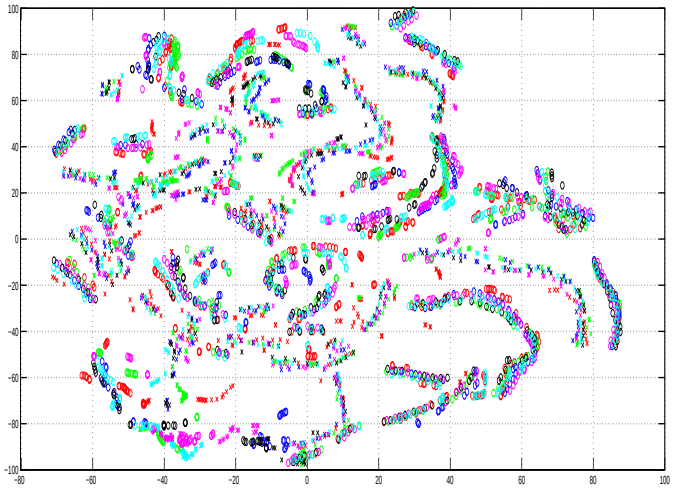

Figure 4.10: t-SNE 2-D map of the 6th layer of the fine-tuned network features using MFSC inputs.

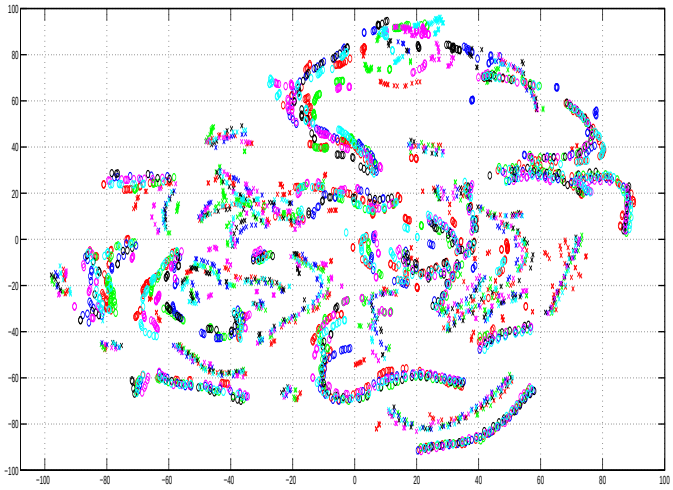

Figure 4.11: t-SNE 2-D map of the 7th layer of the fine-tuned network features using MFSC inputs.

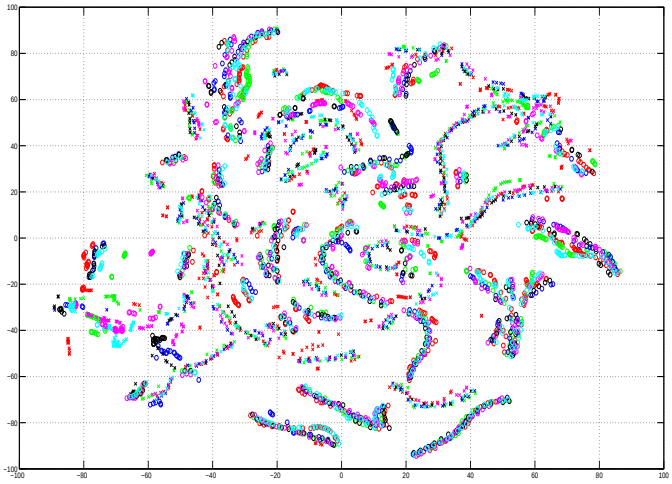

Figure 4.12: t-SNE 2-D map of the 8th layer of the fine-tuned network features using MFSC inputs.

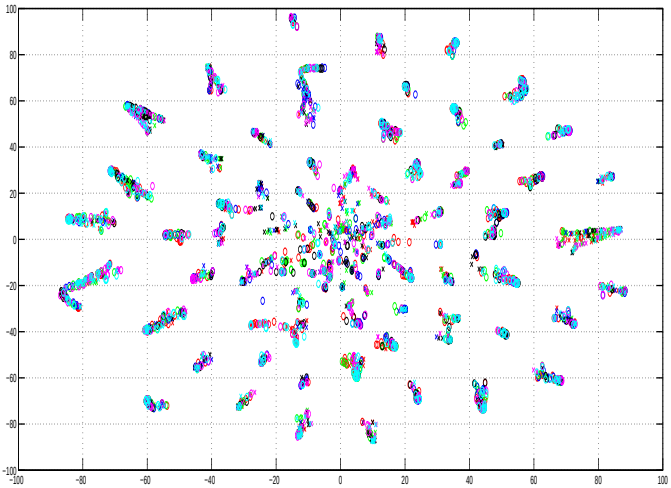

Figure 4.13: t-SNE 2-D map of the softmax output of the fine-tuned network features using MFSC inputs.

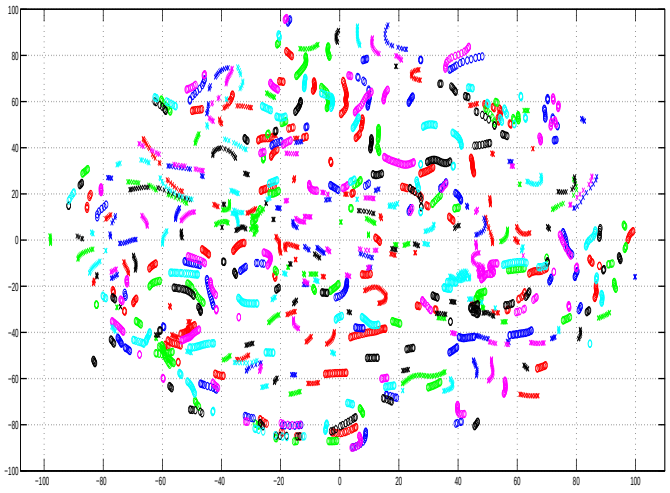

Figure 4.14: t-SNE 2-D map of MFCC inputs.

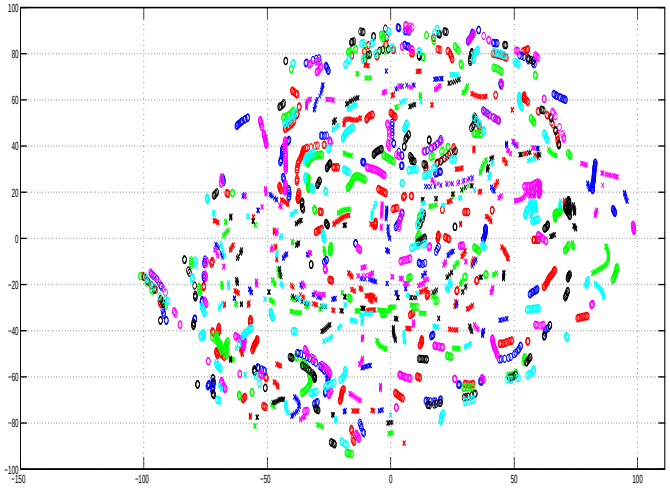

Figure 4.15: t-SNE 2-D map of the 1st layer of the fine-tuned network features using MFCC inputs.

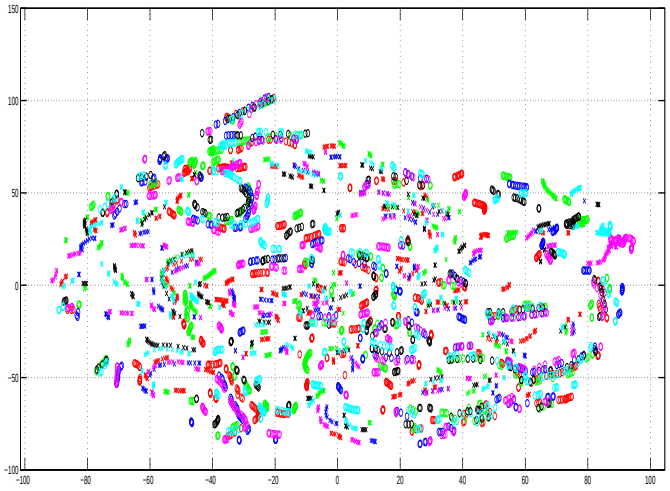

Figure 4.16: t-SNE 2-D map of the 2nd layer of the fine-tuned network features using MFCC inputs.

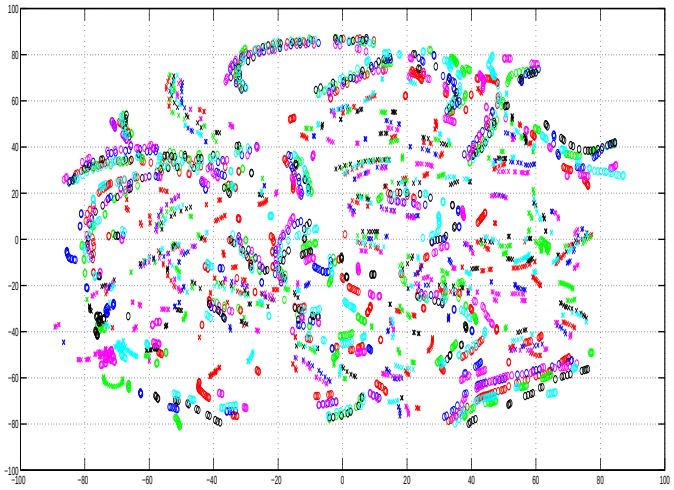

Figure 4.17: t-SNE 2-D map of the 3rd layer of the fine-tuned network features using MFCC inputs.

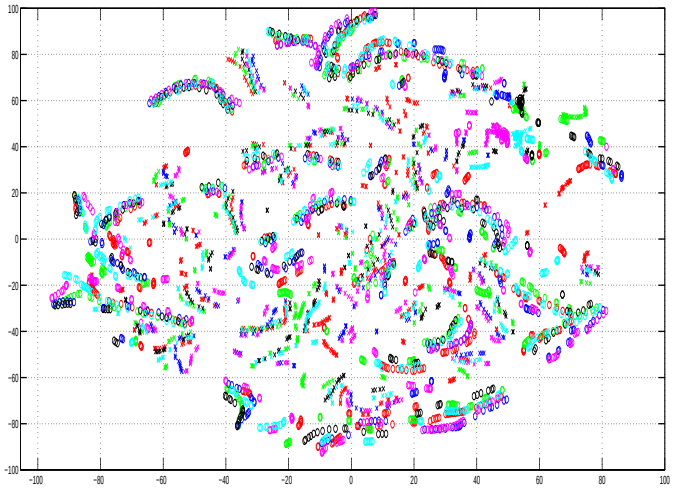

Figure 4.18: t-SNE 2-D map of the 4th layer of the fine-tuned network features using MFCC inputs.

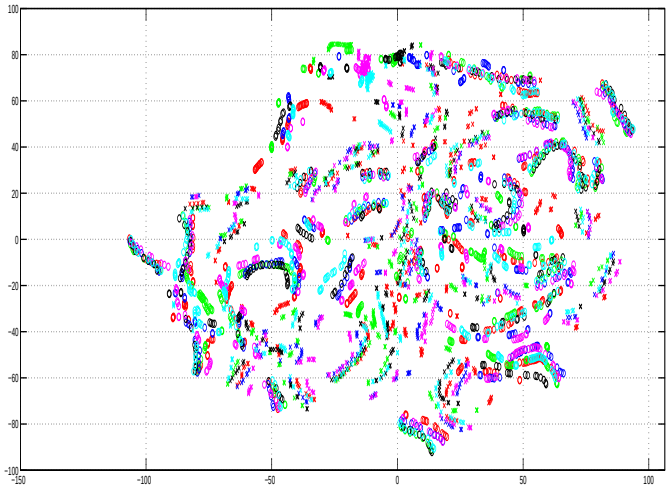

Figure 4.19: t-SNE 2-D map of the 5th layer of the fine-tuned network features using MFCC inputs.

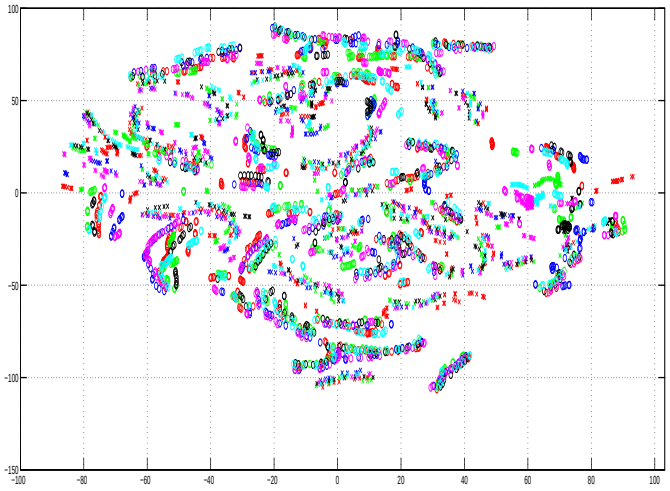

Figure 4.20: t-SNE 2-D map of the 6th layer of the fine-tuned network features using MFCC inputs.

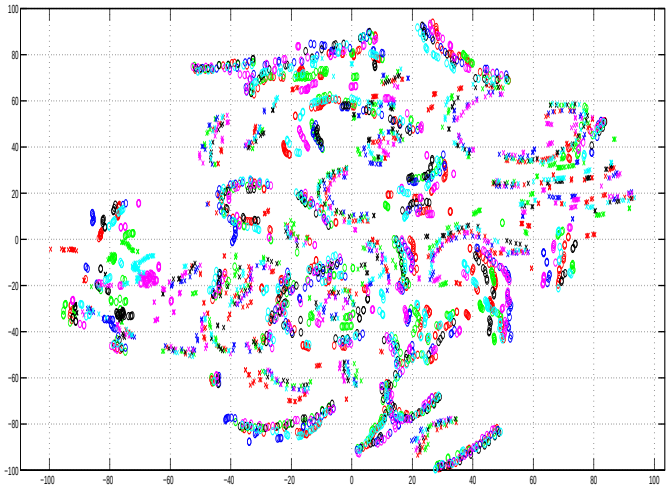

Figure 4.21: t-SNE 2-D map of the 7th layer of the fine-tuned network features using MFCC inputs.

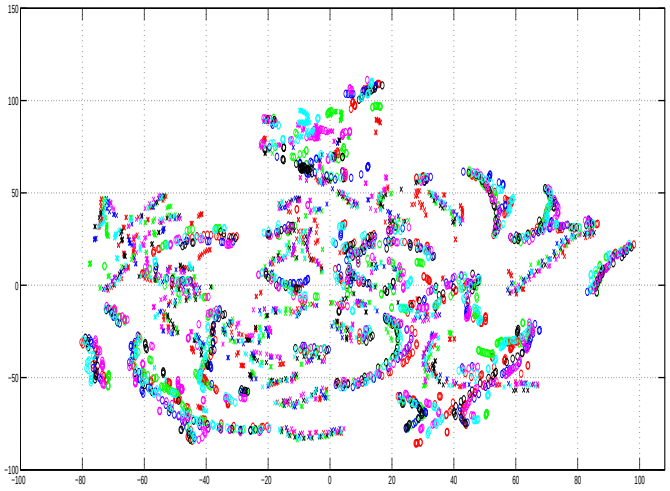

Figure 4.22: t-SNE 2-D map of the 8th layer of the fine-tuned network features using MFCC inputs.

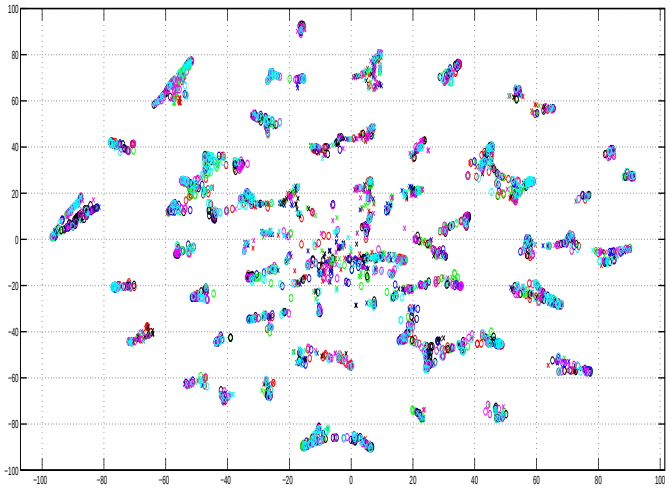

Figure 4.23: t-SNE 2-D map of the softmax output of the fine-tuned network features using MFCC inputs.

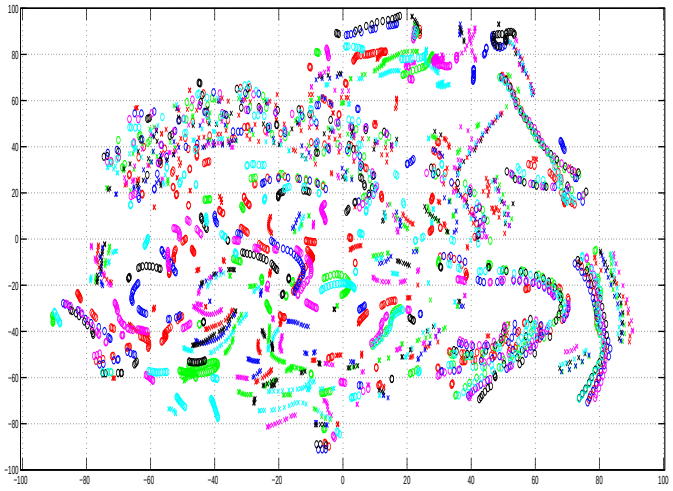

Figure 4.24: t-SNE 2-D map of the 1st layer of the pretrained network features using MFSC inputs.

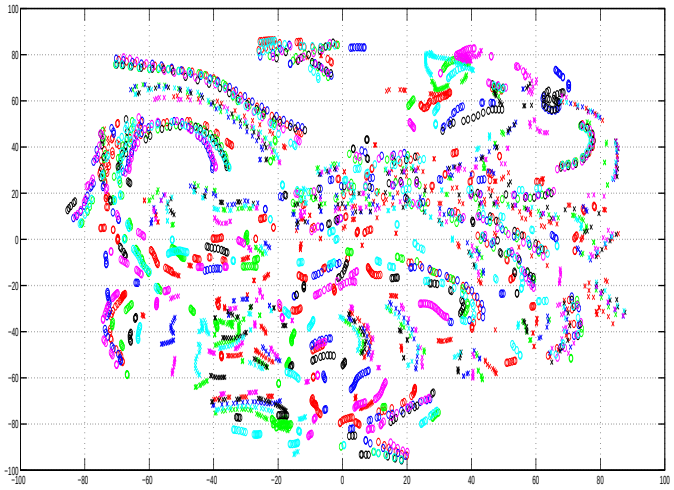

Figure 4.25: t-SNE 2-D map of the 2nd layer of the pretrained network features using MFSC inputs.

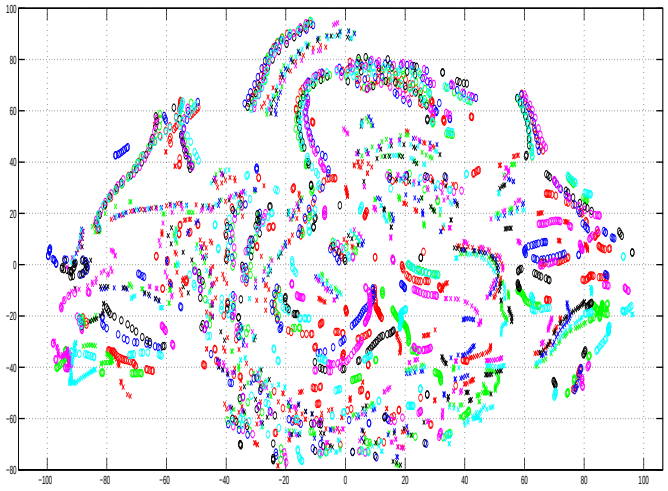

Figure 4.26: t-SNE 2-D map of the 3rd layer of the pretrained network features using MFSC inputs.

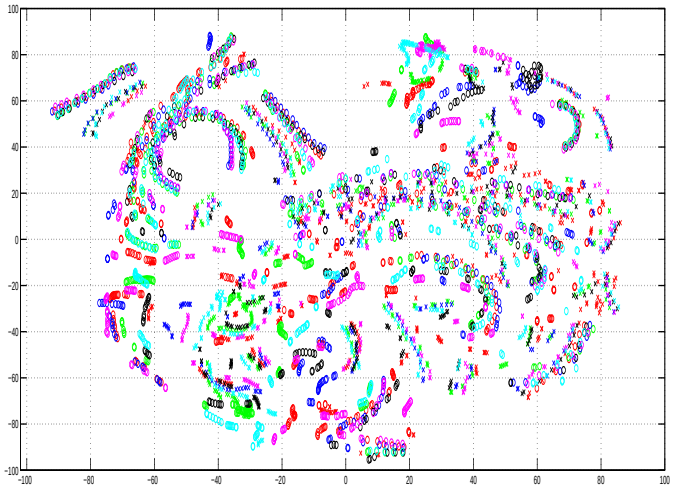

Figure 4.27: t-SNE 2-D map of the 4th layer of the pretrained network features using MFSC inputs.

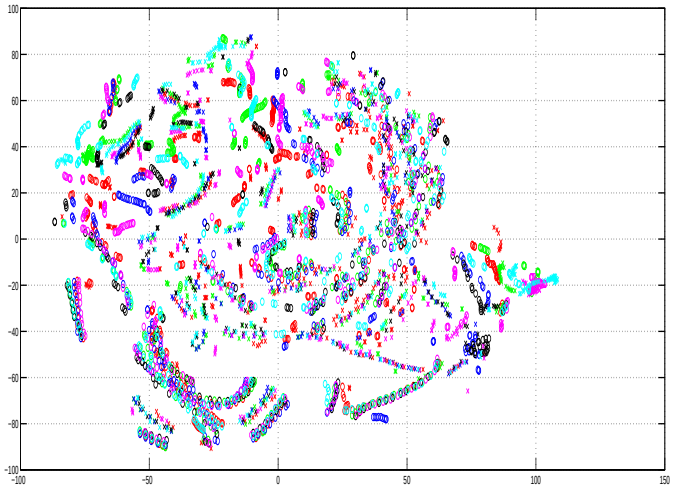

Figure 4.28: t-SNE 2-D map of the 5th layer of the pretrained network features using MFSC inputs.

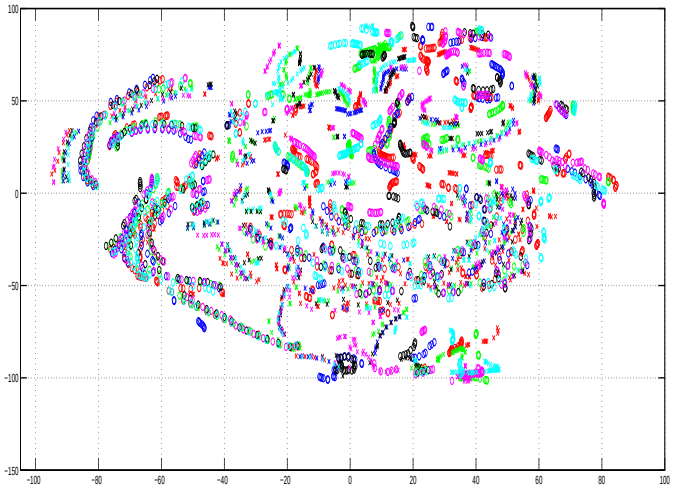

Figure 4.29: t-SNE 2-D map of the 6th layer of the pretrained network features using MFSC inputs.

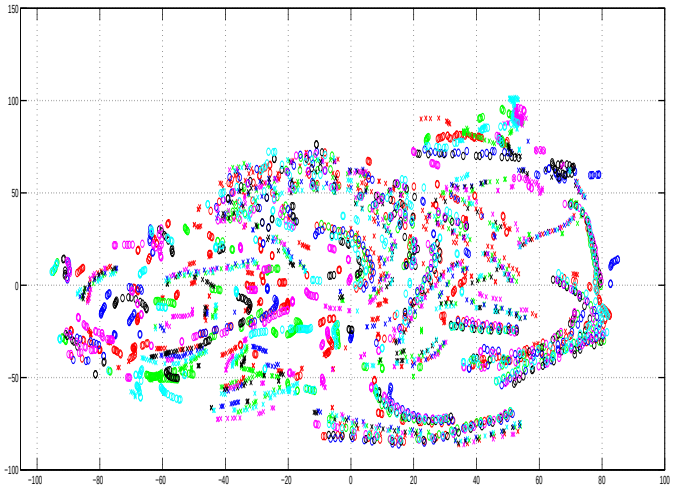

Figure 4.30: t-SNE 2-D map of the 7th layer of the pretrained network features using MFSC inputs.

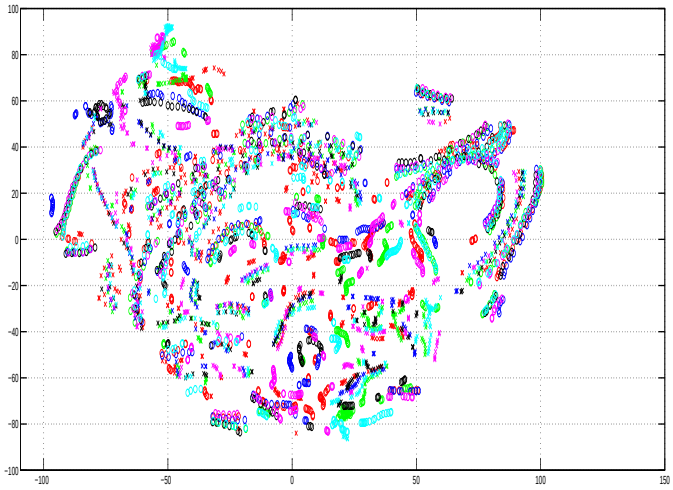

Figure 4.31: t-SNE 2-D map of the 8th layer of the pretrained network features using MFSC inputs.

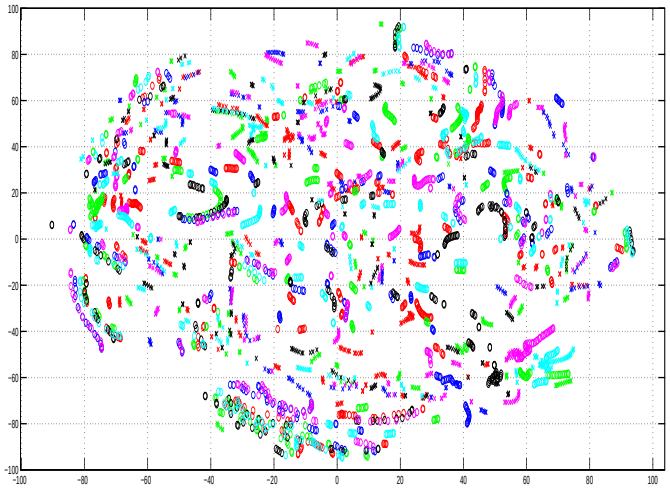

Figure 4.32: t-SNE 2-D map of the 1st layer of the pretrained network features using MFCC inputs.

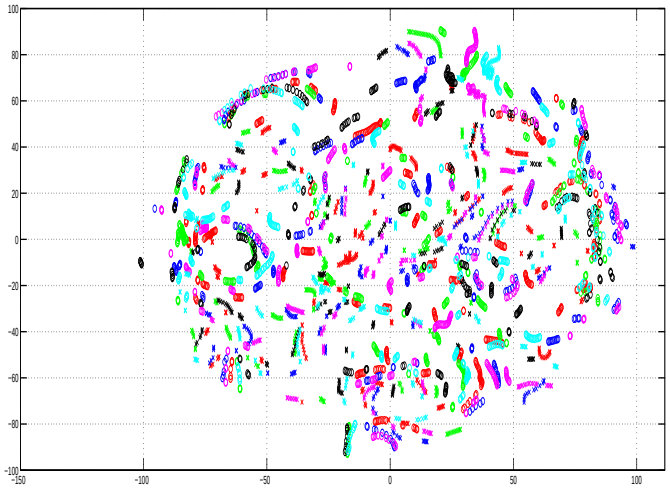

Figure 4.33: t-SNE 2-D map of the 2nd layer of the pretrained network features using MFCC inputs.

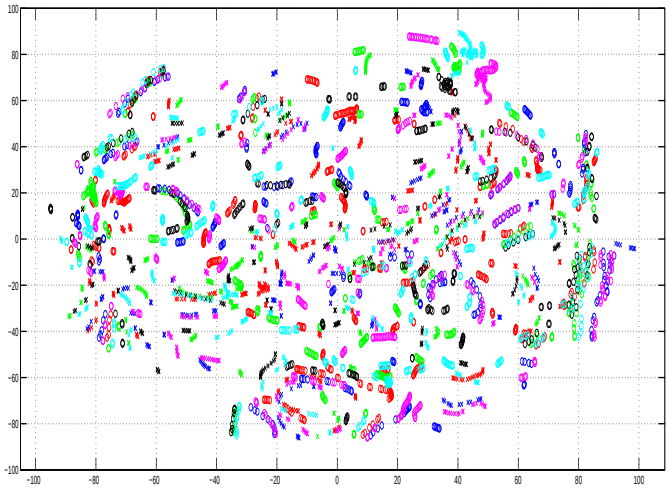

Figure 4.34: t-SNE 2-D map of the 3rd layer of the pretrained network features using MFCC inputs.

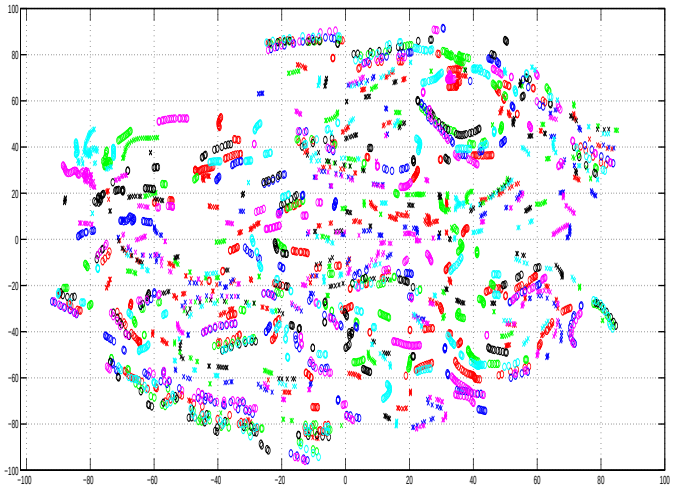

Figure 4.35: t-SNE 2-D map of the 4th layer of the pretrained network features using MFCC inputs.

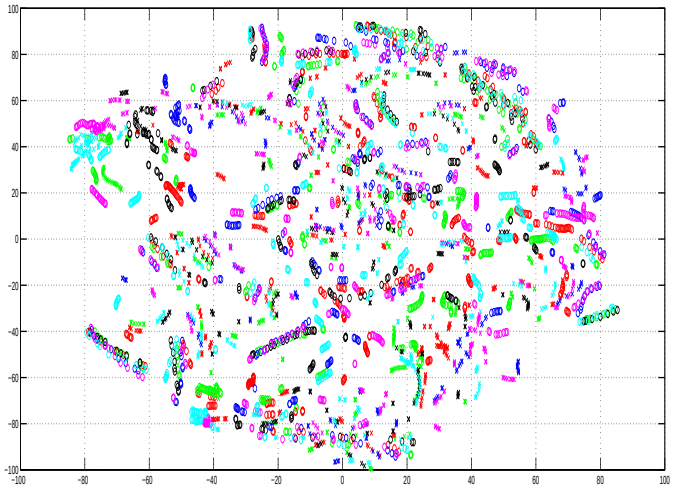

Figure 4.36: t-SNE 2-D map of the 5th layer of the pretrained network features using MFCC inputs.

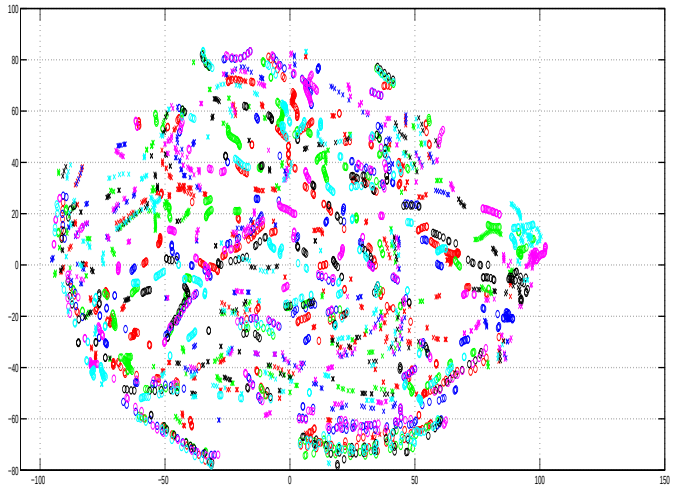

Figure 4.37: t-SNE 2-D map of the 6th layer of the pretrained network features using MFCC inputs.

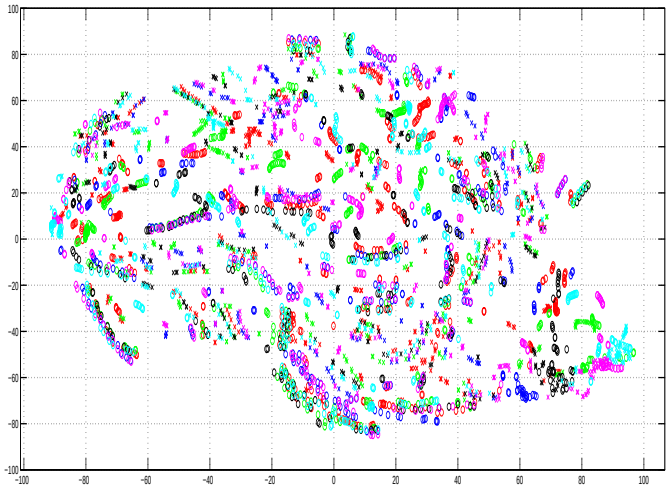

Figure 4.38: t-SNE 2-D map of the 7th layer of the pretrained network features using MFCC inputs.

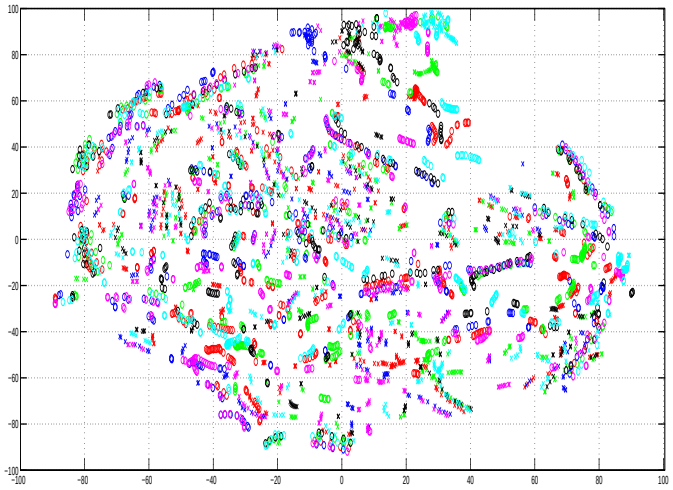

Figure 4.39: t-SNE 2-D map of the 8th layer of the pretrained network features using MFCC inputs.

Table 4.1: *The PER deep nets using various features on the development set*

Feature	Dim	1lay	2lay	3lay	4lay
MFSC	123	23.33%	21.45%	21.06%	21.5%
MFSC+norm	123	22.25%	21.3%	21.31%	21.46%
DCT	123	25.55%	23.67%	23.62%	23.23%
DCT+norm	123	24.48%	22.9%	22.58%	23.31%
MFCC	39	25.95%	24.06%	23.99%	23.98%
MFCC+norm	39	23.2%	21.87%	22.02%	21.99%

Table 4.2: *The PER deep nets using various features on the core test set*

Feature	Dim	1lay	2lay	3lay	4lay
MFSC	123	24.9%	23.58%	22.62%	23.06%
MFSC+norm	123	23.86%	22.58%	22.88%	22.83%
DCT	123	27.22%	25.42%	25.75%	25.58%
DCT+norm	123	26.13%	24.04%	24.49%	25.27%
MFCC	39	27.15%	26.09%	26.2%	25.56%
MFCC+norm	39	24.72%	23.67%	23.62%	23.66%

Table 4.3: *Effect of temporal derivatives on the PER of the development set*

Feature	Dim	1lay	2lay	3lay	4lay
MFSC	41	23.14%	22.31%	22.25%	22.08%
MFSC+D	82	22.53%	21.56%	20.96%	21.46%
MFSC+D+DD	123	22.25%	21.3%	21.31%	21.46%
MFCC	13	24.19%	23%	23.11%	23.16%
MFCC+D	26	23.32%	22.12%	22.17%	22.4%
MFCC+D+DD	39	23.2%	21.87%	22.02%	21.99%

Table 4.4: *Effect of temporal derivatives on the PER of the core test set*

Feature	Dim	1lay	2lay	3lay	4lay
MFSC	41	24.52%	24.07%	23.88%	23.76%
MFSC+D	82	23.84%	23.02%	22.64%	23.24%
MFSC+D+DD	123	23.86%	22.58%	22.88%	22.83%
MFCC	13	25.68%	25.19%	24.89%	25.6%
MFCC+D	26	24.61%	24.03%	23.88%	24.74%
MFCC+D+DD	39	24.72%	23.67%	23.62%	23.66%

Chapter 5

Speaker adaptive training in DNN acoustic models

Humans have an amazing ability to recognize and adapt to a large range of speech, speaker, channel, and environmental conditions which current ASR systems fail dramatically to do. Accurate ASR output for such diverse conditions has been selected as one of the "Grand Challenges" facing ASR research by a team of ASR leading researchers [7].

Many "adaptation" techniques have been developed to deal with background and speaker variability [2, 21, 26]. One way to think about adaptation, that was found successful, is to transform the trained model (the training distribution) to comply with the testing conditions (the testing distribution) so that the likelihood of the test data is maximized under the new model. This type of adaptation is performed during the testing phase.

A different kind of adaptation is to eliminate differences in the training data that do not contribute towards better system accuracy, e.g., normalizing inter-speaker variability in the training data while keeping intra-speaker variability by mapping all training speakers to a similar canonical speaker. Here we focus on this second type of adaptation, which takes place during model training. It focuses only on speaker adaptation but the

work presented is applicable to background and channel adaptation as well.

The DNN acoustic model proposed in previous chapters does not include any special procedure to take care of speaker variability during training and testing. In this chapter, we first examine the benefit of speaker-adapted features to DNN acoustic models. Then two different adaptation techniques that have been developed for DNN acoustic models are presented.

5.1 Speaker adapted features for DNN

Speaker adaptation techniques [21,26] consistently help reduce word error rates in GMM acoustic models where the GMM model and/or the input features are adapted. This section investigates using different types of speaker-adapted features as inputs for DNN acoustic models.

Most of these feature transformations implicitly assume a diagonal covariance GMM acoustic model. They are also optimized to work best on top of Linear-Discriminant Analyzed (LDA) MFCC features. The following is a description of all feature transformations used.

5.1.1 LDA Features

Following the setup in [83], to create a set of Linear Discriminant Analysis (LDA) features, a speech utterance is first chunked into 20ms frames, with a frame-shift of 5 ms, a different frame rate than that used in the previous chapters. Each frame is represented by a 13-dimensional MFCC feature vector. Features are then mean-and-variance-normalized on a per-utterance basis. Then, at each frame, a context of 8 frames to the left and right of the current frame are joined together and an LDA transform is applied to project the feature vector down to 40 dimensions in order to improve discrimination between the context-dependent target states.

5.1.2 Speaker Adapted Features

Two steps are performed to create a set of speaker-adapted (SA) features. First, vocal tract length normalization (VTLN) is applied to the LDA features, followed by a feature/model space adaptation. Both steps are discussed below in more detail.

Vocal Tract Length Normalization

The length of a speaker's vocal tract is often a major factor in speaker variability. VTLN [5, 17, 61] is a popular technique used to reduce this variability. In this procedure, a scaling factor is learned for each speaker that warps the speech from this speaker into a canonical speaker with an average vocal tract length. The warp is applied to the given set of acoustic features before they are LDA-transformed. After the warp, the features are again spliced together at each frame and an LDA transform is applied to produce a set of 40-dimensional "warped" feature vectors.

Feature/Model Space Adaptation

After VTLN, the "warped" features are adapted for each speaker using feature-space Maximum Likelihood Linear Regression (fMLLR) [21]. In this method, a linear-regression-based transformation is applied to the VTLN features for each speaker to create a set of features in a canonical feature space.

5.1.3 Discriminative Feature

Discriminatively trained features and models have been shown to significantly improve error rates, as these discriminative models have more power to differentiate between confusable sounds, such as "ma" and "na". We use a large margin discriminative training approach using the Boosted Maximum Mutual Information (BMMI) criterion [76]. In this approach, a set of ML-trained models is used to bootstrap the training of a set of

feature-space Boosted Maximum Mutual Information (fBMMI) features. fBMMI features are created on top of the SA features.

5.1.4 Experiments

The following experiments use a contextual window of 11 frames of input features to a train multi-layer DNN with each layer containing 1024 hidden units. All networks are first pre-trained then fine-tuned.

Figure 5.1 shows the effect of using different input features and numbers of hidden layers. The main trend visible in the figure is that adding more hidden layers gives better performance, though the gain diminishes as the number of layers increases. There is no significant difference in performance between the MFCC features and LDA, as the network is capable of capturing local discriminative information present in the context window. A jump of about 2% in accuracy is observed when speaker information is utilized to transform all speakers to a canonical speaker using the SA features. Performing fBMMI complements the DNN local discrimination within the input context window by maximizing the margin between competing phone classes using an objective function that spans the whole utterance. Table 5.1 shows the best achieved PER for each type of input feature on the core test set. By analyzing errors that different systems produce, it is apparent that the vowels have benefited the most from speaker-adapted features (vowel gains are about 1.5% to 1.8% absolute). This is expected because most speaker variance is expressed in vowels.

The best speaker-adapted feature performance in table 5.1 is very similar to the best PER achieved using normalized MFSC features. t-SNE plots from the previous chapter showed that DNNs normalize speaker variation in vowel classes in their deeper layers which coincides with the trend observed with speaker-adapted features.

The following two sections introduce two different techniques for normalizing speaker variation in DNN acoustic models while using MFSC features as the input. Both tech-

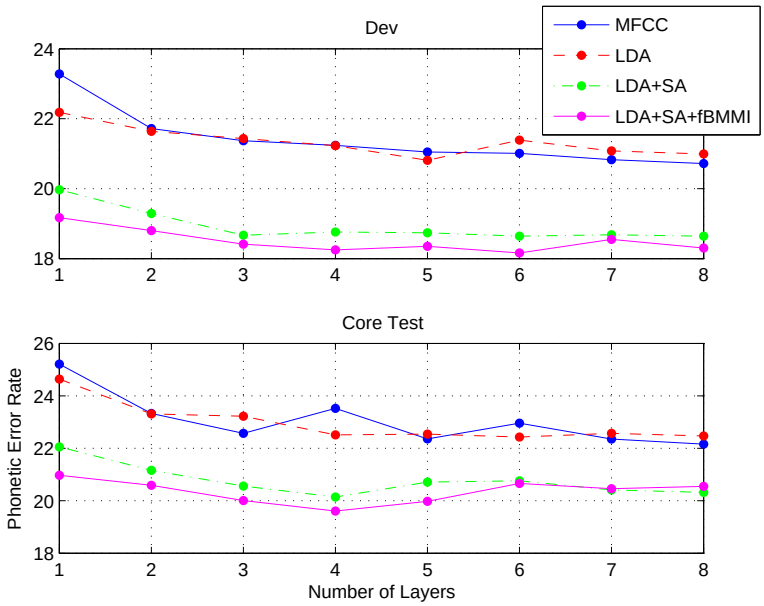

Figure 5.1: Effect of Increasing DNN Hidden Layers with Diff. Features

Feature Type	PER
MFCC	22.1
LDA	22.2
LDA+SA	20.3
LDA+SA+fBMMI	**19.6**

Table 5.1: PER of TIMIT Core Test Set

niques aim at helping the DNN extract speaker-invariant, representations either by allowing the network to use style features during training and then marginalizing them out during testing, or by explicitly conditioning on features that describe the current speaker to help the network focus on the spoken content.

5.2 The gated softmax classifier

The Gated Softmax model (GSM) [66] extends the logistic regression model, which is based on a log-linear relationship between inputs and labels, to a log-bilinear model with a set of probabilistic hidden variables that cooperate to model the decision surface jointly.

To obtain classification decisions at test time, and for training the model, the GSM needs to marginalize over these hidden variables.

To solve the standard classification task of mapping an input vector x to a class label y, the GSM introduces a vector $\mathbf{h}$ of binary latent variables $(h_1, ..., h_K)$. The joint probability that the model assigns to the class label and one hidden configuration is:

$$p(y, \mathbf{h}|x) = \frac{exp(\mathbf{h}^t W_y x)}{\sum_{y' \mathbf{h}'} exp(\mathbf{h}'^t W_{y'} x)}. \tag{5.1}$$

The score for each class is parametrized by a class-specific matrix W_y. The conditional probability of class labels given the input is obtained by marginalizing over $\mathbf{h}$:

$$p(y|x) = \sum_{\mathbf{h} \in \{0,1\}^K} p(y, \mathbf{h}|x). \tag{5.2}$$

For any single and fixed instantiation of $\mathbf{h}$ in eqn. 5.1 we obtain the logistic regression model. So the GSM is equivalent to a mixture of 2^K logistic regressors with shared weights. Another way to think about the GSM is to view the hidden vector $\mathbf{h}$ as a set of style features while the model assigns high probability to combinations of a class label and a set style features that are compatible with the input features x. The model allows the 2^K possible combinations of the K learned style features to be integrated out.

Integrating over the hidden variables make it easy to compute the exact gradient of the log probability of the correct label on training data, which scales linearly with K. The derivative with respect to a single parameter $W_{y'ik}$ takes the form:

$$\frac{\partial \log p(y|x)}{\partial W_{y'ik}} = (\delta_{y'y} - p(y^{'}|x))\sigma(\sum_i x_i W_{y'ik}) x_i \tag{5.3}$$

with $\sigma(a) = (1 + exp(-a))^{-1}$.

To reduce the parameters learned in the GSM, the three way tensor W can be factorized as:

$$W_{yik} = \sum_{f=1}^{F} W_{if}^{x} W_{yf}^{y} W_{kf}^{\mathbf{h}}. \tag{5.4}$$

So the model parameters are now given by three matrices, $W^x, W^y, W^{\mathbf{h}}$, and each component W_{yik} of W is defined as a three-way inner product of column vectors taken from these matrices. Plugging the factorized form for the weight tensor into the probability in eqn. 5.1 and re-arranging terms yields:

$$p(y, \mathbf{h}|x) \propto exp\left[\sum_{f}\left(\sum_{i} x_i W_{if}^{x}\right)\left(\sum_{k} h_k W_{kf}^{\mathbf{h}}\right) W_{yf}^{y}\right]. \tag{5.5}$$

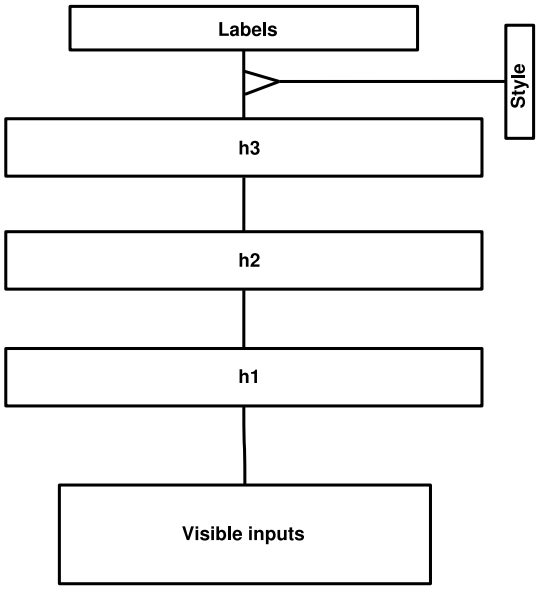

Figure 5.2: A three hidden layer DNN with gated softmax classifier.

This shows that, after factorizing, we obtain a classification decision by first projecting the input vector x and the vector of hidden variables $\mathbf{h}$ onto F basis functions or filters. The resulting filter responses are multiplied and combined linearly using class-specific weights W_{yk}^{y} as shown in figure 5.2.

Table 5.2: The PER of a GSM with two hidden layers compared to a similar DNN.

	GSM	DNN
Dev	20.0%	20.0%
Core	21.6%	22.0%

The logistic regression layer on top of the DNN can be replaced with a GSM to add extra modeling power by utilizing the hidden variables in the GSM to model different interactions between the top layer inputs and the labels for different speaking styles.

Using the gated softmax classifier on top of the DNN does modestly improve the performance on the core test set, as shown in table 5.2.

5.3 Distributed speaker adaptation for DNN

The distributed speaker-adaptation (DSA) model is based on the factored RBM model [65] which allows a set of hidden variables $\mathbf{h}$ to control the interaction between two other visible sets of variables, the inputs $\mathbf{x}$ and the outputs $\mathbf{y}$, through a set of factors. The three-way energy of a joint configuration is defined as:

$$\begin{aligned} E(\mathbf{y},\mathbf{h}|\mathbf{x}) = & - \sum_{f=1}^{F}\sum_{ijk} x_i y_j h_k W_{if}^{\mathbf{x}} W_{jf}^{\mathbf{y}} W_{kf}^{\mathbf{h}} \\ & - \sum_{k} w_k^{\mathbf{h}} h_k - \sum_{j} w_j^{\mathbf{y}} y_j. \end{aligned} \tag{5.6}$$

Having only one set of hidden variables makes inference easy, while learning could be done using contrastive divergence [42].

In the distributed speaker-adaptation model (DSA), unlike the factored RBM model, there is one group of hidden style variables that interact mutliplicatively with the input to form another hidden feature layers that represents the content. The RBM assigns lower energies to compatible configurations of content, style, and input variables.

The learned content hidden features are more invariant to changes in the style of the input data. The distributed representation of the style features does not require a huge amount of training data in order to be learned because each style feature focuses on a single aspect of an input instance and reuses it over all other input instances that have the same style aspect. This allows for data sharing while learning the style features. Also, it allows for keeping the number of style features as small as possible, because they grow linearly with the number of input styles rather than exponentially as in mixture of experts models. Having distributed style features allows for better generalization of new input data styles in test scenarios, because any new input style could be composed of the existing style aspects, i.e., any new style will be modeled by a distribution over existing styles learned while training.

First the style features are inferred and fixed, then inferring the content features conditioned on both the input vector and the fixed style features is done. This simplifies inference, given that there is a way to decide upon the style features. So we need to learn a set of distributed codes that represent each speaker in the training data and that generalizes well for new test speakers.

Usually, utterances in the training data are labeled by speaker, or the boundaries between speakers are given for long conversations. Otherwise, speaker role detection methods could be used. If we have N_s different speakers in our training data, we could use this information to train a separate neural network to predict the speaker given a contextual window of acoustic frames with 1-of-K targets, i.e., $K = N_s$. We will call it the speaker network. The visible-to-hidden connections of the network are generatively pre-trained as an RBM using the contrastive divergence algorithm to get a set of hidden features that represent both the speaker and the speech which help regularize the network. Every test speaker is represented using a distribution over the training speakers which is conditioned on a certain input speech window (about 150ms), so this predicted style distribution varies, even for the same test speaker, over the acoustic unit that spans

the visible input. This allows for more flexibility in the model because there is no fixed speaker representation over all phonetic classes.

The speaker network should be trained to generalize well to new speakers. So the learning should stop as the network starts to overfit to the training speakers. To achieve this goal we need a score that measures learning progress while being valid for test speakers. The cross entropy that is used as the training objective cannot be computed for new test speakers because there are no true labels, i.e., there is no true distribution over training speakers for a new test speaker. One score that could be used is the ratio between the global variance of the speaker prediction distribution and the sum of the variances of the predicted distribution for all test speakers:

$$R = \frac{\sum_{s=1}^{S} \sum_{f=1}^{F_s} \|\mu_s - P_f\|^2}{\sum_{i=1}^{D} \|\mu - P_i\|^2} \tag{5.7}$$

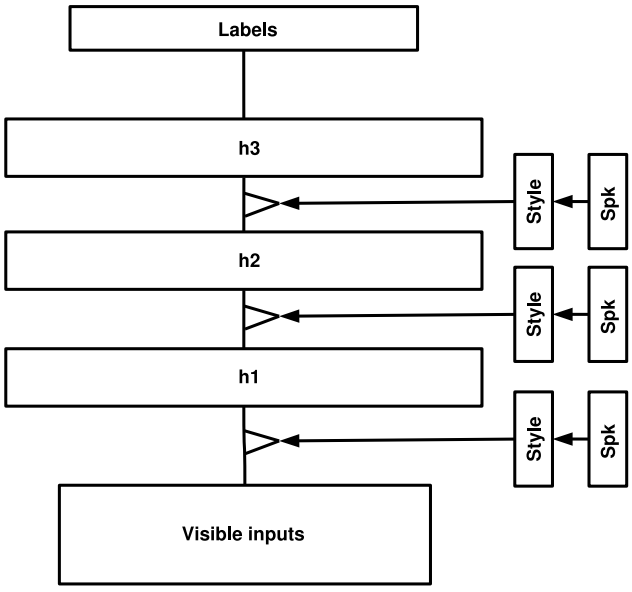

Figure 5.3: Distributed speaker adaptation for a three hidden layer DNN with labels.

where S is the total number of speakers in the held-out data that we run this measure

on, F_s is the total number of frames pronounced by speaker s, D is the total number of frames in the held-out data, and P_f is the predicted distribution over the training speakers for frame f.

Figure 5.3 shows the full network with a linear layer to map the multinomial distribution over training speakers to linear distributed features that are shared between similar speakers. During network training, the speaker predictions for every training frame are used rather than the true speaker label, which helps the network generalize well by coping with the uncertainty in the speaker distribution. The speaker-to-feature matrices are learned by backpropagating generative and discriminative error derivatives during the two phases of training.

The distributed speaker-adaptation (DSA) technique combines Speaker-Adaptive Training (SAT), as it aims at normalizing training utterances to reach a speaker-invariant representation, and Cluster Adaptive Training (CAT) [25] as it models the new speakers with a distribution over training speakers but it is even more powerful since this distribution over speakers is a function of the phonetic class rather than a fixed one. For the test data, the proposed technique does not do a first-pass decoding step, which is important for other state-of-the-art adaptation methods. The speaker transformations in the proposed method are learned jointly in the same framework with the phone recognition (content) model, while other GMM/SAT methods alternate between updating the speaker transformations and updating the GMM means and covariances.

Using distributed speaker representations to adapt the higher-level features to be more invariant does help the DNN perform very well on training data without generalizing well to the held-out data, as shown in table 5.3 and 5.4. Different regularization techniques have been tried to fix the overfitting in the DSA model but they did not work. One explanation is that the speaker codes carry too much training data noise in spite of the early stopping performed during training of the speaker network.

Table 5.3: The PER of the development set using distributed speaker adapted DNNs compared to similar unadapted DNNs.

	DSA	DNN
1 layer	21.9%	20.9%
2 layers	20.5%	19.8%
3 layers	20.5%	19.3%
4 layers	20.3%	19.2%

Table 5.4: The PER of the core test set using distributed speaker adapted DNNs compared to similar unadapted DNNs.

	DSA	DNN
1 layer	23.4%	22.8%
2 layers	22.2%	22.0%
3 layers	21.3%	20.9%
4 layers	21.7%	21.0%

5.4 Conclusions

In this chapter, DNN performance with MFSC features was found to be similar to the performance when speaker-adapted features are used. t-SNE pictures of DNN hidden activations show speaker normalization taking place in higher network layers for the TIMIT dataset. This indicates that DNNs are taking care of most of the speaker normalization needed for the TIMIT task implicitly. This finding coincides with findings in [63] where gains are observed with small network sizes, but gains vanish with large network sizes, where DNNs marginalize out speaker information. In the next chapter, a different method of speaker adaptation is proposed that does not explicitly use speaker information during training, but rather simulates the procedure of the VTLN algorithm

explicitly by using a hand-engineered network structure.

Chapter 6

Convolutional Neural Networks for acoustic modeling

In previous chapters, DNN acoustic models were shown to achieve very competitive performance compared to other acoustic models. Using MFSC features as inputs, DNNs were found to be capable of implicitly normalizing speaker differences in deeper layers of the network. Each layer of the network learns feature projection weights that aim at producing the right phone label. The distributed representations used by neural networks make it easy for DNNs to marginalize out speaker-related aspects in their deeper layers, focusing only on the spoken content.

Vocal tract length normalization (VTLN) [5,17,61] is one effective way of performing speaker normalization. It has been found that different people have different vocal tract lengths which in turn affects formant locations for different sounds. The VTLN algorithm searches for the best factor to stretch or compress the spectrum by so that different speakers have formants at similar locations along the frequency axis.

An alternative way to deal with variation in the location of features on the frequency axis is to replicate feature detectors across a range of similar frequencies. All the replicas of each feature detector are constrained to have the same weights as each other, but these

weights can still be learned. Replicating feature detectors does not, by itself, create an invariant representation in the feature activities because *different* replicas get activated when the location of the feature changes. This is an equivariant representation rather than an invariant one. Replicating a feature detector does, however, ensure that the knowledge in the weights is the same at all locations across which the feature detector is replicated. A limited amount of invariance in the vector of feature activations can be achieved by pooling the outputs of a set of replicated features so that the precise location of the feature is lost. The range over which the vector of activations is invariant can be progressively extended by using multiple layers of replicated feature detectors interleaved with pooling layers. This approach is called "convolutional neural networks" (CNNs) and has been very successful in computer vision where it is currently the most effective way to recognize objects in images [49, 54, 56].

6.1 Convolutional Neural Networks (CNNs)

Convolutional Neural Networks (CNNs) [56] introduce three new concepts to the standard neural networks framework: local filters, weight sharing and pooling. In normal neural networks, the whole input space is mapped with a different weight vector to each of the units in the first hidden layer. In CNNs, each hidden activity represents the presence or absence of a particular feature in a "local" subspace (a patch of contiguous dimensions) of the input space using a filter, i.e., weight vector, of the same dimensionality as the input patch. Each filter in the CNN is replicated across the whole input space producing a "feature map", i.e., a set of hidden activities, that summarize the presence or absence of one feature type over all local locations in the input space. "Weight sharing" refers to the idea that all hidden units forming one feature map *share* the same filter, i.e., weight vector. The first layer of a CNN where shared weights are applied to generate many feature maps is called a "convolutional layer" because the filter is *convolved* with the

input. Actually it is only a convolution if the "stride" by which a filter is translated to be applied to the next patch is 1. "Convolutional" nets often use a stride greater than 1.

To deal with the fact that objects in the input space do not always appear in the same location, CNNs use a mechanism called "pooling" to *subsample* feature maps produced by the convolutional layer in order to generate lower-resolution feature maps, which can tolerate small changes in the feature location without any change in the subsampled representations. Examples of pooling operators are the maximum or the average over a certain pooling window of input feature map from the convolutional layer. This stage of a CNN is called the subsampling or pooling layer.

The combination of these three new concepts provides tolerance to minor translations of object parts. Higher convolutional layers could use broader filters, acting on lower resolution inputs to produce more complex representations of the input. After a few pairs of convolutional and pooling layers, fully connected layers (as in normal neural networks) are typically used to combine these complex representations to perform classification using a final softmax layer.

This hierarchical structure of CNNs was found to be key for producing the best performing systems over many image processing and vision tasks [49, 54, 56, 57].

CNNs have been applied to speech recognition before [51, 55, 59], with convolution and pooling operations taking place over the time axis. DNNs already perform temporal convolution, as they are applied to successive windows of frames when scanning the input utterance, as proposed by [51]. When applied over the time domain, CNNs perform convolutions not only in the input layer but also in all subsequent hidden layers. Also CNNs offer pooling as a means to account for small temporal shifts.

6.2 A new way to apply Convolutional Neural Networks to speech recognition

In a vision task, we would like to know which objects appear in a scene and at which locations. Extending this line of thought, we can think of an ASR task as a kind of a scene analysis task. An interesting mapping, one that is favored in this chapter, thinks of phones as higher-level causes for lower level spectro-temporal energy patterns which we consider to be the objects. Each pattern gets deformed differently depending on context, speaker, accent and gender. Different arrangements of these patterns can realize the same underlying sound. A small deformation in one of these patterns can discriminate one phone from another, whereas the location of these patterns is related to the identity of the speaker.

Convolutional Neural Networks (CNNs) are a perfect match for ASR in this view. When applied on the frequency axis as shown in figure 6.1, CNNs, like VTLN, are resilient to small translations of patterns caused by speaker differences.

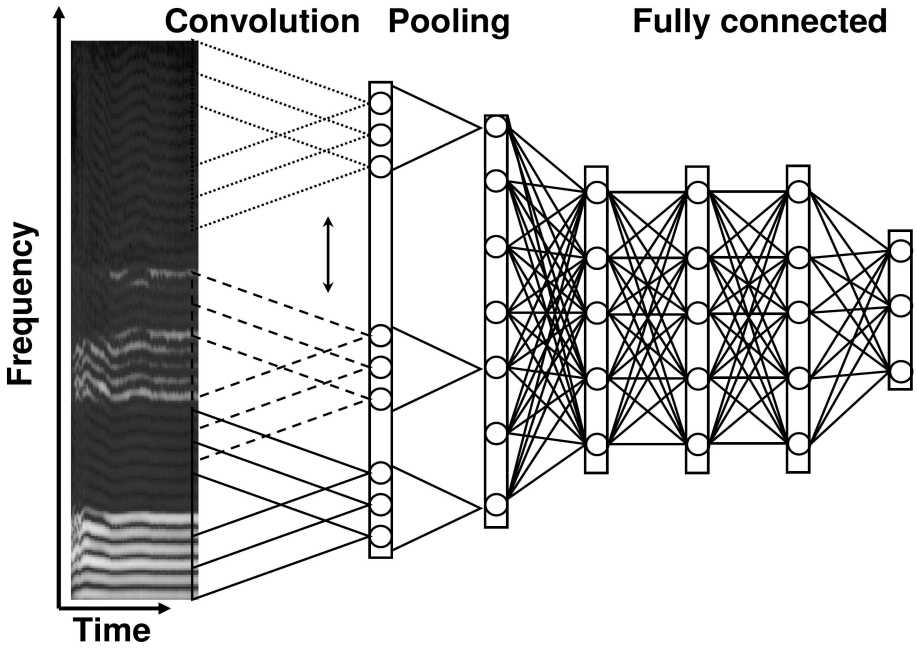

Figure 6.1: A deep convolutional NN applied along the frequency axis.

One important fact to note is that MFCCs cannot be used as input features for a system where a CNN is used on the frequency axis, while MFSC features can, because MFCCs do not have physical meaning after the DCT decorrelation step. As a result, filters with shared weights cannot be applied at different locations over the input space and no pooling operation can be performed.

In this section, CNNs are used as acoustic models, utilizing their locality, pooling, and weight sharing properties for better modeling of speech signals.

6.2.1 Locality

As shown in figure 6.2, speech signals have clear local spectro-temporal structure, while different phones have a slightly deformed energy pattern. Spectral energy peaks represents *formant* frequencies, which are resonance frequencies of the human vocal tract. The relative locations of different formants, along with their patterns, determine the spoken phone.

CNN local filters provide an efficient way of representing these spectro-temporal structures and their combinations along the different parts of the frequency axis. They help discriminate different phones. This framework is much more flexible than traditional GMM acoustic models that represent the entire frequency spectrum as a whole.

Another benefit of using filters that are local in frequency is their potential to achieve better robustness against noisy backgrounds, especially when dealing with coloured noise, that is concentrated in certain frequency locations. Local filters in comparatively clean parts of the spectrum can still detect discriminative speech features to compensate for ambiguity in the noisy parts.

CNNs are capable of modeling such local frequency structures by allowing each hidden unit of the convolutional layer to receive input only from local feature subspaces representing a limited bandwidth of the whole speech spectrum. The input to the CNN is a context window of n frames, each with 40-dimensional MFSC features along with

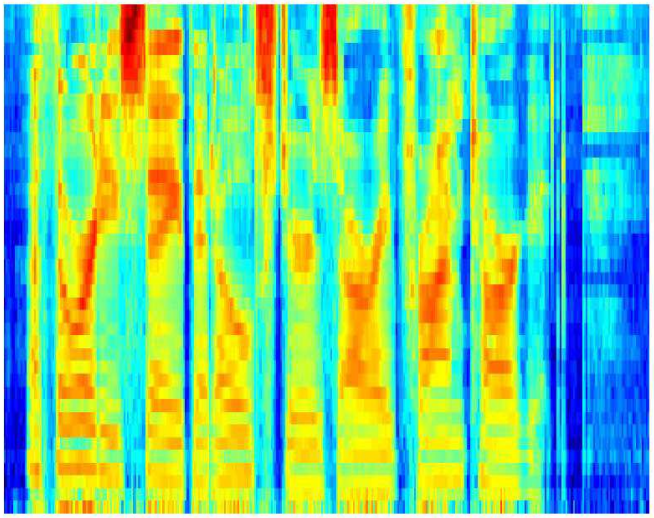

Figure 6.2: MFSC features for one of the TIMIT utterances.

energy and first and second time derivatives. Ignoring the energy coefficient for the time being, we may rearrange the input into a matrix of 40 x $3n$, where each row of the matrix consists of one frequency band along with its time derivatives, the total number of frequency bands are 40 in our case, but this can be changed as needed. Each filter in the convolutional layer receives input from only s frequency bands, so it has a weight dimension of s x $3n$ plus a bias. s is selected to be neither too large to average many patterns together nor too small. In our setup we fix it to be one fifth of the input frequency dimensionality, i.e., $s = 40/5 = 8$. A sigmoid function is applied to the filter output.

In a "full" weight sharing setup as we will discuss more in 6.2.3, the same filter scans the whole frequency axis, creating a feature map of size $K = 40 - 8 + 1 = 33$, assuming filter shift of 1. This feature map represents only one aspect of the input, so the convolutional layer applies J different filters to generate J different feature maps. The convolutional layer size is thus K x J. The full weight-sharing scheme is dominant

in the vision community, but for speech recognition we are going to propose a *limited* weight sharing regime in 6.2.3 better suited to speech signals.

Regarding the energy coefficient and its temporal derivatives, there is no obvious reason to add them to one filter location over the other, e.g., low-frequency filters over high-frequency ones, so they are added to all filters in the convolutional layer. So the size of each filter becomes $s + 1$ x $3n$ where the extra dimension is for energy.

6.2.2 Max Pooling

The speech spectrum includes many local spectro-temporal structures that are distributed over the frequency axis, where each of these patterns exhibit certain frequency ranges with little variation. For example, central frequencies of formants for the same phone may vary within a limited frequency range and they normally differ among different speakers and sometimes even between different utterances spoken by the same speaker. Some techniques try to normalize speaker variability by transforming the speech features of each speaker into a canonical speaker space [5, 21].

In CNNs this problem is addressed through the use of a max-pooling layer on top of the convolutional layer. For one feature map of size K, a pooling layer maximum operator of size r, i.e., the pooling size $= r$, scans the K dimensions, producing a lower resolution, i.e., subsampled, feature map of size $P = 1 + (K - r)/m$ where m is the subsampling factor, i.e., the maximum-operator shift. The output of the max-pooling layer is a matrix of P x J lower-resolution feature maps that contain summary information to be further processed by higher layers of the network.

6.2.3 Weight Sharing

As we discussed in section 6.2.1, a feature map is produced by scanning the input space using the same filter, i.e., the same weight vector and bias; this is called *full* weight-sharing. This concept is important in vision tasks where objects to be detected show up

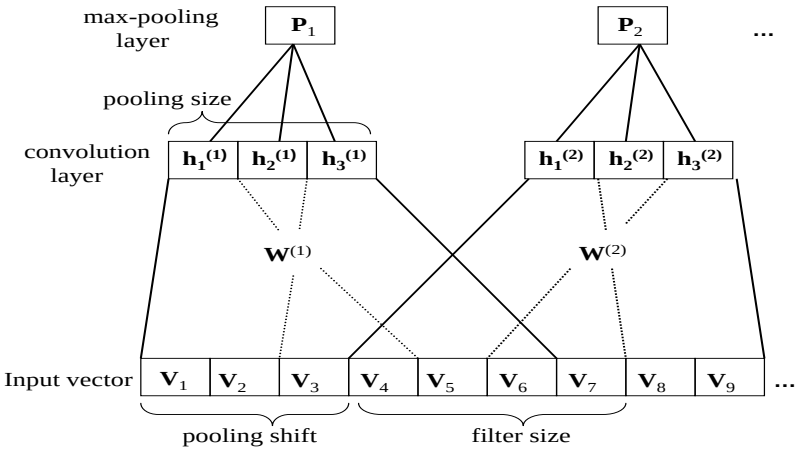

Figure 6.3: A CNN with limited weight sharing uses different weight vector for different pooling unit.

in random places in the input space. For acoustic modeling, however, the local patterns that show up in some parts of the input space simply cannot appear in other parts due to restrictions of the human speech production system. For example, vowels are embodied using lower-frequency spectro-temporal patterns that are different from those of fricatives which appear in the upper part of the spectrum.

This property in speech signals suggests a different, *limited* scheme for weight-sharing, where filters are shared only over neighbouring frequency locations as shown in figure 6.3. The pooling operator is only applied over locations that share the same weight vector.

In limited weight sharing, the max-pooling layer divides the input space into overlapping regions where filters are shared only within each region. If we proceed through figure 6.3 top-down, assuming there is only one filter to be applied, we first see the pooling unit p_1 acts on three hidden units in the convolutional layer, i.e., pooling size=3, all of which use the same weight vector $W^{(1)}$ to scan the input vector with a convolutional layer shift size of 1. As a result, the pooling unit p_1 operates over 6 dimensions of the input space,

i.e., filter size + pooling size - 1 = 6. The pooling unit, p_2, applies a different weight vector $W^{(2)}$, starting from the 4^{th} dimension. The pooling shift parameter determines the shift between input regions where different weight vectors are applied.

There is one main disadvantage of limited weight-sharing: further convolutional and pooling layers cannot be applied on top of the max-pooling layer because pooling units in different weight-sharing regions use different filters, and so they are not related. Therefore, this type of weight-sharing is normally used only in the topmost convolutional and pooling layer pair.

6.3 Experiments

The CNNs used in the experiments consist of one or more pairs of convolution and max-pooling layers, then one or more of fully connected hidden layers. In this section, we study the effects of some design parameters on CNN TIMIT phone recognition performance. For all experiments, the input number of MFSC feature vectors is fixed to 15 and the filter size over the frequency axis is fixed to 8. For training, we used mini-batch stochastic gradient descent with an annealed learning rate and early stopping. Only the fine-tuning phase is performed for all networks starting from random initial Gaussian noise.

6.3.1 Limited weight sharing

In all the limited weight sharing experiments, the number of feature maps, i.e., filters, in the convolutional layer is fixed to 90 per weight sharing region. The number of hidden units in the fully connected layers is fixed to 1000.

Figure 6.4 shows the effect of pooling-layer-shift size in limited weight-sharing CNNs, when fixing the pooling window size at 6 and using only one fully connected layer before the softmax layer. In a limited weight sharing setup, pooling-layer-shift size refers to the distance between two successive weight sharing regions. As the pooling-layer-shift

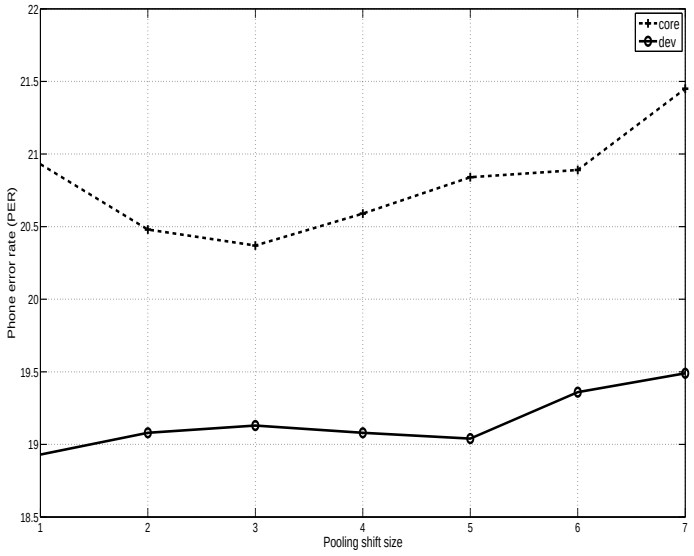

Figure 6.4: The effect of pooling-layer-shift size on PER.

increases, the number of trainable weights in the system decreases. The PER on the development set is about the same for shift sizes from 1 up to 5. High error rates are expected for higher shift sizes where the amount of overlap between different weight-sharing regions decreases.

While fixing the pooling-layer-shift size at 4, figure 6.5 examines the effect of the max-pooling window size on PER. Higher window sizes means more overlap between weight-sharing regions, which improves system performance on the development set. The core test set performance is noisy, with no obvious trend for PER.

In figure 6.6, the optimal number of fully connected layers before the softmax layer is investigated. The pooling-layer-shift size is fixed to 4 and the pooling-window size is fixed to 6. For DNNs we found that adding more hidden layers consistently improves system performance as the deep structure better removes speaker variance. In CNNs, normalizing speaker variance is taken care of using max-pooling operations over the frequency axis. Only one fully-connected layer is needed to aggregate information from all learned feature maps before the softmax layer. There is no obvious accuracy gain

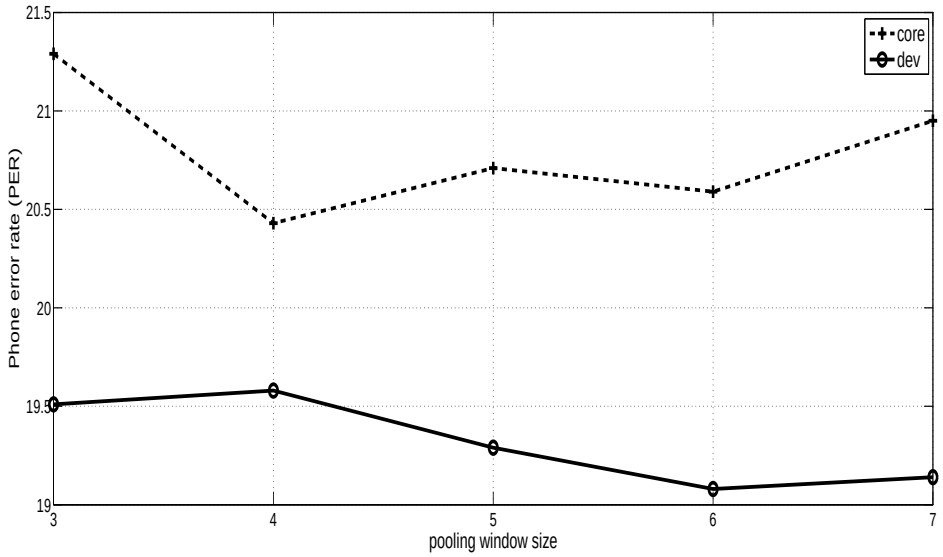

Figure 6.5: The effect of pooling window size on PER.

by adding more hidden layers. The performance of a shallow CNN is comparable to the best performing pre-trained DNN on the TIMIT phone recognition task. This conclusion, however, cannot be easily generalized to all speech recognition tasks where more hidden layers might be needed to model other acoustic complexities in the training data.

6.3.2 Full weight sharing

In all the full weight sharing experiments the number of hidden units in the fully connected layers used is fixed to 1000.

Table 6.1: *The effect of pooling-layer-shift size*

Shift size	2	4	6
Development set	19.45%	19.27%	19.45%
Core test set	21.06%	20.77%	20.84%

Table 6.1 shows the effect of pooling-layer-shift size in full weight-sharing CNNs when fixing the pooling window size at 6. In a full weight sharing setup, pooling-layer-shift size refers to the shift, in the pooling layer, between two successive pooling windows. Table

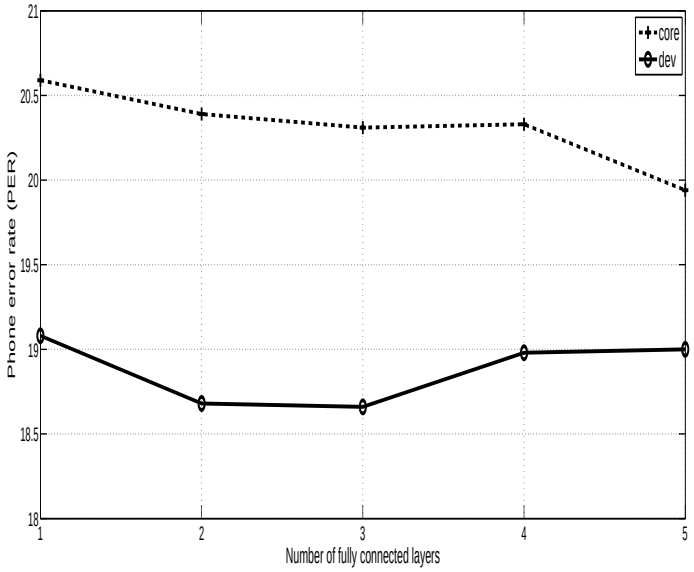

Figure 6.6: The effect of the number of fully connected layers on PER for limited weight sharing.

Table 6.2: *The effect of pooling window size*

Window size	4	6	8
Development set	19.52%	19.27%	19.81%
Core test set	20.96%	20.77%	21%

6.2 shows the effect of pooling-window size when fixing the pooling-layer-shift size at 4. Both experiments use only one fully-connected layer before the softmax layer. There is no significant PER gains by using certain setup over another because, in a full weight-sharing setup, pooling-layer-shift and pooling-window sizes don't change the number of parameters in the convolutional layer, as opposed to the limited weight-sharing setup. Increasing the number of parameters in the fully-connected layer, on top, doesn't seem to help much.

Figure 6.7 examines the effect of varying the number of feature maps in the convolutional layer in the full weight-sharing setup. As expected, the network benefits from adding more feature maps but adding more than 200 feature maps does not push gains

further.

As it is the case with limited weight sharing CNNs, adding more fully connected layers for full weight sharing CNNs makes only small improvements compared to the observed improvement in fully connected deep networks as shown in figure 6.8.

The best performance achieved by the full weight sharing CNNs is very close to that of the limited weight sharing CNNs. So filters that are *limited* to particular ranges of frequencies do not offer any performance gains compared to filters that are shared across all frequencies.

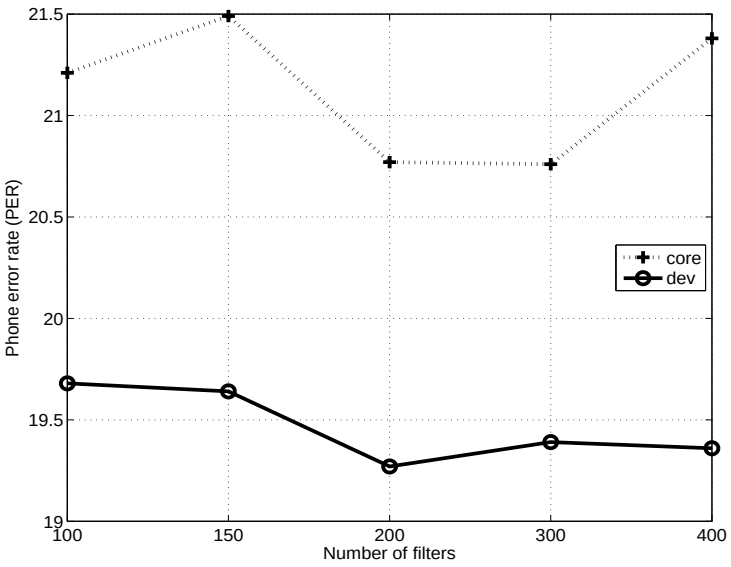

Figure 6.7: The effect of the number of feature maps for full weight sharing.

The full weight-sharing CNN has been also applied to two standard large vocabulary tasks: the 400-hours Broadcast News task, and the 300-hours Switchboard task [82]. Tables 6.3 and 6.4 show comparisons between the best GMM and DNN systems versus the best CNN systems.

Where tandem systems utilize a low dimensional representation of the output posterior probabilities of neural networks to train a baseline GMM/HMM systems [37]. The best DNN systems, for large vocabulary tasks, use six fully connected layers. The best

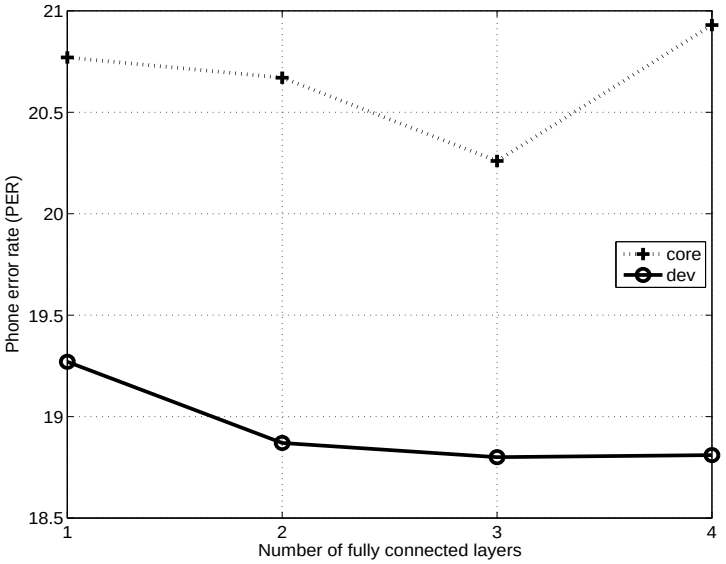

Figure 6.8: The effect of the number of fully connected layers on PER for full weight sharing.

model	dev04f	rt04
GMM/HMM	16.0	13.8
DBN/HMM	15.1	13.4
Tandem DBN-GMM/HMM	14.9	13.3
Tandem CNN-GMM/HMM	13.1	12.0

Table 6.3: WER on Broadcast News, 400 hrs

	Hub5'00	rt03	
model	SWB	FSH	SWB
GMM/HMM	14.5	17.0	25.2
DBN/HMM	12.2	14.9	23.5
Tandem CNN-GMM/HMM	11.5	14.3	21.9

Table 6.4: WER on Switchboard, 300 hrs

CNN systems achieve about 4-12% relative improvement over the best DNN systems. They use two convolutional layers and four fully connected layers. This is different from the small TIMIT task where only one convolutional and one fully connected layers were enough to model all the variability in the input signal.

6.4 Nested Hidden Markov Models

Inspired by the CNN acoustic models, this section extends the GMM acoustic model to have the product of experts flavor of deep models utilizing concepts learned from convolutional neural networks. In CNN acoustic models, local subspaces of the input are used to activate the convolutional layer filters. Then pooling introduces local translation invariance along the frequency axis. In the NHMM model, each local subspace is modeled by a Gaussian Mixture Model (GMM) instead, as shown in figure 6.9. We can think of the frequency-GMMs as states in an HMM model running over the frequency axis. A whole frequency-HMM models single state of another temporal-HMM that models the sequential evolution of speech hence the name Nested HMM. The likelihood of the frequency-HMM is a product of all the frequency-GMMs' likelihoods. Similar models have been previously proposed: the hierarchical HMM model [18], pseudo 2d HMM [50], HMM2 [94]. Product GMM acoustic models have been investigated in [22].

The new aspect of this model is that, motivated by CNNs, GMMs are applied to local spectro-temporal patterns along the frequency axis. To deal with the case where overlapping frequency subspaces are modeled by two different GMMs, the input space could be thought of as a one with lots of replicated frequencies so that overlapping locations become disjoint.

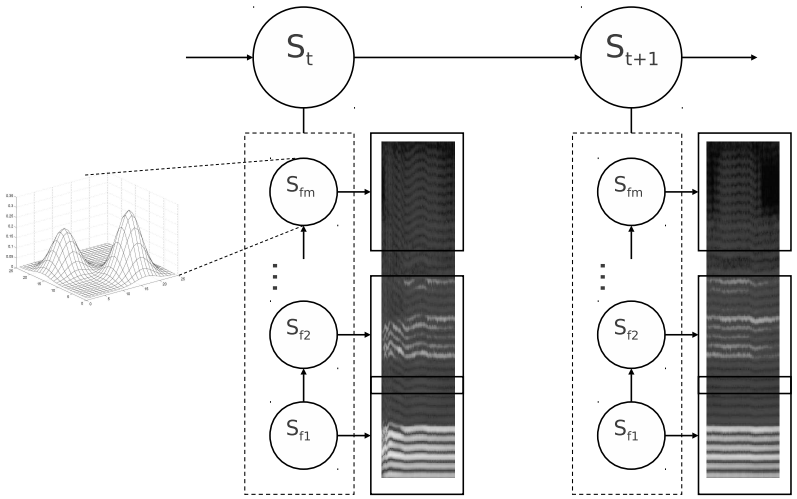

Figure 6.9: The nested hidden Markov model (NHMM).

6.4.1 The NHMM update

The EM for HMMs optimizes:

$$\mathcal{Q}(\theta, \theta^{old}) = \sum_{t=1}^{T} \sum_{k=1}^{K} \gamma_{tk} \log p(x_t|\phi_k) \tag{6.1}$$

where, T is the number of time frames and K is the total number of HMM states, γ_{tk} is the posterior probability of being at state k at time t, and θ denotes the set of parameters of the whole HMM model. Each HMM state is modelled using a GMM, ϕ_k. So,

$$p(x_t|\phi_k) = \sum_{m=1}^{M} \pi_m \mathcal{N}(x_t|\mu_{km}, \Sigma_{km}) \tag{6.2}$$

with each state k contains M Gaussian components. The objective function becomes

$$\mathcal{Q}(\theta, \theta^{old}) = \sum_{t=1}^{T} \sum_{k=1}^{K} \gamma_{tk} \log \sum_{m=1}^{M} \pi_m \mathcal{N}(x_t|\mu_{km}, \Sigma_{km}) \tag{6.3}$$

In the NHMM, each temporal state is represented by a HMM running over the frequency axis with frequency states s_b. For simplicity of the model, we assume that there

are a number of frequency states equal to the number of frequency blocks while transition probabilities all equal one. As a result, there is only one possible frequency state sequence S_f to sum over. So,

$$p(x_t|\phi_k) = \sum_{S_f} p(x_t|S_f,\phi_k)p(S_f|\phi_k) = p(x_t|S_f,\phi_k) \tag{6.4}$$

$$p(x_t,\phi_k) = p(s_1)\left(\prod_{b=2}^{B} p(s_b|s_{b-1})\right)\left(\prod_{b=1}^{B} p(x_b|s_b)\right) \tag{6.5}$$

$$p(x_t,\phi_k) = \prod_{b=1}^{B} p(x_b|s_b) \tag{6.6}$$

$$p(x_t,\phi_k) = \prod_{b=1}^{B}\sum_{c=1}^{C} \pi_{kbc}\mathcal{N}(x_b|\mu_{kbc},\Sigma_{kbc}) \tag{6.7}$$

$$\mathcal{Q}(\theta,\theta^{old}) = \sum_{t=1}^{T}\sum_{k=1}^{K}\gamma_{tk}\sum_{b=1}^{B}\log\sum_{c=1}^{C}\pi_{kbc}\mathcal{N}(x_t|\mu_{kbc},\Sigma_{kbc}). \tag{6.8}$$

By differentiating the $Q(\theta,\theta^{old})$ with respect to μ_{kbc} we get the update equations. For the case where the same GMM is shared between all the frequency states in the same frequency HMM, the update equation is

$$\mu_{kbc} = \frac{\sum_{t=1}^{T}\sum_{b=1}^{B}\gamma_{tkbc}x_b}{\sum_{t=1}^{T}\sum_{b=1}^{B}\gamma_{tkbc}} \tag{6.9}$$

$$\Sigma_{kbc} = \frac{\sum_{t=1}^{T}\sum_{b=1}^{B}\gamma_{tkbc}(x_{tb}-\mu_{kbc})(x_{tb}-\mu_{kbc})^T}{\sum_{t=1}^{T}\sum_{b=1}^{B}\gamma_{tkbc}}. \tag{6.10}$$

But in case there is a different GMM for each frequency state,

$$\mu_{kbc} = \frac{\sum_{t=1}^{T}\gamma_{tkbc}x_{tb}}{\sum_{t=1}^{T}\gamma_{tkbc}} \tag{6.11}$$

$$\Sigma_{kbc} = \frac{\sum_{t=1}^{T}\gamma_{tkbc}(x_{tb}-\mu_{kbc})(x_{tb}-\mu_{kbc})^T}{\sum_{t=1}^{T}\gamma_{tkbc}}. \tag{6.12}$$

6.4.2 Experiments

In this section, we show preliminary experiments of the NHMM versus the baseline model with the whole frequency space represented by a single GMM. A separate model is estimated for each monophone state so there are 183 total models in each system. Diagonal covariance GMMs are used for both the NHMM and baseline. Mean and variance normalized MFSC features are used with a context window of 9 frames as inputs. The frequency axis is split into overlapping local subspaces then linear discriminant analysis (LDA) is applied to reduce the input vector dimensionality for robust GMM estimation.

One problem we discovered while training the NHMM acoustic model is that for some frequency states the posterior probabilities over Gaussian components in that GMM are uniform. This happens in the high frequency states in vowels where all the activities are taking place in the lower part of the spectrum while the upper part is almost always empty. Another related point is that the NHMM model, as a product of many GMMs, represents a single GMM with exponential number of components resulting from the cross product of all Gaussian components in each frequency location. Many of these resulting components are unnecessary and they appear at weird locations in the acoustic space. To get rid of these unnecessary components, a max approximation is used instead of the sum in the GMM model. Only one component is active for each input observation while all the other components have zero responsibility.

Also, we needed to adjust the scale of the resulting NHMM likelihood to fit into the same dynamic range of the baseline in order not to have to readjust the language model scaling factor and decoder pruning parameters. Table 6.5 shows that the performance of the NHMM acoustic model on the TIMIT core test set is about the same as that of the baseline system.

Table 6.5: *Comparing the NHMM and baseline acoustic models on the TIMIT core test set*

Baseline	27.7%
NHMM with maximum overlapping	28.8%
+ max approximation in GMMs	28.3%
+ increased LDA dimensionality	28.1%
+ adjusting likelihood scale	27.9%

6.5 Conclusions

In this chapter, a new acoustic model was proposed that is based on Convolutional Neural Networks (CNNs) concepts. The convolution operation is applied along the frequency axis leading to a speaker invariant representation similar to these of VTLN techniques. The state-of-the-art performance on TIMIT core test set was achieved using shallow networks that use only one pair of convolutional and pooling layers, and one fully connected layer. Two weight-sharing schemes were introduced: full weight-sharing, which is the same scheme used for various vision tasks, and limited weight-sharing, which is motivated by the speech production process. By tuning the model parameters on the development of the TIMIT database, a PER of 20.3% was achieved on the core test set of the TIMIT benchmark using a limited weight-sharing CNN with an input window of 15 MFSC frames, 90 filters per weight-sharing region, a pooling-layer-shift size of 4, a pooling-window size of 6, and three fully connected hidden layers each containing 1000 units.

Full weight-sharing, deep CNNs have shown to provide superior performance to DNNs on two standard large vocabulary tasks. Motivated by the success of the CNN acoustic models, Nested Hidden Markov Models (NHMM), a new GMM-based acoustic model was proposed to leverage the gains speed of GMM and accuracy of CNNs. Initial experiments showed that more work is still needed for the NHMM acoustic model to beat the baseline GMM system. Future directions for improving the NHMM model includes training a

proper HMM along the frequency axis and training another module on top of the NHMM, e.g. an RBM, to remove the useless Gaussian components.

Chapter 7

Conclusions and future directions

In this thesis a new acoustic model that is based on Deep Neural Networks (DNNs) was presented and a new state of the art phone recognition accuracy was reported using deep models. The depth of the model is used to normalize out speaker differences. This was demonstrated using t-SNE visualizations for similar utterances pronounced by different speakers. The visualizations show that DNNs are capable of marginalizing out speaker variation while focusing on the spoken content. The performance of DNNs using MFSC features was found to be similar to the performance using other speaker-adapted features.

Using our understanding of how DNNs perform implicit speaker adaptation, DNNs can be designed in a way that takes care of speaker differences explicitly through network structure. Using Convolutional Neural Networks (CNNs) that perform the convolution operation over the frequency axis, state-of-the-art performance was achieved with a shallow architecture. The proposed limited weight-sharing CNN system could be considered as a hybrid of knowledge based systems and statistical systems, where we used our understanding of the structure of the speech spectrum to share parameters locally and have different sets of parameters for different locations in the spectrum, while allowing the network to learn the kind of features that it likes at each of these locations.

If we know how exactly a DNN acoustic model works along with domain experience in

the problem to be solved, a system that is as good as the DNN system can be constructed and it is more economical. This line of thought led us to think about the baseline GMM acoustic model and how it could be amended, in the light of our understanding of what is done in the DNN model, to have better performance. DNN models are very good models if there is not much understanding of the complex task at hand, but if such knowledge is available, there are more economical ways to achieve the same performance are possible.

Table 7.1: *Reported results on the TIMIT benchmark core test set*

Method	PER
Stochastic Segmental Models [16]	36%
Conditional Random Field [74]	34.8%
Large-Margin GMM [89]	33%
CD-HMM [97]	27.3%
Augmented conditional Random Fields [97]	26.6%
Recurrent Neural Nets [79]	26.1%
Bayesian Triphone HMM [68]	25.6%
Monophone HTMs [14]	24.8%
Heterogeneous Classifiers [33]	24.4%
Triphone HMMs discriminatively trained w/ BMMI [83]	22.7%
Monophone Deep Neural Networks(DNNs) (chapter 4)	**20.7%**
Monophone Deep convolutional Neural Networks(DNNs) (chapter 6)	**20.3%**

Table 7.1 compares the best performing acoustic models, which were proposed in this thesis, with previously reported results on the TIMIT benchmark core test set. [1]

The work done in this thesis opens the space for more research to be done in improving acoustic models, and it adds many techniques to our arsenal of tools. Different kinds of

[1] In [88] a PER of 21.48% is reported on the **complete** test set of the TIMIT database.

binary, discrete, and continuous features were used in the past for NN acoustic model training. In DNN models, features could be combined in the input layer or later in subsequent higher layers. Also pre-training of DNN acoustic models was found not to be necessary for training deep models; however, it is expected to play an important role in tasks where tiny amounts of data are available, and also in cases where we want to utilize the huge amounts of unlabelled spoken data currently available. Further work is still needed to develop pre-training techniques that are faster than the existing ones.

CNN acoustic models need more research along multiple directions. First, we need to improve our understanding of how deep CNN models interact with other feature-based speaker adaptation techniques and whether they replace or complement each other. Although limited weight sharing did not provide improvement over a multi-layer CNN with full weight sharing [84], limited weight sharing can be seen as a generalization of the mel-frequency spectral coefficients applied to the FFT features in the process of generating MFSC features. Hence, it could be used in CNNs for extracting richer features from high dimensional spectral input [85]. One other direction for further improvement is to use convolution and pooling layers in tandem with fully connected layers with temporal connections. This way the lower part of the network acts more like the ears of the system, while the upper part acts like the brain which aggregates information across time over multiple layers to produce the best output prediction.

Speaker adaptation for DNN acoustic models is another rich area for further improvement. One extension of the Distributed Speaker Adaptation (DSA) technique introduced in chapter 5 is to use the GMM first order statistics, as in [13], to learn speaker codes in the speaker NN. Another possibility is to train the speaker NN and the main DNN jointly. Some recent work that is along the same lines has been introduced. In [86], identity vectors (i-vectors) as described in [13] are fed to the DNN while training, while [1] uses the backpropagation algorithm to learn the speaker codes.

Motivated by the recent success in unsupervised phonetic-units learning and pronun-

ciation modelling [58] and the successes of recurrent neural networks (RNNs) in acoustic modelling [30] and language modelling [67], one important future direction is to build a giant neural network that does phonetic-units learning, acoustic modelling, pronunciation modelling, and language modelling jointly.

Bibliography

[1] Ossama Abdel-Hamid and Hui Jiang. Rapid and effective speaker adaptation of convolutional neural network based models for speech recognition. In *Interspeech*, 2013.

[2] Alex Acero, Li Deng, Trausti Kristjansson, and Jerry Zhang. HMM adaptation using vector taylor series for noisy speech recognition. In *Proc. ICSLP*, volume 3, pages 869–872, 2000.

[3] Jont B. Allen. How do humans process and recognize speech? *IEEE Trans. Speech Audio Processing*, 2(4):567–577, 1994.

[4] T. Anastasakos, J. McDonough, R. Schwartz, and J. Makhoul. A compact model for speaker-adaptive training. In *ICSLP 1996*, pages 1137 –1140 vol.2, 1996.

[5] A. Andreou, T. Kamm, and J. Cohen. Experiments in vocal tract normalization. In *In Proc. CAIP Workshop: Frontiers in Speech Recognition II*, 1994.

[6] L. Bahl, P. Brown, P. de Souza, and R. Mercer. Maximum mutual information estimation of hidden Markov model parameters for speech recognition. In *In ICASSP 1986*, pages 49 – 52, 1986.

[7] J. Baker, Li Deng, Sanjeev Khudanpur, Chin-Hui Lee, J.R. Glass, N. Morgan, and D. O'Shaughnessy. Updated minds report on speech recognition and understanding, part 2 [dsp education]. *Signal Processing Magazine, IEEE*, 26(4):78–85, 2009.

[8] Yoshua Bengio. *Artificial neural networks and their application to sequence recognition*. PhD thesis, 1991.

[9] Jeff A. Bilmes. Buried Markov models: a graphical-modeling approach to automatic speech recognition. *Computer Speech & Language*, 17(2-3):213 – 231, 2003.

[10] H. Bourlard and N. Morgan. *Connectionist Speech Recognition: A Hybrid Approach*. Kluwer Academic Publishers, 1993.

[11] Peter Brown. *The Acoustic-Modeling Problem in Automatic Speech Recognition*. PhD thesis, Carnegie-Mellon University, USA, 1987.

[12] S. Davis and P. Mermelstein. Comparison of parametric representations for monosyllabic word recognition in continuously spoken sentences. *Acoustics, Speech and Signal Processing, IEEE Transactions on*, 28(4):357–366, 1980.

[13] N. Dehak, P. Kenny, R. Dehak, P. Dumouchel, and P. Ouellet. Front-end factor analysis for speaker verification. *IEEE Transactions on Audio, Speech, and Language Processing*, 19(4):788–798, 2011.

[14] L. Deng and D. Yu. Use of differential cepstra as acoustic features in hidden trajectory modelling for phonetic recognition. In *Proc. ICASSP*, pages 445–448, 2007.

[15] Li Deng, Dong Yu, and A. Acero. Structured speech modeling. *IEEE Transactions on Audio, Speech & Language Processing*, 14(5):1492–1504, 2006.

[16] V. V. Digalakis, M. Ostendorf, and J. R. Rohlicek. Fast algorithms for phone classification and recognition using segment-based models. *IEEE Transactions on Signal Processing*, 40:2885–2896, 1992.

[17] E. Eide and H. Gish. A parametric approach to vocal tract length normalization. In *In ICASSP 1996*, pages 346 –348 vol. 1, 1996.

[18] Shai Fine, Yoram Singer, and Naftali Tishby. The hierarchical hidden markov model: Analysis and applications. *Machine Learning*, 32(1):41–62, July 1998.

[19] H. Fletcher. Speech and hearing in communication. *(Krieger, New York.)*, 1953.

[20] S. Furui. Speaker-independent isolated word recognition using dynamic features of speech spectrum. *Acoustics, Speech and Signal Processing, IEEE Transactions on*, 34(1):52 – 59, 1986.

[21] M. J. F. Gales. Maximum likelihood linear transformations for HMM-based speech recognition. *Computer Speech & Language*, 12(2):75–98, 1998.

[22] M. J. F. Gales and S. S. Airey. Product of gaussians for speech recognition. *Computer Speech Language*, 20(1):22–40, January 2006.

[23] Mark Gales and Steve Young. The application of hidden Markov models in speech recognition. *Found. Trends Signal Process.*, 1:195–304, 2007.

[24] M.J.F. Gales. Semi-tied covariance matrices for hidden Markov models. *Speech and Audio Processing, IEEE Transactions on*, 7(3):272 –281, 1999.

[25] M.J.F. Gales. Cluster adaptive training of hidden Markov models. *Speech and Audio Processing, IEEE Transactions on*, 8(4):417 –428, 2000.

[26] J-L Gauvain and Chin-Hui Lee. Maximum a posteriori estimation for multivariate gaussian mixture observations of markov chains. *Speech and Audio Processing, IEEE Transactions on*, 2(2):291–298, 1994.

[27] Zoubin Ghahramani. Learning dynamic Bayesian networks. In *Adaptive Processing of Sequences and Data Structures, International Summer School on Neural Networks, "E.R. Caianiello"-Tutorial Lectures*, pages 168–197, 1998.

[28] L. Gillick and S. Cox. Some statistical issues in the comparison of speech recognition algorithms. In *Proc. ICASSP*, pages 532–535, 1989.

[29] James R. Glass. A probabilistic framework for segment-based speech recognition. *Computer Speech & Language*, 17(2-3):137–152, 2003.

[30] A. Graves, A. Mohamed, and G. Hinton. Speech recognition with deep recurrent neural networks. In *ICASSP*, pages 6645–6649, 2013.

[31] S. Greenberg. The representation of speech in the auditory periphery. *J. Phonetics*, 16:1–151, 1988.

[32] T. Hain, P.C. Woodland, T.R. Niesler, and E.W.D. Whittaker. The 1998 HTK system for transcription of conversational telephone speech. In *In ICASSP 1999*, pages 57 –60 vol.1, 1999.

[33] A. Halberstadt and J. Glass. Heterogeneous measurements and multiple classifiers for speech recognition. In *Proc. ICSLP*, 1998.

[34] Andrew K Halberstadt. *Heterogeneous acoustic measurements and multiple classifiers for speech recognition.* PhD thesis, Massachusetts Institute of Technology, 1998.

[35] M. Hasegawa-Johnson, J. Baker, S. Borys, K. Chen, E. Coogan, S. Greenberg, A. Juneja, K. Kirchhoff, K. Livescu, S. Mohan, J. Muller, K. Sonmez, and Tianyu Wang. Landmark-based speech recognition: Report of the 2004 Johns Hopkins summer workshop. In *In ICASSP 2005*, pages 213 – 216, 2005.

[36] Timothy J. Hazen. A comparison of novel techniques for rapid speaker adaptation. *Speech Communication*, 31(1):15 – 33, 2000.

[37] H. Hermansky, D. Ellis, and S. Sharma. Tandem connectionist feature extraction for conventional HMM systems. pages 1635–1638, 2000.

[38] Hynek Hermansky. Perceptual linear predictive (plp) analysis of speech. *The Journal of the Acoustical Society of America*, 87:1738, 1990.

[39] Hynek Hermansky and Nelson Morgan. Rasta processing of speech. *Speech and Audio Processing, IEEE Transactions on*, 2(4):578–589, 1994.

[40] Hynek Hermansky and Sangita Sharma. Traps - classifiers of temporal patterns. In *Proc. International Conference on Spoken Language Processing (ICSLP)*, pages 1003–1006, 1998.

[41] G. Hinton, Li Deng, Dong Yu, G.E. Dahl, A. Mohamed, N. Jaitly, A. Senior, V. Vanhoucke, P. Nguyen, T.N. Sainath, and B. Kingsbury. Deep neural networks for acoustic modeling in speech recognition: The shared views of four research groups. *Signal Processing Magazine, IEEE*, 29(6):82–97, 2012.

[42] G. E. Hinton. Training products of experts by minimizing contrastive divergence. *Neural Computation*, 14:1771–1800, 2002.

[43] G. E. Hinton. A practical guide to training restricted boltzmann machines. In *Technical report 2010-003, Machine Learning Group, University of Toronto*, 2010.

[44] G. E. Hinton, S. Osindero, and Y. W. Teh. A fast learning algorithm for deep belief nets. *Neural Computation*, 18(7):1527–1554, 2006.

[45] G. E. Hinton and R. R. Salakhutdinov. Reducing the dimensionality of data with neural networks. *Science*, 313:504–507, 2006.

[46] N. Jaitly and G. Hinton. Learning a better representation of speech soundwaves using restricted boltzmann machines. In *Acoustics, Speech and Signal Processing (ICASSP), 2011 IEEE International Conference on*, pages 5884–5887, 2011.

[47] A. Jansen and P. Niyogi. A hierarchical point process model for speech recognition. In *Proc. IEEE International Conference on Acoustics, Speech and Signal Processing (ICASSP)*, pages 4093–4096, 2008.

[48] Hui Jiang, Xinwei Li, and Chaojun Liu. Large margin hidden Markov models for speech recognition. *Audio, Speech, and Language Processing, IEEE Transactions on*, 14(5):1584 –1595, 2006.

[49] Alex Krizhevsky, Ilya Sutskever, and Geoff Hinton. Imagenet classification with deep convolutional neural networks. In *Advances in Neural Information Processing Systems 25*, pages 1106–1114. 2012.

[50] S.-s. Kuo and O.E. Agazzi. Machine vision for keyword spotting using pseudo 2d hidden markov models. In *ICASSP*, 1993.

[51] Kevin J. Lang, Alex H. Waibel, and Geoffrey E. Hinton. A time-delay neural network architecture for isolated word recognition. *Neural Networks.*, 3(1):23–43, January 1990.

[52] H. Larochelle, D. Erhan, A. Courville, J. Bergstra, and Y. Bengio. An empirical evaluation of deep architectures on problems with many factors of variation. In *International Conference on Machine Learning*, pages 473–480, 2007.

[53] Geoffrey Hinton Laurens van der Maaten. Visualizing data using t-sne. *Journal of Machine Learning Research*, 9:2579–2605, 2008.

[54] Steve Lawrence, C Lee Giles, Ah Chung Tsoi, and Andrew D Back. Face recognition: A convolutional neural-network approach. *Neural Networks, IEEE Transactions on*, 8(1):98–113, 1997.

[55] Y. LeCun and Y. Bengio. Convolutional networks for images, speech, and time-series. In M. A. Arbib, editor, *The Handbook of Brain Theory and Neural Networks.* MIT Press, 1995.

[56] Y. Lecun, L. Bottou, Y. Bengio, and P. Haffner. Gradient-based learning applied to document recognition. In *Proceedings of the IEEE*, pages 2278–2324, 1998.

[57] Y. LeCun, F. Huang, and L. Bottou. Learning methods for generic object recognition with invariance to pose and lighting. In *Proceedings of CVPR'04*. IEEE Press, 2004.

[58] C. Lee, Y. Zhang, and J. Glass. Joint learning of phonetic units and word pronunciations for asr. In *EMNLP*, 2013.

[59] H. Lee, P. Pham, Y. Largman, and A. Ng. Unsupervised feature learning for audio classification using convolutional deep belief networks. In *Advances in Neural Information Processing Systems 22*, pages 1096–1104. 2009.

[60] K. F. Lee and H. W. Hon. Speaker-independent phone recognition using hidden Markov models. *IEEE Transactions on Audio, Speech & Language Processing*, 37(11):16411648, 1989.

[61] Li Lee and R.C. Rose. Speaker normalization using efficient frequency warping procedures. In *In ICASSP 1996*, pages 353 –356 vol. 1, 1996.

[62] C. J. Leggetter and P. C. Woodland. Maximum likelihood linear regression for speaker adaptation of continuous density hidden Markov models. *Computer Speech & Language*, 9(2):171 – 185, 1995.

[63] Hank Liao. Speaker adaptation of context dependent deep neural networks. In *Proc. ICASSP*, 2013.

[64] R. P. Lippmann. Speech recognition by machines and humans. *Speech Commun.*, 22(1):1–15, 1997.

[65] Roland Memisevic and Geoffrey E. Hinton. Learning to represent spatial transformations with factored higher-order boltzmann machines. *Neural Computation*, 22(6):1473–1492, June 2010.

[66] Roland Memisevic, Christopher Zach, Geoffrey Hinton, and Marc Pollefeys. Gated softmax classification. In J. Lafferty, C. K. I. Williams, J. Shawe-Taylor, R.S. Zemel,

and A. Culotta, editors, *Advances in Neural Information Processing Systems 23*, pages 1603–1611. 2010.

[67] T. Mikolov, S. Kombrink, L. Burget, J.H. Cernocky, and Sanjeev Khudanpur. Extensions of recurrent neural network language model. In *ICASSP*, pages 5528–5531, 2011.

[68] J. Ming and F. J. Smith. Improved phone recognition using Bayesian triphone models. In *Proc. ICASSP*, page 409412, 1998.

[69] V. Mnih. Cudamat: a CUDA-based matrix class for python. Technical Report UTML TR 2009-004, Department of Computer Science, University of Toronto, November 2009.

[70] A. Mohamed and Geoffrey Hinton. Phone recognition using restricted Boltzmann machines. In *ICASSP 2010*, 2010.

[71] Abdel-rahman Mohamed, George E Dahl, and Geoffrey Hinton. Acoustic modeling using deep belief networks. *Audio, Speech, and Language Processing, IEEE Transactions on*, 20(1):14–22, 2012.

[72] N. Morgan. The ring array processor (RAP): Algorithms and architecture. Technical report, International Computer Science Institute, 1990.

[73] N. Morgan, Q. Zhu, A. Stolcke, K. Sonmez, S. Sivadas, T. Shinozaki, M. Ostendorf, P. Jain, H. Hermansky, D. Ellis, G. Doddington, B. Chen, O. Cretin, H. Bourlard, and M. Athineos. Pushing the envelope - aside. *Signal Processing Magazine, IEEE*, 22(5):81–88, 2005.

[74] J. Moris and E. Fosler-Lussier. Combining phonetic attributes using conditional random fields. In *Proc. Interspeech*, pages 597–600, 2006.

[75] A. Nadas. Optimal solution of a training problem in speech recognition. *Acoustics, Speech and Signal Processing, IEEE Transactions on*, 33(1):326 – 329, 1985.

[76] D. Povey, D. Kanevsky, B. Kingsbury, B. Ramabhadran, G. Saon, and K. Visweswariah. Boosted mmi for model and feature-space discriminative training. In *In ICASSP 2008*, pages 4057 –4060, 2008.

[77] D. Povey, B. Kingsbury, L. Mangu, G. Saon, H. Soltau, and G. Zweig. fmpe: Discriminatively trained features for speech recognition. In *In ICASSP 2005*, pages 961 – 964, 2005.

[78] D. Povey and P.C. Woodland. Minimum phone error and I-smoothing for improved discriminative training. In *In ICASSP 2002*, pages I–105 – I–108 vol.1, 2002.

[79] A. Robinson. An application to recurrent nets to phone probability estimation. *IEEE Transactions on Neural Networks*, 5(2):298–305, 1994.

[80] Antti-Veikko I. Rosti and M. J. F. Gales. Factor analysed hidden Markov models for speech recognition. *Computer Speech & Language*, 18(2):181–200, 2004.

[81] T. N. Sainath, B. Kingsbury, V. Sindhwani, E. Arisoy, and B. Ramabhadran. Low-rank matrix factorization for deep neural network training with high-dimensional output targets. In *ICASSP*, 2013.

[82] T. N. Sainath, A. Mohamed, B. Kingsbury, and B. Ramabhadran. Deep convolutional neural networks for LVCSR. In *Proc. ICASSP*, 2013.

[83] T. N. Sainath, B. Ramabhadran, and M. Picheny. An explortation of large vocabulary tools for small vocabulary phonetic recognition. In *IEEE Automatic Speech Recognition and Understanding Workshop*, 2009.

[84] Tara N. Sainath, Brian Kingsbury, Abdel-rahman Mohamed, George Dahl, George Saon, Hagen Soltau, Tomas Beran, Aleksandr Aravkin, and Bhuvana Ramabhadran. Improvements to deep convolutional neural networks for lvcsr. In *ASRU*, 2013.

[85] Tara N. Sainath, Brian Kingsbury, Abdel-rahman Mohamed, and Bhuvana Ramabhadran. Learning filter banks within a deep neural network framework. In *ASRU*, 2013.

[86] George Saon, Hagen Soltau, David Nahamoo, and Michael Picheny. Speaker adaptation of neural network acoustic models using i-vectors. In *ASRU*, 2013.

[87] L.K. Saul and M.G. Rahim. Maximum likelihood and minimum classification error factor analysis for automatic speech recognition. *Speech and Audio Processing, IEEE Transactions on*, 8(2):115 –125, 2000.

[88] Petr Schwarz, Pavel Matjka, and Jan ernock. Hierarchical structures of neural networks for phoneme recognition. In *Proc. ICASSP*, pages 325–328, 2006.

[89] F. Sha and L. Saul. Large margin gaussian mixture modeling for phonetic classification and recognition. In *Proc. ICASSP*, pages 265–268, 2006.

[90] Fei Sha and Lawrence K. Saul. Large margin hidden Markov models for automatic speech recognition. In *Advances in Neural Information Processing Systems 19*, pages 1249–1256. 2007.

[91] K.C. Sim and M.J.F. Gales. Minimum phone error training of precision matrix models. *Audio, Speech, and Language Processing, IEEE Transactions on*, 14(3):882 – 889, 2006.

[92] I. Sutskever and G. E. Hinton. Using matrices to model symbolic relationships. In *Advances in Neural Information Processing Systems*, volume 21.

[93] G. W. Taylor, G. E. Hinton, and S. Roweis. Modeling human motion using binary latent variables. In *Proc. NIPS*, 2007.

[94] Katrin Weber. *HMM Mixtures (HMM2) for Robust Speech Recognition.* PhD thesis, Ecole Polytechnique Federale de Lausanne, 2003.

[95] P.C. Woodland, D. Pye, and M.J.F. Gales. Iterative unsupervised adaptation using maximum likelihood linear regression. In *In ICSLP 1996*, pages 1133 –1136 vol.2, 1996.

[96] Phil C. Woodland. Speaker adaptation for continuous density HMMs: A review. In *ITRW on Adaptation Methods for Speech Recognition*, 2001.

[97] Hifny Y. and Renals S. Speech recognition using augmented conditional random fields. *IEEE Transactions on Audio, Speech & Language Processing*, 17(2):354–365, 2009.

[98] Victor Zue, James Glass, Michael Phillips, and Stephanie Seneff. The MIT SUMMIT speech recognition system: a progress report. In *Proceedings of the workshop on Speech and Natural Language*, HLT '89, pages 179–189, 1989.

[99] Geoffrey Zweig and Stuart Russell. Speech recognition with dynamic Bayesian networks. In *AAAI 1998*, pages 173–180, 1998.